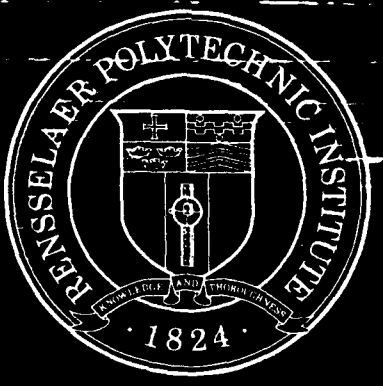

Rensselaer Polytechnic Institute

Troy, New York 12181

Final Report

ANALYTICAL AND EXPERIMENTAL CHARACTERIZATION OF DAMAGE PROCESSES IN COMPOSITE LAMINATES

by

George J. Dvorak
Civil Engineering Department
Rensselaer Polytechnic Institute
Troy, NY 12180

and

Norman Laws
Department of Mechanical Engineering
University of Pittsburgh
Pittsburgh, PA 15261

Submitted to

Air Force Office of Scientific Research
Bolling Air Force Base, Washington, DC

Contract AFOSR-84-0366

June 1988

Unclassified

SECURITY CLASSIFICATION OF THIS PAGE

REPORT DOCUMENTATION PAGE

1a. REPORT SECURITY CLASSIFICATION: Unclassified	1b. RESTRICTIVE MARKINGS
2a. SECURITY CLASSIFICATION AUTHORITY	3. DISTRIBUTION/AVAILABILITY OF REPORT: Approved for public release. Distribution unlimited.
2b. DECLASSIFICATION/DOWNGRADING SCHEDULE	
4. PERFORMING ORGANIZATION REPORT NUMBER(S): CECM-2	5. MONITORING ORGANIZATION REPORT NUMBER(S): AFOSR-TR- 88-0707
6a. NAME OF PERFORMING ORGANIZATION: Rensselaer Polytechnic Inst. / 6b. OFFICE SYMBOL (If applicable):	7a. NAME OF MONITORING ORGANIZATION: AFOSR
6c. ADDRESS (City, State and ZIP Code): Civil Engineering Department, Troy, NY 12180	7b. ADDRESS (City, State and ZIP Code): AFOSR/NA Bldg 410, Bolling AFB, DC 20332
8a. NAME OF FUNDING/SPONSORING ORGANIZATION: AFOSR/NA / 8b. OFFICE SYMBOL (If applicable): NA	9. PROCUREMENT INSTRUMENT IDENTIFICATION NUMBER: AFOSR-84-0366
8c. ADDRESS (City, State and ZIP Code): Building 410, Bolling Air Force Base, DC 20332	10. SOURCE OF FUNDING NOS. — PROGRAM ELEMENT NO.: 61102F / PROJECT NO.: 2302 / TASK NO.: B2 / WORK UNIT NO.:
11. TITLE (Include Security Classification): Analytical & Experimental Characterization of Damage Processes in Composite Laminates	(U)
12. PERSONAL AUTHOR(S): George J. Dvorak and Norman Laws	
13a. TYPE OF REPORT: FINAL / 13b. TIME COVERED: FROM 9/1/86 TO 2/29/88	14. DATE OF REPORT (Yr., Mo., Day): June 1988 / 15. PAGE COUNT: 35
16. SUPPLEMENTARY NOTATION	

17. COSATI CODES		
FIELD	GROUP	SUB. GR.

18. SUBJECT TERMS (Continue on reverse if necessary and identify by block number): Composite materials, cracking, damage accumulation. (KEY)

19. ABSTRACT (Continue on reverse if necessary and identify by block number)

This report presents a brief summary of the principal results obtained in a research program on damage development in fibrous composite laminates. The following technical subjects are described: (i) Effect of transverse cracks and fiber breaks on stiffness changes in unidirectional and laminated plates. (ii) Effect of ply thickness on initial failure and on progressive cracking in brittle matrix laminates, and (iii) Analysis of progressive cracking in metal and polymer composite laminates. Work in progress is discussed as well.

(Keywords)

20. DISTRIBUTION/AVAILABILITY OF ABSTRACT: UNCLASSIFIED/UNLIMITED ☒ SAME AS RPT. ☐ DTIC USERS ☒	21. ABSTRACT SECURITY CLASSIFICATION: UNCLASSIFIED
22a. NAME OF RESPONSIBLE INDIVIDUAL: Lt. Col. George K. Haritos	22b. TELEPHONE NUMBER (Include Area Code): (202)767-0463 / 22c. OFFICE SYMBOL: NA

DD FORM 1473, 83 APR — EDITION OF 1 JAN 73 IS OBSOLETE.

UNCLASSIFIED

ABSTRACT

This report presents a brief summary of the principal results obtained in a research program on damage development in fibrous composite laminates. The following technical subjects are described: (i) Effect of transverse cracks and fiber breaks on stiffness changes in unidirectional and laminated plates. (ii) Effect of ply thickness on initial failure and on progressive cracking in brittle matrix laminates, and (iii) Analysis of progressive cracking in metal and polymer composite laminates. Work in progress is discussed as well.

TABLE OF CONTENTS

1. INTRODUCTION

This research project was conducted as a cooperative effort of two investigators. Dr. George J. Dvorak was the principal investigator of the program at Rensselaer Polytechnic Institute, which was the primary contractor. Dr. Norman Laws was the principal investigator of the part of the program subcontracted from RPI to the University of Pittsburgh.

The program addressed several basic problems in damage mechanics of both brittle and ductile fibrous composite materials, and produced many new results. The principal accomplishments can be summarized as follows:

1. Formulation of self-consistent and bounding techniques for a deterministic evaluation of stiffness changes caused by transverse cracks or by fiber breaks in plies of any orientation in fibrous laminates. The accuracy of stiffness predictions obtained from the self-consistent method was verified by comparison with available and our own experimental data.
2. Evaluation of the effect of ply thickness on initial failure and on progressive cracking in polymer matrix laminates under incrementally increasing load. The significant conclusion obtained in the analysis, and in the related experimental confirmation, was that damage development in such brittle matrix laminates could be retarted or completely eliminated by keeping the thickness of each ply to a minimum.
3. Analysis of progressive cracking in metal and polymer composite laminates. In this effort we were able to predict stiffness changes which were observed experimentally under monotonically increasing loads in glass and graphite/epoxy laminates. Also, we analyzed the process of fatigue damage development in metal matrix B/Aℓ laminates, which is caused by cyclic plastic straining of the matrix. We found that damage in this system

served as a shakedown mechanism which allowed the composite to resume an elastic deformation response in the saturation damage state. An incremental procedure was formulated to find the stiffness changes associated with saturation damage states reached under any steady-state loading program. The predicted stiffness changes were found to be in excellent agreement with experimentally measured magnitudes.

These principal findings, together with other related results are described in the sequel.

2. SIGNIFICANT ACHIEVEMENTS

2.1 Loss of Stiffness

The first important technical results obtained in the course of this research relate to the loss of stiffness of unidirectional composites, or individual plies in a laminate, due to transverse matrix cracks and due to fiber breaks and consequent aligned penny-shaped cracks. The general analysis of Laws, Dvorak and Hejazi [1] was simplified and, for transverse matrix (slit) cracks the self-consistent results were extensively discussed by Dvorak, Laws and Hejazi [2]. Subsequently these results were favorably compared by Laws and Dvorak [3] with some exact results of Delameter, Herrmann and Barnett [4], see Table 1. Further, Dvorak and Laws [5] showed that the predictions of the self-consistent model were in good agreement with the experimental data of Highsmith and Reifsnider [6] for $(0,90_3)_s$ E-glass epoxy laminates, see Fig. 1. In addition we note that the model may be used to give results for transverse cracking of $(90_3,0)_s$ laminates. However, Highsmith [7] advises that the reported [6] data for $(90_3,0)_s$ E-glass epoxy laminates is not reliable.

It is worth noting here that the model developed by the present authors [3,5] is entirely consistent [8] with bounds obtained by Hashin [9] for the loss of stiffness of cracked laminates.

At the time of writing, a popular alternative to the self-consistent model is the differential scheme. We remark that the first application of the differential scheme to cracked solids was given by Laws and Dvorak [10]. As far as cracked laminates are concerned, it is straightforward to use the differential scheme rather than the self-consistent scheme in the Dvorak-Laws model for cracked laminates. Indeed, in many cases, the results are almost

identical.

We emphasize that the Dvorak-Law model for the loss of stiffness of cracked laminates is completely deterministic in the sense that the model does not contain any adjustable parameters.

Next we turn to the analysis of fiber breaks in a unidirectional composite, or in an individual ply of a laminate. An essential prerequisite to this study is the analysis of crack opening displacements by Laws [10]. It is, perhaps, relevant to point out that the analysis of Laws [10] corrects a rather serious error in the literature. The paper by Laws and Dvorak [11] breaks new ground in many important areas. In particular we gave

(i) the self-consistent model for the loss of stiffness of a unidirectional composite due to fiber breaks accompanied by penny-shaped cracks at the ends of the broken fibers,

(ii) the differential scheme for the same problem,

(iii) the appropriate Hashin-Shtrikman bound for cracked solids,

(iv) a succinct derivation of the Mori-Tanaka [12] model which showed that the model coincided with the Hashin-Shtrikman bound,

(v) a complete numerical comparison of the various models, see e.g. Figs. 2, 3,

(vi) the calculation of various energy release rates, thus indicating the likelihood of multiple cracking rather than the catastrophic propagation of a single crack.

We note that the results described briefly above have been used extensively by Laws and Brockenbrough [13,14,15], and others, in the study of microcracked polycrystalline ceramics.

2.2 First Ply Failure of Composite Laminates

The mechanics of crack initiation in an elastic fibrous ply were explained in [16] and [17]. Cracks were assumed to initiate from a nucleus created by localized fiber debonding and matrix cracking. Conditions for the onset of unstable cracking from such nuclei were evaluated with due regard to the interaction of cracks with adjacent plies of different elastic properties. It was found that crack propagation in the direction of the fiber axis controls the strength of thin plies, whereas cracking in the direction perpendicular to the fiber axis determines the strength of thick plies. The theory relates ply thickness, crack geometry and ply toughness to ply strength.

In order to apply the theory presented by Dvorak and Laws [16,17] to a specific laminate, it is necessary to evaluate the reduction in the stress intensity factor, at the crack tip of a transverse crack, due to the interaction with the adjacent plies in the laminate. This calculation is especially difficult and involves the solution of a complicated singular integral equation - the details are to be reported in a forthcoming Ph.D. thesis [18]. When use is made of these stress intensity reduction coefficients together with experimental data reported by Wang [19], one obtains the comparisons shown in Fig. 4.

2.3 Progressive Cracking of Cross Ply Laminates

A further significant achievement has been the formulation of a simple shear-lag model to predict progressive transverse cracking of cross ply laminates under monotonic loading. The model is based upon fracture mechanics but accounts for the statistical nature of the transverse cracking process observed in experimental tests. The theory has been developed in references

[8] and [20]. In particular we suggested a definite choice of probability density function to account for the statistical variations in the locations of the respective cracks. Thus the model does not involve any adjustable parameters. The model allows us to predict the loss of stiffness, progressive crack density, initiation of H-cracking at interfaces, etc. when we are given basic data on ply thermo-elastic properties, ply toughness and laminate geometry.

Figure 6 shows the predicted loss of stiffness for the bench-mark data of Highsmith and Reifsnider [6]. Also shown in Figure 6 are the Hashin [9] lower bound and the Highsmith-Reifsnider [6] prediction. We observe that the Dvorak-Laws self-consistent result is not shown in Fig. 6 since it is almost indistinguishable from the Hashin [9] bound. In the final analysis one can conclude that predicting the loss of stiffness is quite a forgiving process. Indeed, when one considers graphite-epoxy systems, the loss of stiffness due to transverse cracking is so small that all models must give almost identical results. However, when we consider the prediction of progressive crack density, a totally different picture emerges.

As far as we are aware the only other work which addresses the problem of determining crack density under monotonic load is due to Wang, Crossman and co-workers [19,21,22,23,24]. The predictions of the model developed by the present authors [8,20] are extremely close to the observed values, see Figs. 9 and 10. We note that we have omitted Wang's [24] numerical predictions from Fig. 9 since it is impossible to do justice by attempting to reproduce the published graphs. Nevertheless, it is significant that both the Wang-Crossman model and the Laws-Dvorak model give excellent predictions.

In our own experimental program conducted by Dvorak and Martine at RPI, we examined glass-epoxy tube specimens of the $0_n/90_m/0_n$ (n = 1, 2; m = 1, 2, 4)

layup under incrementally applied, combined tension and torsion loads. The crack density in the 90° plies and the stiffness losses in the laminated tubes were measured in the experiments. In agreement with the predictions of our analysis of the role of ply thickness in damage development, we found no pre-failure damage in single-ply, i.e., 0/90/0 specimens. The single ply thickness in our specimens was 0.254 mm. Some incomplete cracks were found in $0/90_2/0$ tubes, and many circumferential cracks were observed in four-ply, $0/90_4/0$ laminates. The implication is that the amount of damage in laminates can be reduced if ply thickness is kept to a minimum.

The above experimental investigation also showed that transverse cracking in the tested system was caused almost exclusively by transverse normal stresses in the 90° layer. Combined loading in tension and shear showed that the shear stress made no significant contribution to transverse cracking, but that it was responsible for delamination between plies prior to final failure.

The experiments also confirmed predictions of stiffness losses by the self-consistent method. The agreement was very good in the case of axial elastic modulus of the tube, but less satisfactory in the case of the shear modulus. Viscous effects were apparently responsible.

2.4 Fatigue of Metal Matrix Laminates

The experimental results of Dvorak and Johnson [26] on B/Al laminates, as well as subsequent studies by Johnson on SiC/Ti plates suggest that cyclic plastic straining of the matrix is the principal cause of fatigue damage growth. No damage is typically observed if the laminate is loaded by an elastic load cycle, either in the initial or shakedown state. This argument can be extended to damaged laminates. In particular, one can assume that all

damage growth will terminate if the laminate reaches an elastic deformation state. As illustrated by the example in Fig. 8, elastic deformation can be restored under an initially inelastic cycle of loading, if the amount of damage in the plies, and the applied strain cycle cause, respectively, expansion and translation of the ply relaxation surfaces such that the prescribed load cycle or the corresponding strain cycle can be accommodated within the new elastic range. The damage evolution process can then be regarded as a mechanism that the composite laminate employs to reach an elastic state. In this new state, the originally inelastic part of the total strain in each ply is accommodated, in part, by the strain caused by opening of the cracks.

Viewed from a different perspective, the damage process can be thought of as a part of a shakedown mechanism in the composite laminate. According to the static or Melan shakedown theorem, an elastic-plastic solid or structure will shake down if any admissible residual stress field can be found such that its superposition with the stresses caused by the applied loading will not violate the yield condition anywhere in the solid. In other words, the laminate will shake down if a subsequent yield surface, or its relaxation surface counterpart in the strain space, can be found which contains the applied load or strain cycle. Of course, shakedown can take place only if the structure is loaded within its failure envelope, and if early collapse by incremental plastic straining can be prevented. That is usually the case in laminated plates where the elastic fibers support a major part of the load so that the total strains are small, yet substantially larger than the initial yield strains of a ply.

Modeling of the incremental shakedown-damage process in a metal matrix laminate can be illustrated with the help of relaxation surfaces shown in

Fig. 8. In this example, the yield surfaces in strain space, so-called relaxation surfaces, were plotted for a $(0/90)_s$ laminate subjected to in-plane normal strains $\bar{\varepsilon}_{22}$, $\bar{\varepsilon}_{33}$. The top bars indicate laminate strains, which are equal in all plies; the x_3 direction coincides with the fiber orientation in the 0° ply, and x_2 is the fiber direction in the 90° ply. Cracks have been added after completion of the load cycle, and the relaxation surfaces are therefore plotted from the end position at 50 MPa. The dashed line indicates the crack opening condition. As one would expect, a larger overall strain is needed to cause the initial yield strain in the matrix of a cracked ply. Therefore, the open crack branches of the relaxation surfaces expand with increasing crack density β.

It is useful to point out that cyclic plastic loading of the laminate creates cyclic *plastic strains* in individual plies which, as illustrated by Fig. 8, tend to reach a steady state after relatively few cycles. On the other hand, the plastic deformation cycle also promotes low cycle fatigue damage growth which, in comparison, proceeds very slowly. Typically, several thousand cycles may be needed to cause a significant change. One may then expect the relaxation surfaces to translate much more rapidly than expand. The direction of translation should be such as to minimize the magnitude of plastic work per cycle. Under such circumstances, the relaxation surfaces will tend to translate into such most favorable positions which will assure that the amount of expansion - which is to say extent of ply damage - will reach only the minimum amount necessary for an elastic accommodation of the loading program.

Another consequence of the large disparity between deformation and damage rates is that in each damage state the effect of past deformation history will

fade very quickly. That is to say that the deformation field in the laminate at a particular state of ply damage will be very similar to that which one would reach if this amount of damage was introduced into an elastic laminate prior to the application of the corresponding load cycle. The implication is that the final deformation state in a damaged laminate subjected to a constant load cycle must be independent of previous loading and damage history. Therefore, in arriving at a final damage state, one may follow any convenient path. For example, the damage analysis of the typical case of constant amplitude loading, which causes large excursions into the plastic range during many initial deformation cycles, can be replaced by analysis of damage caused by a load cycle which expands at a rate comparable to that of damage growth. In this particular case each increment in amplitude is followed after few cycles by a saturation damage increment which restores elastic straining within a new shakedown sate.

Apart from the above arguments, available results obtained in tension-tension fatigue tests of B/Aℓ metal matrix composite laminates support the path independence concept. For example, Johnson found that a saturation damage state at a certain maximum load amplitude could be reached by dissimilar loading sequences. Another support for this concept was established by experiments which showed that the amount of damage in a laminate was determined primarily by the load amplitude and not by variations of the mean stress.

We now present some results which illustrate certain aspects of damage development in B/Aℓ laminates subjected to cyclic tension loading. Our objective is to find, for several different load amplitudes, the amount of damage in each ply that is needed to reach a shakedown state in the laminate. Of course, the stiffness loss and the internal stress distribution, particularly

the fiber stress, are also of interest. One specific laminate under consideration, of 0/90 layup, was already discussed in connection with Fig. 8. In addition, a similar analysis was performed for a 0° plate. The final load cycle we wish to reach in both laminates is from S_{min} = 50 MPa to S_{max} = 500_{max} MPa. The actual path we follow starts with cycling of the laminate to a steady state, as in Fig. 8. Then, while S_{min} is kept constant, S_{max} is reduced to bring the laminate into an elastic state. Next, S_{max} is increased in small increments. After each increment, cracks are introduced in the plastically deforming plies to the extent needed to accommodate the deformation path within the expanded relaxation surfaces. This involves both expansion and translation of the surfaces, which cause a new plastic strain state and a stress redistribution through the laminate. Details of the procedure have been described by Wung [27] and Dvorak and Wung [28]. As an example, Fig. 9 shows the current relaxation surfaces at two levels of S_{max}. Note that high values of crack density β are needed here to accomplish the accommodation. It would be unrealistic to expect crack densities exceeding β = 1 in each ply. Therefore, β must be regarded here as a damage parameter which accounts for extension of the cracks onto adjacent plies, for crack intersection at ply boundaries, and for crack extension by delamination along fiber-matrix interfaces. The incremental expansion of the loading range continues until one reaches the desired final magnitude of S_{max}.

Fig. 10 shows the change in the axial elastic modulus caused by saturation damage in the two laminates as a function of the applied tension stress range. The computed results are plotted together with experimental data of Dvorak and Johnson [26]. In the experiments, the saturation damage state was defined as the damage state after 2×10^6 cycles at constant stress amplitude,

as noted in Fig. 10, but actual measurements of stiffness loss indicated that damage usually stabilized after 5×10^5 cycles. Finally, Fig. 11 indicates the computed magnitudes of the axial stress in the 0° layer fibers, in the saturation state at different levels of S_{max}. This stress change has been plotted up S_{max} equal to the experimentally observed endurance limit. Note that while the endurance S_{max} are quite different in the two laminates, the terminal fiber stresses are nearly identical. The implication is that fatigue failure occurs in these composite systems by overloading of the 0° fibers. Of course, the maximum stress is not seen by the fibers until the laminate reaches the saturation damage state at the endurance S_{max}. In the initial stages of damage development, a part of the load is carried by the undamaged off-axis plies, but as damage grows more stress is absorbed by the 0° fibers.

3. WORK IN PROGRESS

Two Ph.D. dissertations are still in progress, one by Mr. A. Kaveh Ahangar [29] at RPI, and one by Mr. J.B. Wang [18] at the University of Pittsburgh. This work in progress can be described as follows.

Mr. Ahangar's dissertation is concerned with evaluation of overall stiffness changes, and the local fields in plies, for cracked laminates of any lay-up. The approach is based on variational principles of elasticity, which allow one to select, among a class of chosen admissible fields in the plies, the best approximation of the actual stress field in a cracked ply. The chosen fields do not take into account crack-tip singularities, this seems to be reasonable in fibrous systems where the crack tip geometry is not well defined. However, interaction between cracks in a ply, and of the cracks with adjacent plies is taken into consideration. This technique leads to much better estimates of ply fields than the self-consistent method which gives only ply stress averages. We have already completed the analysis of laminates with specified crack densities. Current work addresses the problem of crack growth under incrementally applied load. Results of this kind have been available so far only for 0/90 laminates. The method relies on a numerical procedure, but the computing effort is relatively moderate.

Work is also continuing on the exact stress analysis of cracked laminates. To a certain extent this will be reported in the forthcoming Ph.D. thesis by Wang [18]. But we continue to strive for a computer code which is sufficiently user-friendly and cost effective to analyse laminates of arbitrary lay-up. This is not easy and indeed is impossible without use of the supercomputer. As remarked earlier in this report, this program provides the stress intensity factors which are essential in the Dvorak-Laws model for first ply failure.

The work on progressive cracking is continuing and problems associated with other lay-ups, e.g., $(\pm 25,90)_s$, $(\ (0,90)_n)_s$, are being addressed. In addition we are continuing with our work on the onset of additional damage modes together with the progressive nature of such modes. A particular problem of concern here relates to the development of damage during bending.

But the major part of the work in progress is now related to ceramic matrix composites and laminates. Here we are investigating the change of thermomechanical properties of both unidirectional composites and laminates. Typical problems of interest are the loss of stiffness and improvement of toughness of various ceramic matrix ceramic fiber systems. It is clear from the literature and from discussions with Dr. Nicholas Pagano and with Dr. Ted Nicholas at the Air Force Materials Laboratory that unidirectional materials pose significantly different issues to those which must be addressed for laminates. Further, it is also clear that the damage modes in ceramic matrix ceramic fiber systems (unidirectional or laminates) are different from the modes observed in graphite-epoxy or glass-epoxy systems. These problems are under intensive study.

REFERENCES

1. Laws, N., Dvorak, G.J. and Hejazi, M., "Stiffness Changes in Unidirectional Composites Caused by Crack Systems," Mechanics of Materials 2 (1983) 123-127.

2. Dvorak, G.J., Laws, N. and Hejazi, M., "Analysis of Progressive Cracking in compc .te Laminates, I, Thermoelastic Properties of a Ply with Cracks," J. Composite Materials 19 (1985) 216-234.

3. Laws, N. and Dvorak, G.J., "The Loss of Stiffness of Cracked Laminates," Fundamentals of Deformation and Fracture (Eshelby Memorial Symposium, ed. B.A. Bilby, K.J. Miller and J.R. Willis) pp. 119-127, Cambridge University Press 1984.

4. Delameter, W.R., Hermann, G. and Barnett, D.M., "Weakening of an Elastic Solid by a Rectangular Array of Cracks," J. Appl. Mech. 42 (1975) 74, 44 (1977) 190.

5. Dvorak, G.J. and Laws, N., "Analysis of Matrix Cracking in Composite Laminates: Theory and Experiment," Advances in Aerospace Sciences and Engineering, ASME ASD-08 (1984) pp. 69-78.

6. Highsmith, A.L. and Reifsnider, D.L., "Stiffness Reduction Mechanisms in Composite Laminates," ASTM STP775 (1982) p. 103.

7. Highsmith, A.L. Private communication.

8. Laws, N. and Dvorak, G.J., "Progressive Transverse Cracking in Composite Laminates," J. Composite Materials, in press.

9. Hashin, Z., "Analysis of Cracked Laminates: A Variational Approach," Mechanics of Materials 4 (1985) 121.

10. Laws, N., "A Note on Penny-Shaped Cracks in Transversely Isotropic Materials," Mechanics of Materials 4 (1985) 209-212.

11. Laws, N. and Dvorak, G.J., "The Effect of fiber Breaks and Aligned Penny-Shaped Cracks on the Stiffness and Energy Release Rates in Unidirectional Composites," Int. J. Solids Structures 23 (1987) 1269-1283.

12. Mori, T. and Tanaka, K., "Average Stress in Matrix and Average Elastic Energy of Materials with Misfitting Inclusions," Acta. Metall. 21 (1973) 571-574.

13. Laws, N. and Brockenbrough, J.R., "The Effect of Microcrack Systems on the Loss of Stiffness of Brittle Solids," Int. J. Solids Structures 23 (1987) 1247-1268.

14. Laws, N. and Brockenbrough, J.R., "Microcracking in Polycrystalline Solids," J. Engineering Materials and Technology, in press.

15. Laws, N. and Brockenbrough, J.R., "The Effect of Microcracks on the Response of Brittle Solids," IUTAM Symposium on Yielding, Damage and Failure of Anisotropic Solids, (ed. J.P. Boehler) in press.

16. Dvorak, G.J. and Laws, N., "Analysis of Progressive Matrix Cracking in Composite Laminates II: First Ply Failure," J. Composite Materials 2 (1987) 309-329.

17. Dvorak, G.J. and Laws, N., "Analysis of First Ply Failure in Composite Laminates," Eng. Fracture Mechanics 25 (1986) 763-770.

18. Wang, J.B., Ph.D. Thesis (University of Pittsburgh) in preparation.

19. Wang, A.S.D., "Fracture Analysis of Matrix Cracking in Laminated Composites," Report No. NADC-85118-60, Drexel University, 1985.

20. Laws, N. and Dvorak, G.J., "Transverse Matrix Cracking in Composite Laminates," Composite Material Response (ed. G.C. Sih) Elsevier Applied Science, in press.

21. Wang, A.S.D. and Crossman, F.W., "Initiation and Growth of Transverse Cracks and Edge Delamination in Composite Laminates, Part I: An Energy Method," J. Composite Materials Suppl. 14 (1980) 71.

22. Crossman, F.W. Warren, W.J. Wang, A.S.D. and Law, G.E., Jr., "Initiation and Growth of Transverse Cracks and Edge Delamination in Composite Laminates, Part 2: Experimental Correlation," J. Composite Materials Suppl. 14 (1980 88.

23. Wang, A.S.D., Chou, P.C. and Lei, S.C., "A Stochastic Model for the Growth of Matrix Cracks in Composite Laminates," J. Composite Materials 18 (1984) 239.

24. Wang, A.S.D., "Fracture Mechanics of Sublaminate Cracks in Composite Materials," Composites Tech. Review 6 (1984) 45.

25. Laws, N., "Composite Materials: Theory vs. Experiment," J. Composite Materials, in press.

26. Dvorak, G.J., and Johnson, W.S. (1980) Fatigue of metal matrix composites. Intl. Jnl. Fracture, 16, 585.

27. Wung, C.J. (1987) Strain-space analysis of plasticity, fracture, and fatigue of fibrous composites. Ph.D. Dissertation, University of Utah, 202 pp.

28. Dvorak, G.J. and Wung, C.J., "Fatigue Damage Mechanics of Metal Matrix Composite Laminates," Strain Localization and Size Effect Due to Cracking and Damage, edited by J. Mazars and Z.P. Bazant, Elsevier Scientific Publishers, London, 1988.

29. Kaveh-Ahangar, A., Ph.D. Dissertation, Rensselaer Polytechnic Institute, Troy, New York, in preparation.

4. LIST OF PUBLICATIONS

1. Laws, N. and Dvorak, G.J., "The Loss of Stiffness of Cracked Laminates," Fundamentals of Deformation and Fracture (Eshelby Memorial Symposium ed. B.A. Bilby, K.J. Miller and J.R. Willis) pp. 119-127, Cambridge University Press 1984.

2. Dvorak, G.J., Laws, N. and Hejazi, M., "Analysis of Progressive Cracking in Composite Laminates, I, Thermoelastic Properties of a Ply with Cracks," J. Composite Materials 19 (1985) 216-234.

3. Dvorak, G.J. and Laws, N., "Analysis of Matrix Cracking in Composite Laminates: Theory and Experiment," Advance in Aerospace Sciences and Engineering, ASME AS-08 (1984) pp. 69-78.

4. Laws, N., "A Note on Penny-Shaped Cracks in Transversely Isotropic Materials," Mechanics of Materials 4 (1985) 209-212.

5. Dvorak, G.J. and Laws, N., "Mechanics of First Ply Failure in Composite Laminates," Fracture of Fibrous Composites - ASME AMD Vol. 74 (ed. C.T. Herakovich) 1985, pp. 59-69.

6. Dvorak, G.J. and Laws, N., "Analysis of First Ply Failure in Composite Laminates," Eng. Fracture Mechanics 25 (1986) 763-770.

7. Dvorak, G.J. and Laws, N., "Analysis of Progressive Matrix Cracking in Composite Laminates, II, First Ply Failure," J. Composite Materials 21 (1987) 309-329.

8. Laws, N. and Dvorak, G.J., "The Effect of Fiber Breaks and Aligned Penny-Shaped Cracks on the Stiffness and Energy Release Rates in Unidirectional Composites," Int. J. Solids Structures 23 (1987) 1269-1283.

9. Laws, N., "Composite Materials: Theory v. Experiment," J. Composite Materials, in press.

10. Laws, N. and Dvorak, G.J., "Progressive Transverse Cracking in Composite Laminates," J. Composite Materials, in press.

11. Laws, N. and Dvorak, G.J., "Transverse Matrix Cracking in Composite Laminates," Composite Material Response (ed. G.C. Sih) Elsevier Applied Science, in press.

12. Wung, C.J. (1987) Strain-space analysis of plasticity, fracture, and fatigue of fibrous composites. Ph.D. Dissertation, University of Utah, 202 pp.

13. Dvorak, G.J. and Wung, C.J., "Fatigue Damage Mechanics of Metal Matrix Composite Laminates," Strain Localization and Size Effect Due to Cracking and Damage, edited by J. Mazars and Z.P. Bazant, Elsevier Scientific Publishers, London, 1988.

14. Kaveh-Ahangar, A., Ph.D. Dissertation, Rensselaer Polytechnic Institute, Troy, New York, in preparation.

15. Martine, E.A., "Effect of Progressive Matrix Cracking on the Elastic Moduli of Fiberglass-Epoxy Crossply Laminates," M.S. Thesis, Rensselaer Polytechnic Institute, in preparation.

5. LIST OF PRESENTATIONS ON AFOSR-SPONSORED WORK

G.J. Dvorak (September 1, 1985 - September 1988)

Eleventh Annual Mechanics of Composites Review, Dayton, Ohio, October 22-24, 1985 (invited lecture).

Midwestern Mechanics Seminar:

University of Notre Dame, October 29, 1985.
Illinois Institute of Technology, October 30, 1985.
University of Illinois at Urbana-Champaign, October 31, 1985.
Purdue University, November 1, 1985.

Midwestern Mechanics Seminar:

University of Michigan, April 9, 1986.
University of Wisconsin, April 10, 1986.
University of Minnesota, April 11, 1986.
Michigan State, April 29, 1986.

Colloquium, Northwestern University, May 2, 1986. "Analysis of Fatigue Cracking of Fibrous Metal Matrix Laminates."

General Electric Company, Seminar, May 14, 1986.

ASME Winter Annual Meeting, invited lecturer, Anaheim, CA, December 7-12, 1986.

ONR Workshop on Composite Materials - Interface Science, Leesburg, Virginia, March 11, 1987.

Solid Mechanics Seminar, Brown University, April 5, 1987.

Lawrence Livermore Laboratories, Livermore, California, Mechanics Seminar, April 23, 1987.

Alcoa Laboratories Centennial Technical Seminar on Mechanics: Micro-mechanics to Product Design, Hilton Head, South Carolina, June 7, 1987.

Society of Engineering Science 24th Annual Meeting, Salt Lake City, Utah, 3 papers, September 20-23, 1987.

Air Force Mechanics of Composites Review, Ft. Lauderdale, Florida, October 16, 1987.

ASME Winter Annual Meeting, Boston, Massachusetts, 2 lectures, December 14-15, 1987.

Evandale Aircraft Plant Site Visit, Evansdale, Ohio, February 18, 1988.

G.J. Dvorak (CONTINUED)

Short Course on Metal Matrix Composites, Los Angeles, California, February 22-26, 1988.

Rensselaer Composites Center Overview '88, "Plasticity and Fracture of Composite Materials," March 2, 1988.

France-U.S. Research Workshop, Strain-Localization and Size Effect Due to Cracking and Damage, "Fatigue Damage Mechanics of Metal Matrix Composite Laminates," Cachan, France, September 1988.

N. Laws (Sept. 1, 1984 - Sept. 30, 1987)

CCM Decennial Meeting, University of Delaware, September 24-28, 1984.

Society of Engineering Science, VPI, Blacksburg, VA, October 15-17, 1984.

University of Illinois at Urbana-Champaign, April 25, 1985.

Society of Engineering Science, Pennsylvania State University, October 7-9, 1985.

Rensselaer Polytechnic Institute, February 20, 1986.

Texas A & M, March 13, 1986.

University of Houston, March 14, 1986.

University College, Cork, June 16, 1986.

University College, Dublin (Engineering Dept.), June 18, 1986.

University College, Dublin (Engineering Dept.), June 19, 1986.

University College, Dublin (Mathematical Physics), June 20, 1986

Yale University, October 29, 1986.

Virginia Polytechnic & State University, December 3, 1986.

Lehigh University, February 6, 1987.

Pennsylvania State University, April 8, 1987.

Composite Materials Workshop, Glasgow, Scotland, July 29-31, 1987.

Sawcuk Memorial IUTAM Symposium, Grenoble, France, August 24-28, 1987.

Society of Engineering Science, Univeristy of Utah, September 20-23, 1987.

6. LIST OF PROFESSIONAL PERSONNEL

Dr. G.J. Dvorak - Principal Investigator

Dr. N. Laws - Principal Investigator

Dr. C.J. Wung - Postdoctoral Research Associate (Ph.D. 1987)

Mr. J.B. Wang - Gr aduate Student

Mr. W. Li - Graduate Student

Mr. A. Kaveh-Ahangar - Graduate Student

Mr. E. Martine - Graduate Student (M.S. 1988)

	β = 0.1	β = 0.3	β = 0.5
	SCM / DHB	SCM / DHB	SCM / DMB
$(0_4, 90)s$	98 / 97	93 / 94	89 / 90
$(0_3, 90_2)s$	95 / 94	85 / 85	77 / 78
$(0_2, 90_3)s$	92 / 91	77 / 77	65 / 64
$(0, 90_4)s$	90 / 85	70 / 66	53 / 54

Table 1: The predicted remaining % of the initial stiffness at the indicated crack densities according to the Delameter, Herrmann, Barnett [9] analysis and the self-consistent model.

FIGURE CAPTIONS

Figure 1: Comparison of self-consistent model with experimental data [6] for $(0,90_3)_s$ E-glass epoxy laminates.

Figure 2: Longitudinal Young's modulus of various T300/5208 systems:
(a) bound _____ (b) self-consistent method -----
(c) differential scheme . . . . .

Figure 3: Longitudinal shear modulus of various T300/5208 systems:
(a) bound _____ (b) self-consistent method -----
(c) differential scheme . . . . .

Figure 4: Predictions and measurements of strength of various T300/934 graphite epoxy laminates.

Figure 5: Experimental and theoretical values for stiffness loss of $(0,90_3)_s$ E-glass epoxy laminate:
(i) Highsmith-Reifsnider predictions.....
(ii) Shear lag _____ (iii) Lower bound ------
Experimental data from reference [6].

Figure 6: Theory versus experiment for progressive cracking of AS-3501-06 laminates. Data from Wang [24].

Figure 7: Theory versus experiment for progressive cracking of T300/934 laminates. Data from Wang [24].

Figure 8: Motion of ply relaxation surfaces during first and second loading cycle, and expansion of the surfaces at different values of the damage parameter β.

Figure 9: Translated and expanded relaxation surfaces of a damaged laminate at two different levels of S_{max}.

Figure 10: The effect of sustained cyclic loading on reduction of axial elastic modulus of two B-Aℓ laminates. Comparison of prediction with experimental results obtained under constant load amplitudes.

Figure 11: Fiber stresses in zero-degree plies after damage-induced shakedown.

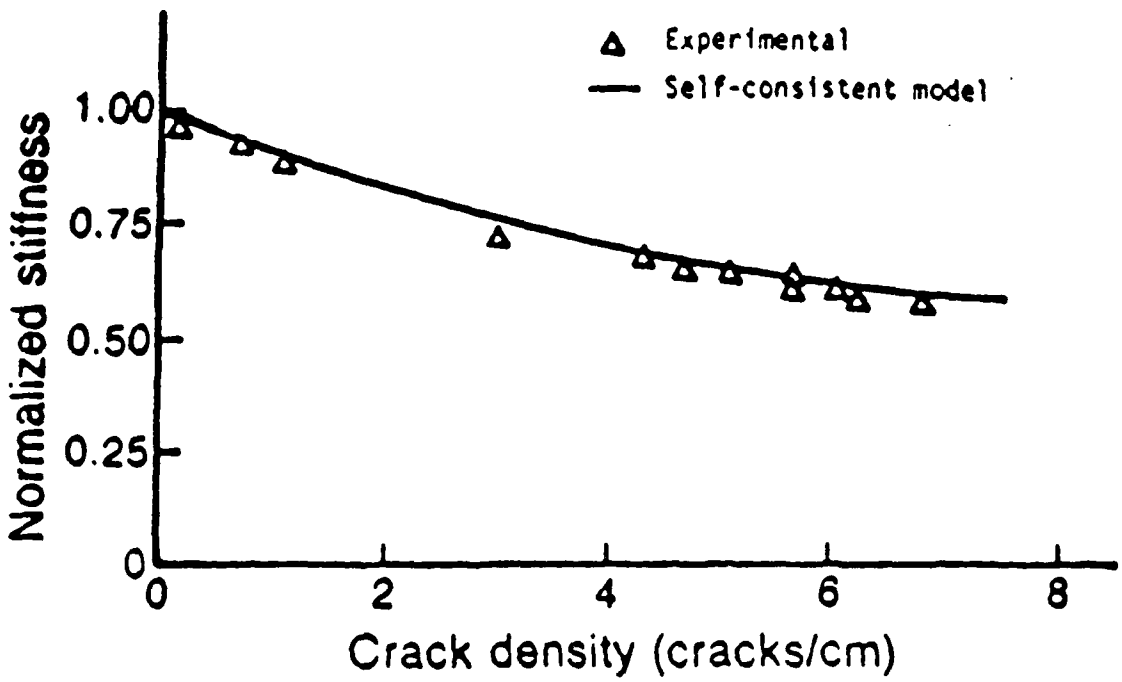

Figure 1: Comparison of self-consistent model with experimental data [6] for $(0,90_3)_s$ E-glass epoxy laminates.

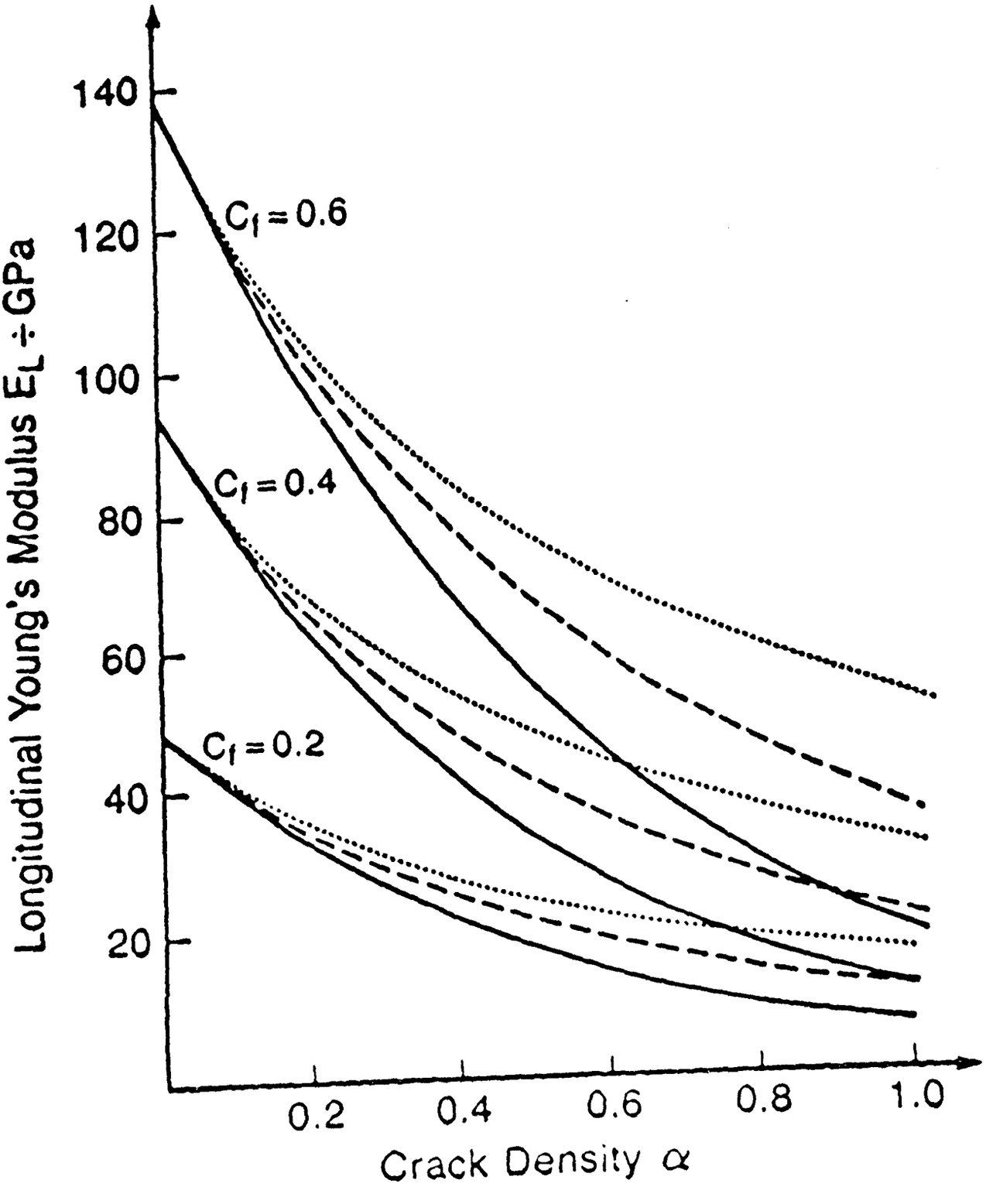

Figure 2: Longitudinal Young's modulus of various T300/5208 systems:
(a) bound _____ (b) self-consistent method -----
(c) differential scheme . . . . .

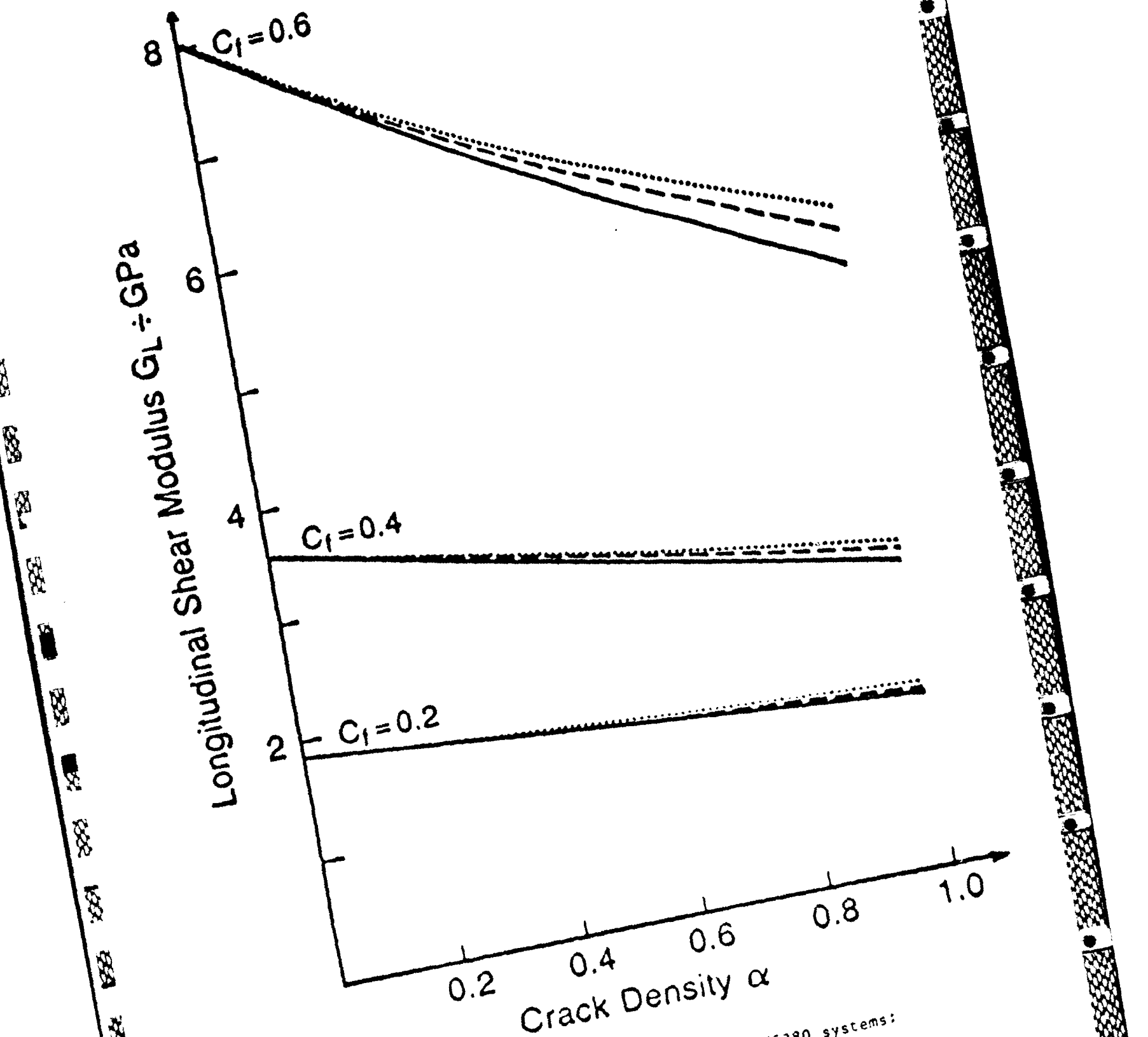

Figure 3: Longitudinal shear modulus of various T300/5280 systems:
(a) bound ——— (b) self-consistent method - - - -
(c) differential scheme . . . . .

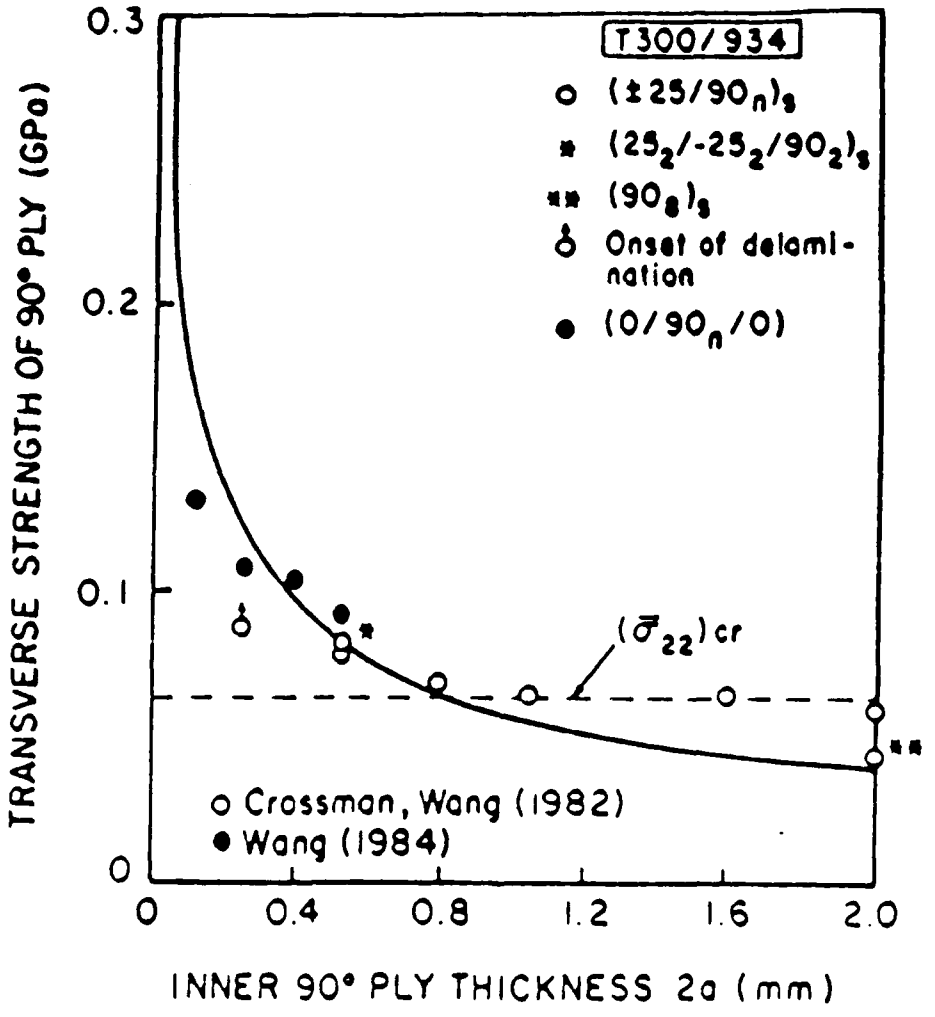

Figure 4: Predictions and measurements of strength of various T300/934 graphite epoxy laminates.

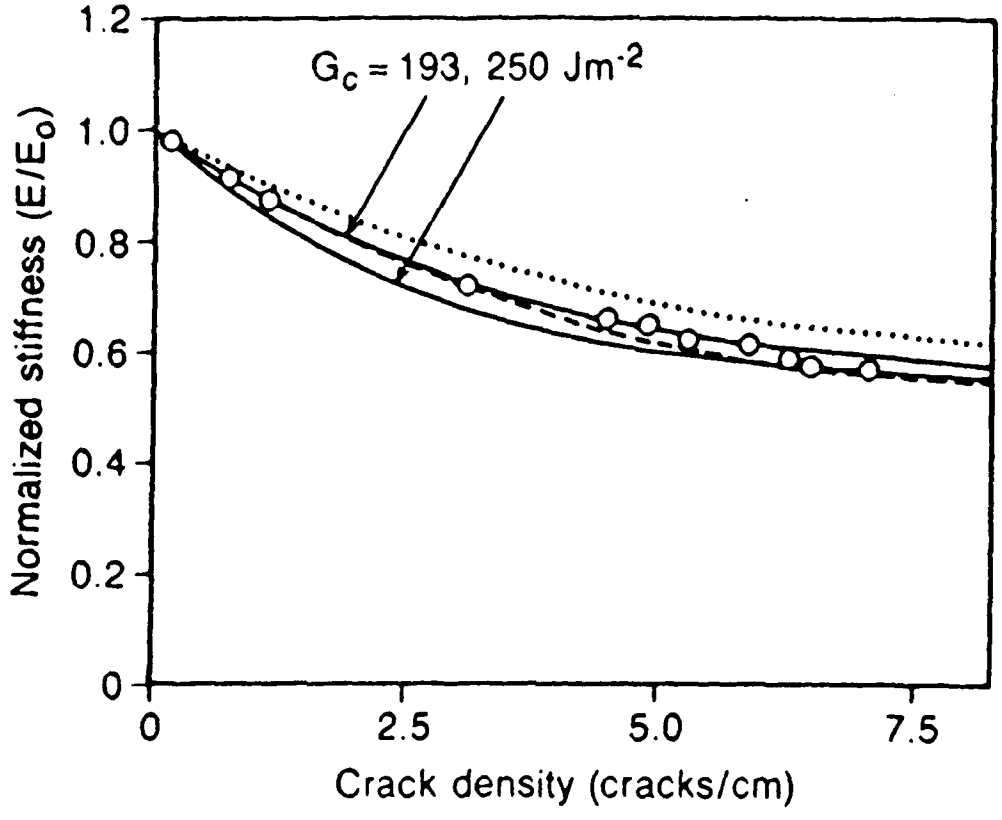

Figure 5: Experimental and theoretical values for stiffness loss of $(0,90_3)_s$ E-glass epoxy laminate:
(i) Highsmith-Reifsnider predictions .....
(ii) Shear lag _____ (iii) Lower bound -------
Experimental data from reference [6].

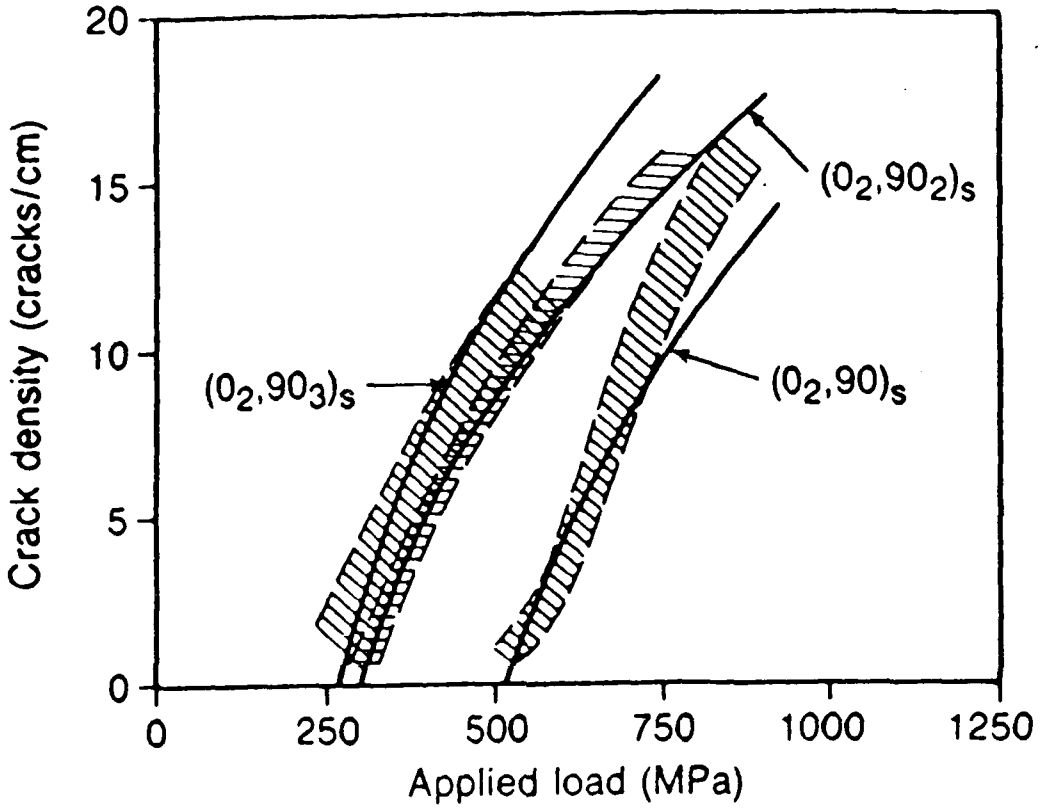

Figure 6: Theory versus experiment for progressive cracking of AS-3501-06 laminates. Data from Wang [25].

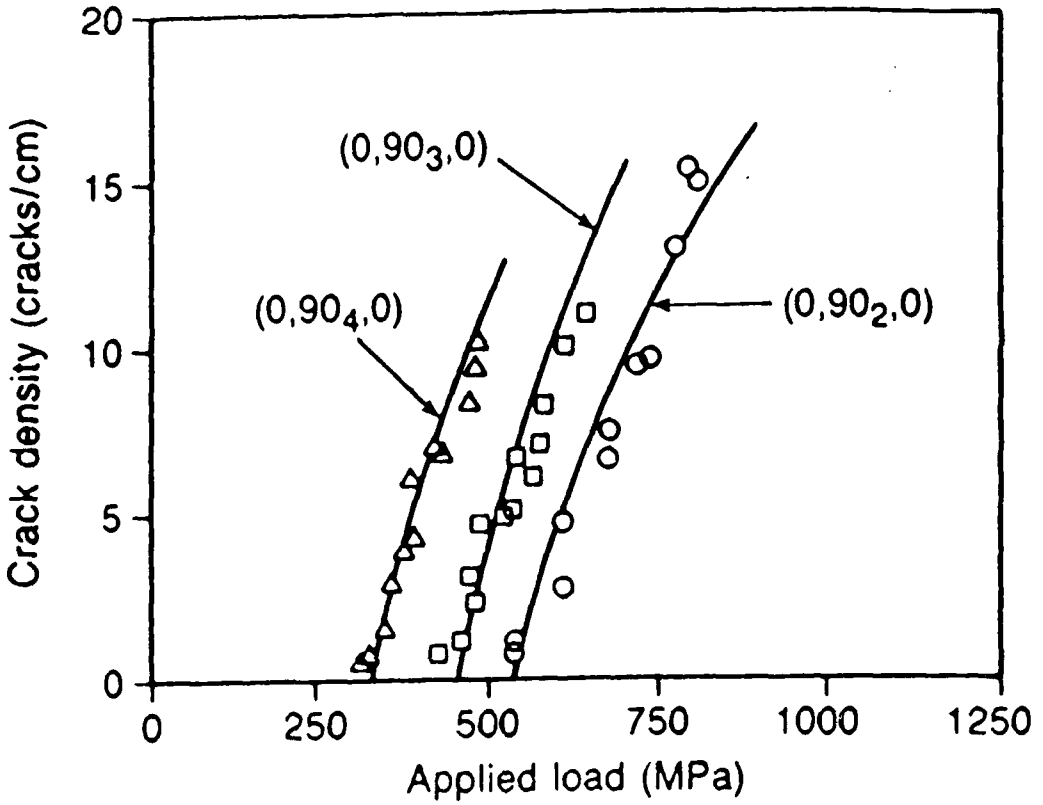

Figure 7: Theory versus experiment for progressive cracking of T300/934 laminates. Data from Wang [25].

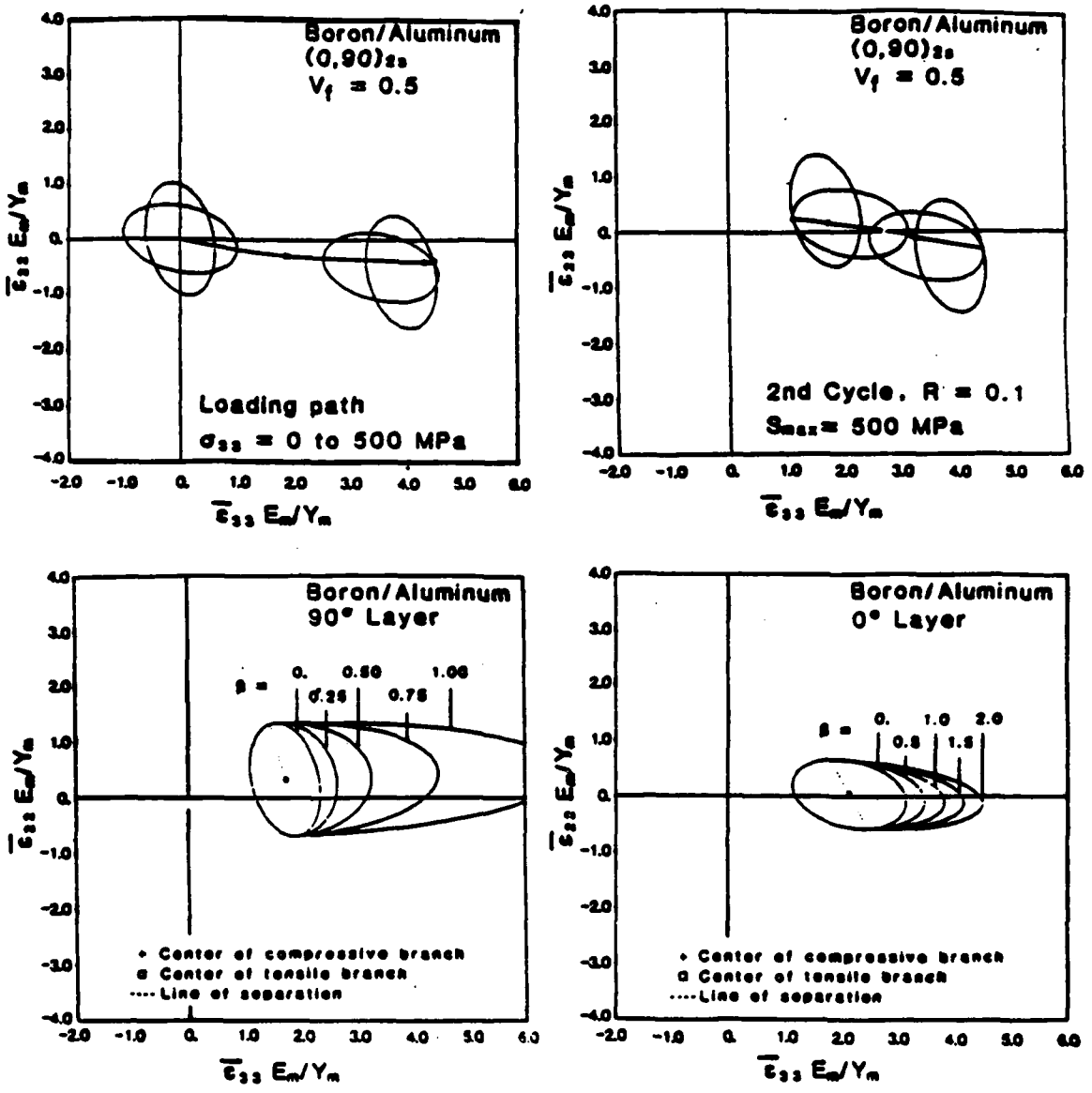

Figure 8: Motion of ply relaxation surfaces during first and second loading cycle, and expansion of the surfaces at different values of the damage parameter β.

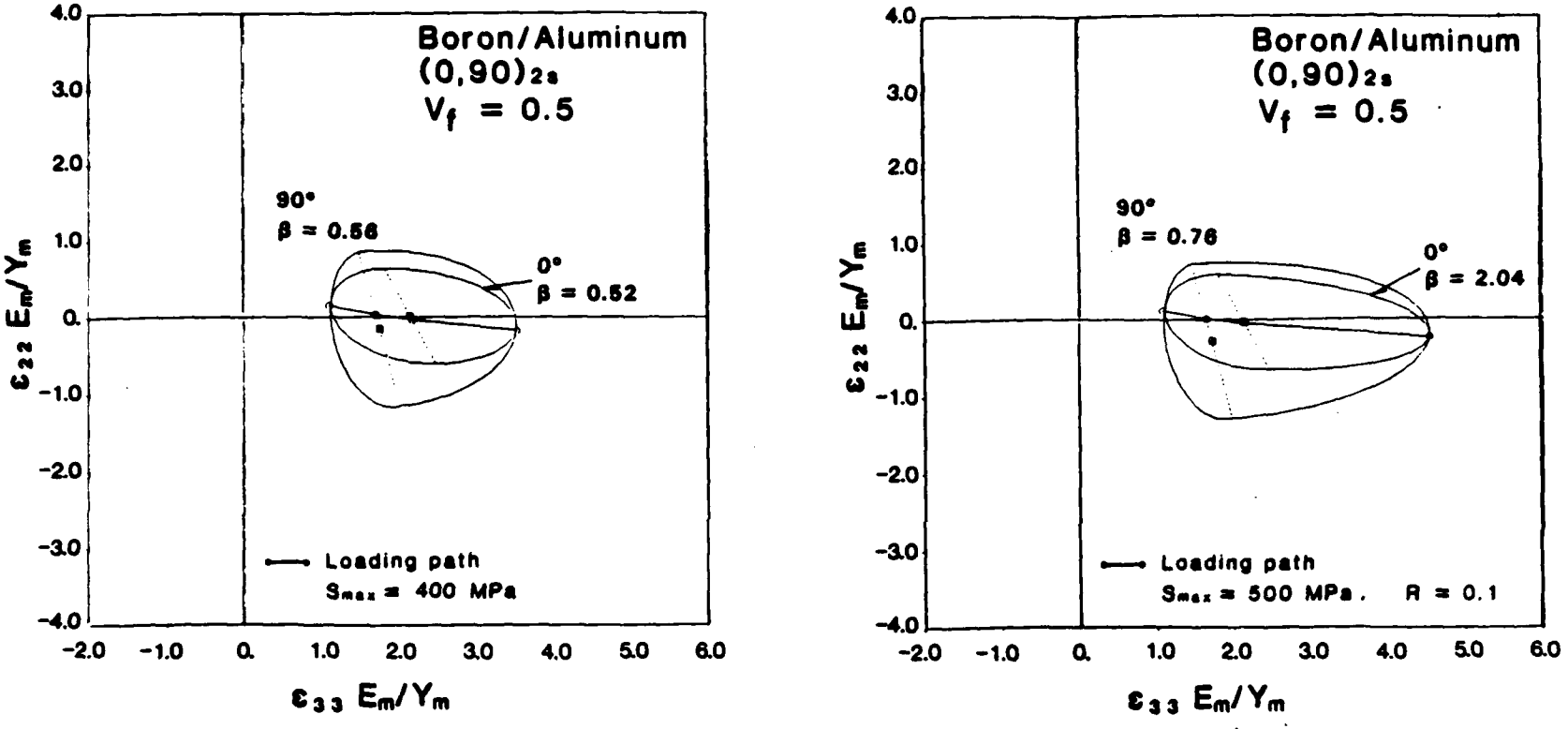

Figure 9: Translated and expanded relaxation surfaces of a damaged laminate at two different levels of S_{max}.

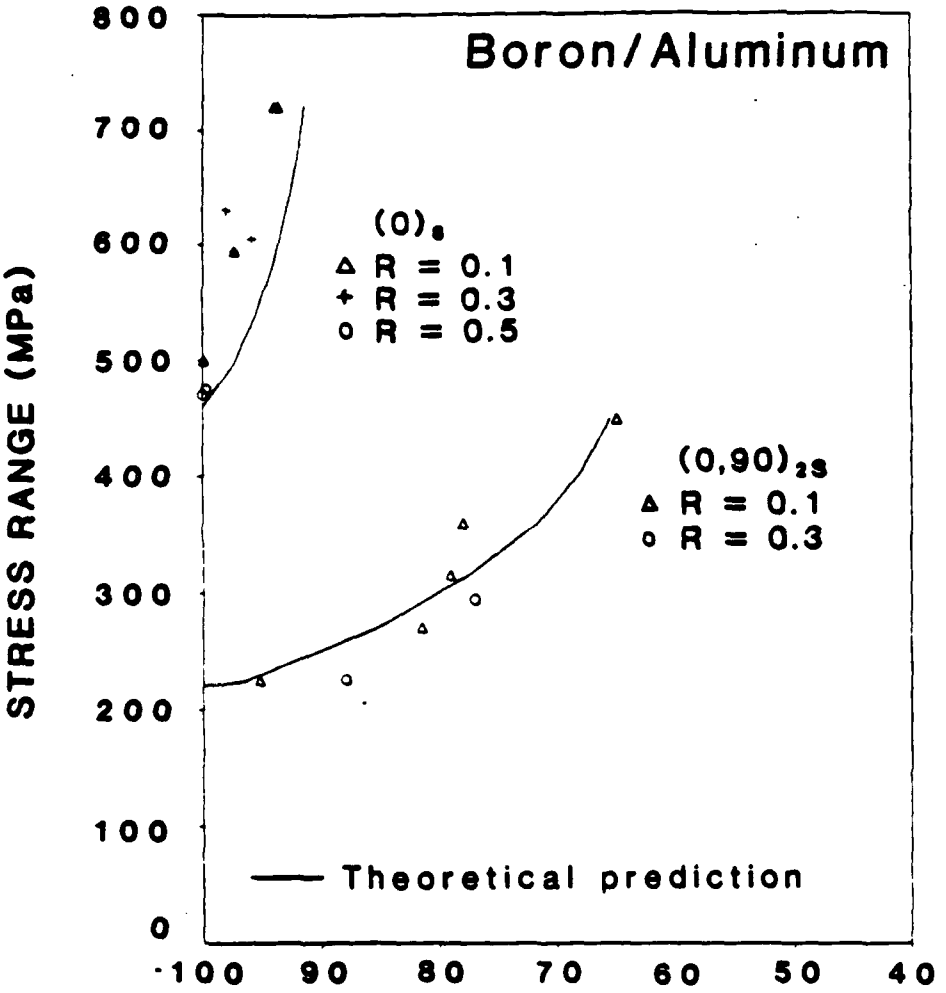

Figure 10: The effect of sustained cyclic loading on reduction of axial elastic modulus of two B-Aℓ laminates. Comparison of prediction with experimental results obtained under constant load amplitudes.

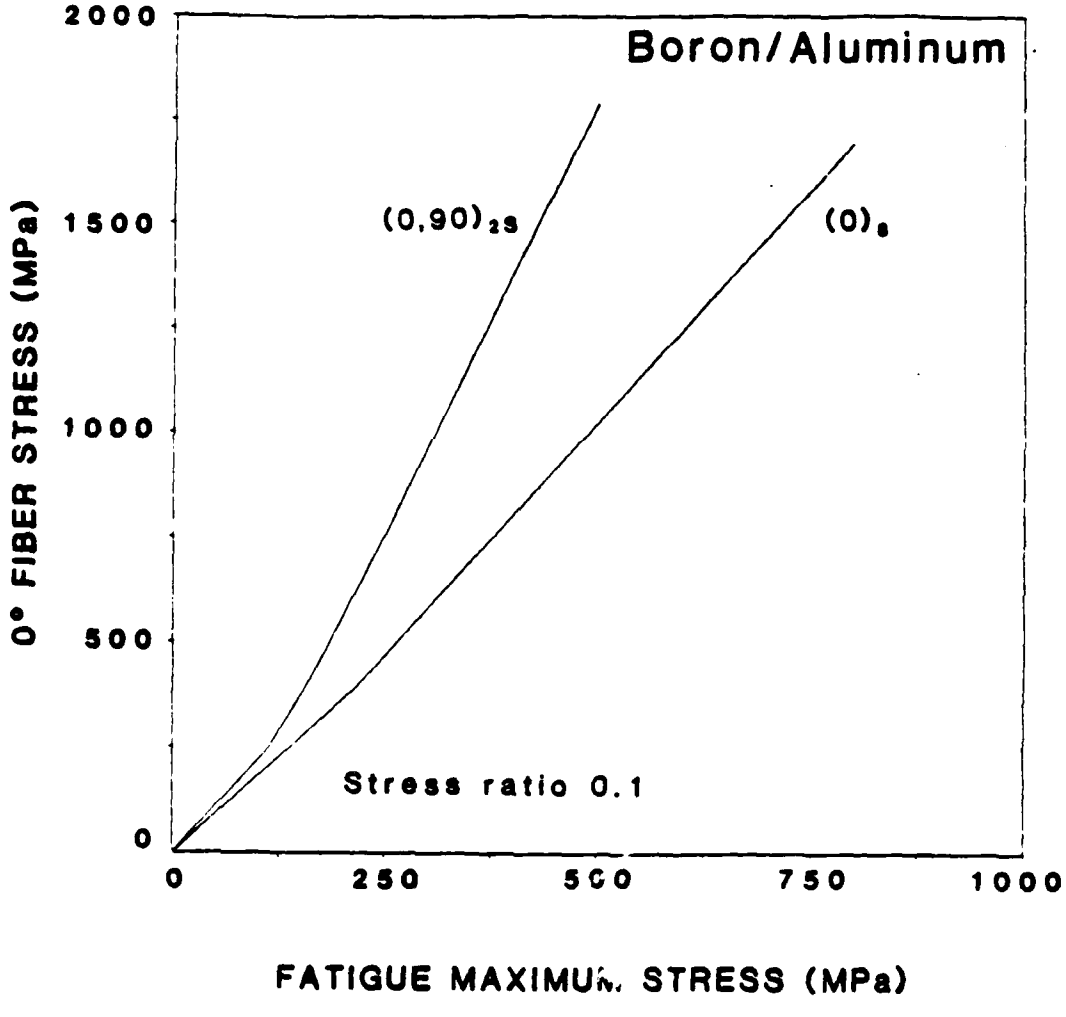

Figure 11: Fiber stresses in zero-degree plies after damage-induced shakedown.

7. COPIES OF SELECTED PAPERS

Analysis of Progressive Matrix Cracking in Composite Laminates
I. Thermoelastic Properties of a Ply with Cracks

Analysis of Progressive Matrix Cracking in Composite Laminates
II. First Ply Failure

Analysis of Matrix Cracking in Composite Laminates: Theory and Experiment

Analysis of First Ply Failure in Composite Laminates

The Effect of Fiber Breaks and Aligned Penny-Shaped Cracks on the Stiffness and Energy Release Rates in Unidirectional Composites

Fatigue Damage Mechanics of Metal Matrix Composite Laminates

Analysis of Progressive Matrix Cracking in Composite Laminates I. Thermoelastic Properties of a Ply with Cracks

GEORGE J. DVORAK
Department of Civil Engineering
Rensselaer Polytechnic Institute
Troy, NY 12180

NORMAN LAWS
Department of Mechanical Engineering
University of Pittsburgh
Pittsburgh, PA 15260

MEHDI HEJAZI
Department of Civil Engineering
University of Utah
Salt Lake City, UT 84112

(Received June 26, 1984)
(Revised September 20, 1984)

ABSTRACT

Overall stiffnesses and compliances, thermal expansion coefficients, and stress and strain averages are evaluated for a fibrous composite lamina which contains a given density of open transverse cracks and is subjected to uniform mechanical loads and thermal changes. The evaluation procedure is based on the self-consistent method and is similar, in principle, to that used in finding elastic constants of unidirectional composites.

1. INTRODUCTION

IN MANY FIBROUS COMPOSITE SYSTEMS THE FAILURE STRAIN OF THE FIBER far exceeds that of the matrix. Under load, the difference is usually accommodated by matrix cracking. This is frequently observed in monotonically or cyclically loaded laminated plates, where each layer may contain a system of aligned slit cracks which grow in the direction of the fibers and across the thickness of the ply. Such cracks are often called ply cracks or transverse cracks, although it is more appropriate to reserve the latter for cracks which

Reprinted from *Journal of* COMPOSITE MATERIALS, *Vol. 19—May 1985*

are perpendicular to the fiber axis, and refer to cracks which grow parallel to the fiber direction as axial cracks.

In polymer matrix composites axial matrix cracking typically starts at low strain levels in the weakest off-axis ply [1-3]. As loading continues, cracks appear in other off-axis plies; also, their density increases until it reaches a certain saturation level. For example, in statically loaded (0/90), graphite-epoxy laminates the minimum crack spacing was observed to be equal to 3.5–4.0 ply thicknesses [4]. In metal matrix composites, matrix cracking appears to be caused only by cyclic loads which exceed the shakedown limit of the laminate [5]. Under such circumstances the matrix experiences cyclic plastic straining and, consequently, low-cycle fatigue failure. Both axial and transverse cracking is present, the former in off-axis plies, the latter in zero degree plies. The crack patterns and densities are generally similar to those found in polymer matrix systems. However, saturation density increases with load amplitude, and it is not unusual to find cracks as close as one ply thickness.

In a typical part of a laminated composite structures, removed from concentrated loads and free edges, matrix cracking is the initial, low-stress damage mode under applied load. It is eventually followed by other types of damage, such as cracking between layers and fiber breaks; but these appear at relatively high loads which may exceed allowable design magnitudes. In contrast, matrix cracks grow at low loads, and they can significantly impair stiffness and strength of composite structures, especially those containing many off-axis plies. For example, fatigue tests on both polymer and metal matrix laminated plates indicate that stiffness and residual static strength reductions caused by cracking in plies may be as high as 10–50% after 2×10^4 cycles of loading [5,6]. It is therefore desirable to consider the effect of matrix cracking on composite properties in design.

Sufficiently general theoretical models of progressive cracking in composite laminates are apparently not to be found in the literature. Such results as are available for angle-ply laminates have been obtained from finite element calculations [4,7], while other studies have focused on $(0/90_n)_s$ laminates [2,3].

The purpose of this group of papers is to introduce a modelling procedure for axial cracking which can be applied to any laminate geometry under general loading conditions.

The first step in the analysis, undertaken in this paper, is an evaluation of overall thermoelastic properties of a fibrous composite which contains a certain density of aligned slit cracks, Figure 1a. In subsequent papers we introduce appropriate fracture criteria for a unidirectional ply, and develop a technique for evaluation of instantaneous crack densities and stiffnesses of a single ply which is strained in a prescribed way. Finally, these results will be incorporated into an analysis of laminated plates which are loaded by in-plane stresses and contain many cracking layers of different orientation. Although the subsequent parts utilize the results obtained herein, the procedures developed there do not depend on the particular method used to evaluate the effect of cracks on thermoelastic properties of a lamina.

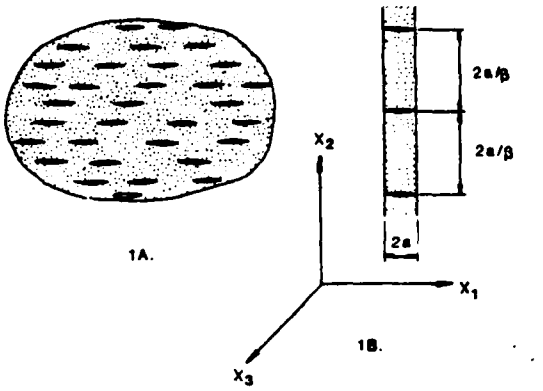

Figure 1. (A) an infinite fibrous medium with aligned slit cracks; (B) a fiber lamina with parallel slit cracks.

In this paper we are concerned with evaluation of overall compliance, thermal expansion coefficients (or thermal strain and stress vectors), and strain and stress averages in the phases of a fibrous lamina which contains aligned slit cracks, and is subjected to uniform mechanical loads and thermal changes. The approach to the problem was outlined in our recent study [8], where we suggested that the effect of matrix crack systems on properties of fibrous composites could be analyzed, in principle, by the techniques which are commonly used to evaluate the elastic constants of composite materials and fibrous laminates, e.g., by the self-consistent method.

The essential approximation in the evaluation of stiffness and compliance changes of laminates consists in the replacement of a cracked layer, Figure 1b, by an effective medium which contains many cracks, Figure 1a. The crack densities can be exactly matched to provide identical stiffnesses. However, the cracks in the layer are not entirely surrounded by the layer material, instead they interact with neighboring layers which have different elastic properties. This interaction is limited to the vicinity of the crack tip [9], thus it may be important in analysis of local crack growth at the interface, but it has only a minor effect on lamina stiffness. We note that a similar approximation is commonly accepted in evaluation of elastic moduli analysis of laminated composite structures reinforced by monolayers of large diameter fibers.

2. CRACK DENSITY

It was emphasized in our earlier work [8] that interest in cracked infinite unidirectional composites is largely determined by the desire to study composite laminates. Certainly in papers of this series we assume that the properties of a cracked ply are adequately predicted by the infinite model. It is, therefore, expedient to interpret the analysis in this paper with particular

reference to cracked laminates. Thus the terms cracked ply and cracked infinite unidirectional composite are here synonymous.

Consider a unidirectional fibrous medium with aligned slit cracks of length 2a, Figure 1a. By way of contrast, there are several ways of viewing the composite on the microscale. In the first place one could distinguish between the three coexistent phases: fiber, matrix, and cracks. On the other hand, one might consider the uncracked fibrous composite as an effective homogeneous solid into which cracks have been introduced. In [8] we referred to the two possibilities as the three phase model and two phase model, respectively. The distinction reflects the fact that in certain laminated composite systems the crack length and fiber diameter are of similar magnitude, while in other systems the fiber diameter is much smaller than the crack length. A significant conclusion which may be drawn from [8] is that for many purposes the predictions of the two models are indistinguishable. In the present paper we concentrate on the simpler two phase model.

In analysis of cracked materials, it is well known that cracks can be modeled either as limiting ellipsoids or as slits—the final results are equivalent. It was convenient in our earlier work [8] to regard cracks as limiting ellipsoids and we adopt the same approach here. On the other hand we note that in a study of crack geometries different from ours, Gottesman, Hashin and Brull [10] use slits a priori. Thus we can consider the cracks in Figure 1 to be elliptic cylindrical cavities. Let a, b respectively denote the major and minor semi-axes of a cavity, and let η be the number of cavities per unit area of the x_1x_2-plane. Then the volume fraction of cavities is $1/4\ \pi\beta\delta$ where $\delta = b/a$ is the aspect ratio and $\beta = 4\eta a^2$ is the crack density parameter. For simplicity, suppose that the cracks have length 2a, then β is the average number of cracks in a square of side 2a. Alternatively, when the cracks are located in a ply, Figure 1b, β measures the average distance between cracks. Clearly, if the cracks are equally spaced in a ply, the distance between successive cracks is $2a/\beta$. Thus when $\beta = 1$ the distance between cracks is equal to 2a. As β *decreases* the distance between cracks *increases* and when $\beta = 0$ there are no cracks. We note that in some experiments [4] the observed minimum separation of cracks (in a saturation state) in Gr-Ep laminates was 3.5 to 4.0 ply thicknesses. The corresponding values of β are 0.28 and 0.25 respectively. These values may be contrasted with B-Al composites where values as high as $\beta = 1$ have been observed [5]. Therefore we present all results for $0 \leqslant \beta \leqslant 1$.

As cracks are generally initiated at preexisting flaws which are randomly distributed in the ply, the crack distribution at any given moment is not regular. However, we assume that it is statistically homogeneous, and that β is a measure of average crack density in the in-plane area of the ply. Also, since cracks sometimes tend to propagate rapidly across the entire loaded width of a ply, the crack density does not change continuously but may increase in discrete steps. These steps can be measured in terms of a change $\Delta\beta$ caused by a single crack in a unit plane area of a ply.

To illustrate the relationship between the crack density β, and the number

Table 1. Cracks in a 1/8 mm thick ply (2a = 0.0125 cm).

Crack density β	0.1	0.25	0.5	0.75	1.0
Crack spacing, $2a/\beta$ mm	1.25	0.50	0.25	0.17	0.125
Number of cracks/Unit square plane area of ply					
No. cracks/cm^2	8	20	40	60	80
No. cracks/in^2	20	50	100	150	203
No. cracks/ft^2	244	610	1220	1830	2438

of cracks in a plane area, we focus for a moment at the x_2x_3-plane in Figure 1b. The trace of each crack in this plane is a straight line parallel to x_3. Table 1 presents some typical numbers calculated for a 1/8 mm thick ply. It shows the distance between cracks $2a/\beta$, and the number of cracks in a unit area (x_2x_3-plane in Figure 1b) of the ply, at specified magnitudes of β. Note that even at low β values, and in small areas, the crack counts are relatively large.

These results also indicate the magnitude of an increment $\Delta\beta$ caused by a single crack in a unit area of the ply, which does not depend on β. For example, even in a small area of 1 cm^2 a single crack changes β by 0.0125. This increment is relatively small, so that β may be regarded as continuous in most applications. A notable exception occurs at stress concentrations where stresses may change significantly within a small area, e.g., 1 mm^2. A single crack will cause $\Delta\beta = 0.125$/crack in a 1 mm^2 area, hence β may not be regarded as continuously changing. Moreover, the crack count becomes small ($\sim$1 crack/mm at $\beta = 0.1$), so that the concept of average crack density may no longer be applied. It follows that the averaging approach is admissible in evaluation of stiffness changes caused by cracks in large in-plane areas of a ply or laminate, but that it may not be suitable for analysis of local properties at small geometrical imperfections such as notches or free edges.

It is also appropriate to discuss the definition of crack density in exterior or surface plies of a laminate. As in Figure 1b, such cracks are open at the surface, hence their effective length is not equal to the ply thickness. However, the surface layer may be regarded as half of a layer of thickness 4a, Figure 2, so that open surface cracks may be approximated by interior cracks of length 4a. The effective crack density, β^e, in exterior layers is easily obtained in terms of the crack density, β, defined for interior layers. In fact, from Figure 2

$$2a/\beta = 4a/\beta^e,$$

hence

$$\beta^e = 2\beta.$$

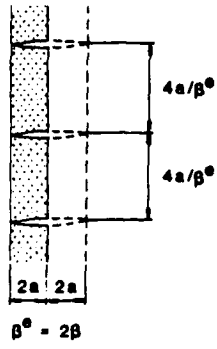

Figure 2. *Evaluation of crack density parameter β^* in exterior layers of a laminate.*

3. EVALUATION OF OVERALL COMPLIANCE

On the macroscale, the cracked unidirectional composite of Figure 1 can be regarded as an orthotropic homogeneous solid. The elastic properties of the "matrix" are identical with those of the fibrous composite and can be easily evaluated. When cracks are introduced, the macroscopic or overall elastic moduli of the solid change. To make the concept of overall moduli meaningful, it is necessary to consider overall uniform loading. Thus, we introduce uniform overall average stresses $\bar{\underline{\sigma}}$ and strains $\bar{\underline{\varepsilon}}$, with components arranged in (6 × 1) column vectors and related by constitutive equations*

$$\bar{\underline{\sigma}} = L\,\bar{\underline{\varepsilon}}, \quad \bar{\underline{\varepsilon}} = M\,\bar{\underline{\sigma}}, \tag{1}$$

where L, and M are the overall stiffness, and compliance (6 × 6) matrices of the cracked composite, respectively. $M = L^{-1}$ when the inverse exists.

Since we are here concerned only with a 2-phase model (in which the uncracked composite is the matrix) it is convenient to adopt a minor variant of the notation of our earlier work [8]; we use the suffix o to denote the properties of the uncracked composite. For example, L_o is the stiffness of the uncracked composite.

According to the derivation given in [8], the self-consistent estimates for the overall stiffness and compliance matrices are given by

$$\begin{aligned} L &= L_o - \bar{\beta}\,L_o\,\Lambda L \\ M &= M_o + \bar{\beta}\,\Lambda, \end{aligned} \tag{2}$$

where

*As in [8], (6 × 6) matrices are denoted by capital Latin or Greek letters, e.g., L, M, Λ, A, B, and (6 × 1) matrices by lower case letters underlined by a tilda, e.g., $\underline{\sigma}$, $\underline{\varepsilon}$, $\underline{m}$, $\underline{l}$.

$$\bar{\beta} = \frac{l}{4}\pi\beta. \tag{3}$$

The matrix Λ has only three nonzero components, which are expressed in terms of compliances M_{ij} of the effective medium as:

$$\Lambda_{22} = \frac{M_{22}M_{33} - M_{23}^2}{M_{33}}(\alpha_1^{1/2} + \alpha_2^{1/2}) \tag{4}$$

$$\Lambda_{44} = (M_{44}\, M_{55})^{1/2} \tag{5}$$

$$\Lambda_{66} = \frac{(M_{22}M_{33} - M_{23}^2)^{1/2}(M_{11}M_{33} - M_{13}^2)^{1/2}}{M_{33}}(\alpha_1^{1/2} + \alpha_2^{1/2}) \tag{6}$$

where α_1 and α_2 are the roots of

$$(M_{22}M_{33} - M_{23}^2)\alpha^2 - \{M_{33}M_{66} + 2(M_{12}M_{33} - M_{13}M_{23})\}\alpha + M_{11}M_{33} - M_{13}^2 = 0. \tag{7}$$

These results imply that only three compliance coefficients M_{22}, M_{44}, and M_{66} are affected by the introduction of cracks, the remaining six terms in M are unchanged, i.e., they remain equal to those of the uncracked fiber composite. In particular

$$M_{11} = M_{11}^0\,, \quad M_{12} = M_{12}^0\,, \quad M_{13} = M_{13}^0\,,$$

$$M_{23} = M_{23}^0\,, \quad M_{33} = M_{33}^0\,, \quad M_{55} = M_{55}^0\,,$$

$$M_{22} = M_{22}^0 + \bar{\beta}(M_{22}M_{33} - M_{23}^2)(\alpha_1^{1/2} + \alpha_2^{1/2})/M_{33}\,, \tag{8}$$

$$M_{44} = M_{44}^0 + \bar{\beta}(M_{44}M_{55})^{1/2}\,, \tag{9}$$

$$M_{66} = M_{66}^0 + \bar{\beta}(M_{22}M_{33} - M_{23}^2)^{1/2}(M_{11}M_{33} - M_{13}^2)^{1/2}(\alpha_1^{1/2} + \alpha_2^{1/2})/M_{33}, \tag{10}$$

and from (7):

$$\alpha_1\alpha_2 = (M_{11}M_{33} - M_{13}^2)/(M_{22}M_{33} - M_{23}^2)$$

$$\alpha_1 + \alpha_2 = [M_{33}M_{66} + 2(M_{12}M_{33} - M_{13}M_{23})]/[M_{22}M_{33} - M_{23}^2].$$

The unknown shear compliance M_{44} can be obtained directly from (9):

$$M_{44} = M_{44}^0 + \frac{\bar{\beta}}{2}[\bar{\beta}\, M_{55} + (\bar{\beta}^2\, M_{55}^2 + 4M_{44}^0\, M_{55})^{1/2}] \tag{11}$$

The remaining unknowns M_{22} and M_{66} are found from (8) and (10). The solu-

tion of these equations is perhaps best explained with the help of additional notation. Thus let

$$x = M_{22}M_{33} - M_{23}^2 \ , \ x_o = M_{22}^o M_{33} - M_{23}^2 \tag{12}$$

$$y = M_{66}M_{33} \qquad , \ y_o = M_{66}^o M_{33} \tag{13}$$

$$p = M_{11}M_{33} - M_{13}^2 \ , \ q = 2(M_{12}M_{33} - M_{13}M_{23}) \tag{14}$$

Now, it is easy to show that

$$y = y_o + (p/x)^{1/2}(x - x_o)$$

and that x is the solution of

$$F(x) \equiv x - x_o - \bar{\beta}[3p^{1/2}\, x^{3/2} + (y_o + q)\, x - p^{1/2}\, x_o\, x^{1/2}]^{1/2} = 0. \tag{15}$$

At this stage it is not clear that the self-consistent estimate for x is unique. This apparent deficiency is easily remedied by noting that the square bracketed terms in (15) is always positive. Thus $x \geqslant x_o$. Next one could for example rewrite (15) as a quartic in $x^{1/2}$ and use the Descartes' rule of signs to show that Equation (15) has one and only one root $x \geqslant x_o$.

Results obtained for several composite systems indicate that an approximate value of the positive root $x = x_1$ can be found as:

$$x_1 \doteq x_o - \frac{F(x_o)}{F'(x_o)} \tag{16}$$

This is illustrated in Figure 3, where $F(x)$ plotted against x is almost a straight line between x_o and x_1.

Once x_1 has been found, M_{22} and M_{66} are obtained from (12) and (13), respectively.

The preceding argument may suggest that it is better to solve equation (2_1) for the compliance matrix then equation (2_1) for the stiffness matrix. This is not the case. The analysis was presented in terms of the compliance to furnish a simple proof of the uniqueness of the self-consistent solution. From a computational standpoint, it is just as easy to solve (2_1) for the stiffness as it is to solve (2_2) for compliance. Once either is known the other is found by inversion.

If the M_{ij} are known, then one can find the three nonzero components of Λ_{ij} in (6) from (4). The overall stiffness L can then be written in terms of Λ_{ij}; the expressions appear in (A-6) in Appendix.

We emphasize that the results obtained above are valid only for the case of open cracks (c.f., (32) below). If cracks are closed, the overall response may be approximated by that of the uncracked composite.

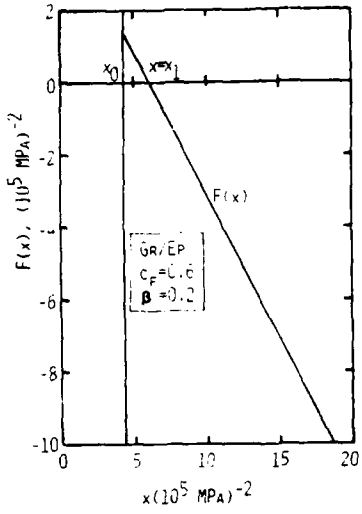

Figure 3. Solution of Equation (15).

4. RESPONSE TO THERMAL CHANGE

Let θ denote a uniform temperature change from a reference temperature θ_o, applied to the composite. The constitutive Equations (1) must be replaced by

$$\bar{\underline{\sigma}} = L\,\bar{\underline{\varepsilon}} - \theta\underline{\ell} \qquad \bar{\underline{\varepsilon}} = M\,\bar{\underline{\sigma}} + \theta\underline{m}\,, \tag{17}$$

where $\underline{m}$ is the thermal expansion vector and $\underline{\ell}$ the thermal stress vector [11]. From (17) one obtains

$$\underline{\ell} = L\,\underline{m}\,. \tag{18}$$

It is probably obvious that the presence of cracks does not affect free thermal expansion of the composite. Thus

$$\underline{m} = \underline{m}_o\,, \tag{19}$$

and from (2) and (18):

$$\underline{\ell} = (I - \bar{\beta}L\Lambda)\underline{\ell}_o \tag{20}$$

Explicit forms of $\underline{m}$ and $\underline{\ell}$ are:

$$\underset{\sim}{m} = \begin{bmatrix} \alpha_T \\ \alpha_T \\ \alpha_A \\ 0 \\ 0 \\ 0 \end{bmatrix}; \quad \underset{\sim}{l} = \begin{bmatrix} (L_{11} + L_{12})\alpha_T + L_{13}\,\alpha_A \\ (L_{12} + L_{22})\alpha_T + L_{23}\,\alpha_A \\ (L_{13} + L_{23})\alpha_T + L_{33}\,\alpha_A \\ 0 \\ 0 \\ 0 \end{bmatrix}, \tag{21}$$

where α_T and α_A are linear thermal expansion coefficients of the uncracked composite in the transverse and axial directions, respectively. Since the coefficients of L_{ij} change with β, $\underset{\sim}{l}$ is also a function of β, while $\underset{\sim}{m}$ remains constant.

Again, the derived expressions are valid only if the cracks are open. Closed cracks do not affect thermal response of the composite.

5. LOCAL STRAIN AND STRESS AVERAGES

Certain applications of the above results require information about local stress and strain fields in the phases. Estimates of local fields are also needed to distinguish between loading conditions which lead to either open or closed cracks and thus delineate limits of validity of the theory.

It is clear that when a fiber reinforced composite containing cavities is subjected to general uniform mechanical loading, part of the applied strain (i.e., the average strain) is accommodated by cavity expansion. Whereas the strain of a typical cavity wall becomes unbounded in the limit of vanishing aspect ratio, the important quantity in the macroscopic study of composites is the wall strain multiplied by the area of the cross-section (or aspect ratio) which tends to a finite limit. Following Laws [12], let $\underset{\sim}{\varepsilon}^w$ be the strain of a typical cavity wall, and set

$$\underset{\sim}{\phi} = \lim_{\delta \to 0} \delta\, \underset{\sim}{\varepsilon}^w . \tag{22}$$

Then it is easy to show that (c.f., [12])

$$\underset{\sim}{\phi} = \Lambda\, \underset{\sim}{\bar{\sigma}} . \tag{23}$$

Furthermore, from the formulae given in [8], and in Section 4 above, it is not difficult to show that in the limit of slit cracks ($\delta \to 0$), the overall strain, $\underset{\sim}{\bar{\varepsilon}}$ is given by

$$\underset{\sim}{\bar{\varepsilon}} = \underset{\sim}{\bar{\varepsilon}}_0 + \underset{\sim}{\bar{\varepsilon}}_c , \tag{24}$$

where $\underset{\sim}{\bar{\varepsilon}}_0$ is the average strain in the composite "matrix":

$$\underline{\bar{\varepsilon}}_o = (I - \bar{\beta} \wedge L)\underline{\bar{\varepsilon}} + \beta \wedge L \, \underline{m} \, \theta \, . \tag{25}$$

In addition, $\underline{\bar{\varepsilon}}_c$ is the *crack accommodation strain*

$$\underline{\bar{\varepsilon}}_c = \bar{\beta} \wedge L(\underline{\bar{\varepsilon}} - \underline{m}\theta) \, ; \tag{26}$$

it represents that part of the applied (average) strain which is accommodated by cracks.

In practice Equations (25) and (26) provide us with estimates of the local stress and strain fields within the composite.

Viewed from another standpoint, Equations (25) and (26) immediately furnish the strain concentration factors. As far as the composite "matrix" is concerned,

$$\underline{\bar{\varepsilon}}_o = A \, \underline{\bar{\varepsilon}} - \theta \underline{a} \tag{27}$$

where

$$\begin{aligned} A &= I - \bar{\beta} \wedge L \\ \underline{a} &= (A - I) \, \underline{m} = - \bar{\beta} \wedge L \, \underline{m} \end{aligned} \tag{28}$$

It is perhaps important to emphasize the different physical interpretations of $\underline{\bar{\varepsilon}}_o$ and $\underline{\bar{\varepsilon}}_c$. Whereas $\underline{\bar{\varepsilon}}_o$ is the average strain in the matrix, $\underline{\bar{\varepsilon}}_c$ represents that part of the overall strain which is accommodated by all the cracks. Therefore, one can write (26) as

$$\underline{\bar{\varepsilon}}_c = A_c \, \underline{\bar{\varepsilon}} - \theta \underline{a}_c \, , \tag{29}$$

where

$$\begin{aligned} A_c &= \bar{\beta} \wedge L \\ \underline{a}_c &= \bar{\beta} \wedge L \, \underline{m} \, . \end{aligned} \tag{30}$$

For example, it is immediately obvious that the average thermal strains in a fully constrained cracked composite ($\underline{\bar{\varepsilon}} = \underline{0}$) are

$$\underline{\bar{\varepsilon}}_o = - \underline{\bar{\varepsilon}}_c = \bar{\beta} \wedge L \, \underline{m} \, \theta \, .$$

The matrix expands at the expense of crack closing.

For computational purposes it is advantageous to review (28$_1$) with the help of (2) in the form

$$A = M_o \, L \, . \tag{31}$$

It is often convenient to have explicit forms of the above results. The nonzero components of A in (28) are:

$$\begin{aligned} A_{11} &= A_{33} = A_{55} = 1 \\ A_{21} &= (M^0_{12} - M_{22})\, L_{12} \\ A_{22} &= (M^0_{12} - M_{22})\, L_{22} + 1 \\ A_{23} &= (M^0_{12} - M_{22})\, L_{23} \\ A_{44} &= M^0_{44}/M_{44} \\ A_{66} &= M^0_{66}/M_{66} \,. \end{aligned} \tag{32}$$

Again, M^0_{ij} are compliances of the uncracked composite; M_{ij}, L_{ij} are listed in (A-3) to (A-6) in the Appendix.

The components of thermal strain concentration factor $\underline{a}$ in (28) are all zero, except for

$$a_{22} = -\bar{\beta}\, \Lambda_{22}[(L_{12} + L_{22})\alpha_T + L_{23}\, \alpha_A] \tag{33}$$

The average strain $\bar{\underline{\varepsilon}}_c$ (26), (29) in the cracks has the following nonvanishing components:

$$\begin{aligned} \bar{\varepsilon}^c_{12} &= \bar{\beta}\, \Lambda_{22}[L_{12}(\bar{\varepsilon}_{11} - \alpha_T\theta) + L_{22}(\bar{\varepsilon}_{22} - \alpha_T\theta) + L_{23}(\bar{\varepsilon}_{33} - \alpha_A\theta)] \\ \bar{\varepsilon}^c_{23} &= (1 - M^0_{44}/M_{44})\bar{\varepsilon}_{23} \qquad \bar{\varepsilon}^c_{12} = (1 - M^0_{66}/M_{66})\bar{\varepsilon}_{12} \,, \end{aligned} \tag{34}$$

We note that the distinction between open and closed cracks is determined by the inequality

$$\varepsilon^c_{12} > 0 \,, \tag{35}$$

which can be evaluated with the help of (34).

The results presented here are valid only if this inequality is satisfied. If the sign is reversed, or if the two sides are equal, then cracks are closed and do not affect the mechanical and thermal response of the composite. An exception arises when the closed crack faces slide in shear. Treatment of this case is beyond the scope of the present paper [13].

Finally, we note that evaluation of stress averages in the phases is trivial. Since open cracks do not support any stress,

$$\bar{\underline{\sigma}}_0 \equiv \bar{\underline{\sigma}} \,, \; \bar{\underline{\sigma}}_c \equiv \underline{0} \tag{36}$$

6. STIFFNESS AT LARGE β

When a fibrous lamina is embedded in a laminated structure, it may crack rather extensively. Under such circumstances, certain components of L_{ij} in (2) become independent of β, or equal to zero. It is worth evaluating these limiting stiffnesses since they correspond to the worst possible damage to a particular ply of a laminate. A good approximation to the actual residual stiffness can be obtained as

$$L^*_{ij} = \lim_{\beta \to \infty} L_{ij} . \tag{37}$$

Now as $\beta \to \infty$ it is easy to see that

$$M_{22},\ M_{44},\ M_{66} \to \infty$$

whereas the remaining components of the compliance matrix remain finite (and equal to the uncracked value). It then follows from simple matrix inversion that

$$\begin{aligned} &L^*_{11} = M^0_{33}/\gamma = L^0_{11} - (L^0_{12})^2/L^0_{22} \\ &L^*_{12} = 0 \qquad L^*_{22} = 0 \qquad L^*_{23} = 0 \\ &L^*_{13} = -M^0_{13}/\gamma = L^0_{13} - L^0_{12}L^0_{23}/L^0_{22} \\ &L^*_{33} = M^0_{11}/\gamma = L^0_{33} - (L^0_{23})^2/L^0_{22} \end{aligned} \tag{38}$$

where $\gamma = M^0_{11}\, M^0_{33} - (M^0_{13})^2$. Also,

$$L^*_{55} = L^0_{55}, \qquad L^*_{44} = L^*_{66} = 0 . \tag{39}$$

For a moderately cracked ply, say $\beta = 1$, a reasonable approximation to the stiffnesses L_{ij} (ij = 1,2,3) is still given by (38), while L_{55} is of course equal to L^0_{55}. However, L_{44} and L_{66} must be calculated either directly from (2) and (A-6), or indirectly from (8), (10), and (11).

7. SELECTED RESULTS

To illustrate the evaluation of compliances of a cracked composite, and of the "matrix" strain averages, we consider a T300 Gr-EP system. Table 2 lists the constituent properties of fiber and matrix, and of the uncracked composite. The composite compliances were obtained from self-consistent estimates of moduli [14].

Figure 4 shows changes in the three compliances M_{22}, M_{44}, and M_{66}, calculated from Equations (8–11) for given values of crack density β. Of

Table 2. Constituent properties and compliances of the T300 Gr-EP system.

	Unit	E_{33}	G_{31}	ν_{31}	E_{11}	G_{12}	Symmetry
Fiber (T300)	10^3ksi	33.00	3.36		2.25	0.78	Transversely Isotropic
				0.410			
	10^3MPa	227.5	23.2		15.5	5.4	
Matrix (Epoxy)	10^3ksi	0.50	0.19		0.50	0.19	Isotropic
				0.350			
	10^3MPa	3.46	1.26		3.4	1.26	

Composite Compliances:

Compliance	$c_f = 0.2$	$c_f = 0.4$	$c_f = 0.6$
M^o_{11}	0.2069	0.1595	0.1192
M^o_{12}	−0.1037	−0.0779	−0.0561
M^o_{13}	−0.0075	−0.0041	−0.0028
M^o_{22}	0.2069	0.1595	0.1192
M^o_{23}	−0.0075	−0.0041	−0.0028
M^o_{33}	0.0207	0.0107	0.0073
M^o_{44}	0.5108	0.2726	0.1244
M^o_{55}	0.5108	0.2726	0.1244
M^o_{66}	0.6211	0.4746	0.3506

All values are in units of $(10^3\ MPa)^{-1}$.

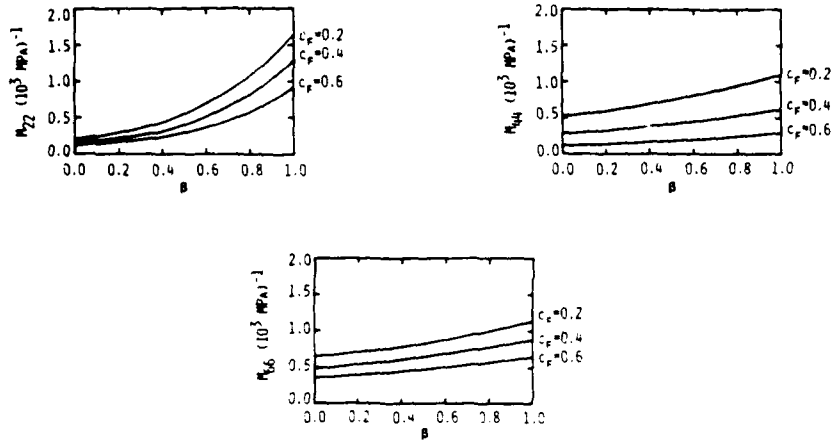

Figure 4. *Compliance changes in the T300 Gr-Ep system caused by cracks of density β.*

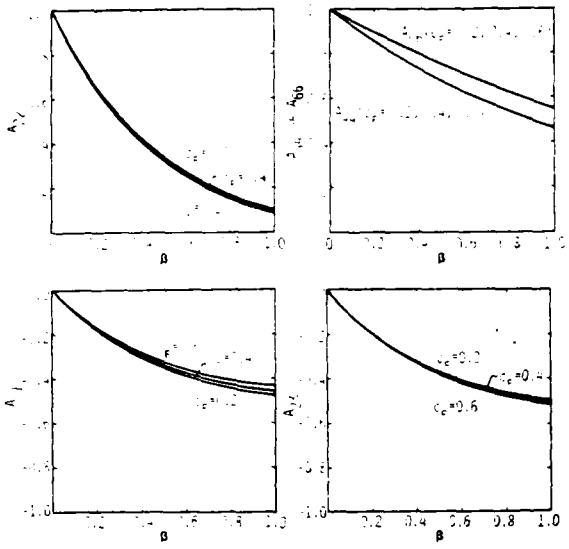

Figure 5. *Changes in strain concentration factor components in composite "matrix" caused by cracks of density β (T300 Gr-Ep).*

course, all these components increase with increasing β, but their change is quite gradual, especially at low β. This contrasts but is not in conflict with the relatively rapid reduction in stiffnesses which we found in [8].

We note that the composite without cracks is transversely isotropic, and has five independent compliances, M_{ij}. When cracks are introduced the coefficient M_{22}, M_{44}, and M_{66} change, the material is no longer transversely isotropic, and the number of independent elastic compliances increases to eight.

The changes caused by β in components of strain concentration factor A in (28) are shown in Figure 5. As required by (32), five of the eight components of A change with β. Note that the fiber volume fraction appears to have a small effect on A_{ij}. However, crack density β can have a significant effect on the strain concentration factor components, especially at relatively low values of β.

ACKNOWLEDGEMENT

This work has been supported by a grant from the Air Force Office of Scientific Research.

SYMBOLS

$2a$ = thickness of a lamina

A, $\underline{a}$ = mechanical and thermal strain concentration factors for unbroken segments of a cracked lamina

I = 6×6 identity matrix
L = instantaneous overall stiffness of a lamina
L^*_{ij} = overall lamina stiffness at large crack density
$\underline{l}$ = instantaneous overall thermal stress vector of a lamina
$\underline{l}_o$ = thermal stress vector of the unbroken segments of a cracked lamina
M = instantaneous overall compliance of a lamina
$\underline{m}$ = overall thermal strain vector of a lamina
$\underline{m}_o$ = thermal strain vector of the unbroken segments of a cracked lamina
α_A = axial linear thermal expansion coefficient of the uncracked composite lamina
α_T = transverse linear thermal expansion coefficient of the uncracked composite lamina
β = crack density parameter in an interior ply
$\beta^s = 2\beta$ = crack density parameter in a surface ply
$\bar{\beta}$ = $\frac{1}{4}\pi\beta$
$\bar{\underline{\xi}}$ = overall uniform strain
$\bar{\underline{\xi}}_c$ = volume average of strain accommodated by cracks (crack accommodation strain)
$\bar{\underline{\xi}}_o$ = volume average of strain in the unbroken segments of a cracked lamina
θ = uniform temperature change
Λ = crack tensor
$\bar{\underline{\sigma}}$ = overall uniform stress
$\bar{\underline{\sigma}}_o$ = volume average of stress in unbroken segments of cracked lamina

REFERENCES

1. Aveston, J. and Kelly, A., "Theory of Multiple Fracture in Fibrous Composites," *J. Materials Science*, Vol. 8, p. 352 (1973).
2. Hahn, H. T. and Tsai, S. W., "On the Behavior of Composite Laminates After Initial Failures," *J. Composite Materials*, p. 228 (1974).
3. Bailey, J. E., Curtis, P. T. and Parvizi, A., "On the Transverse Cracking and Longitudinal Splitting Behavior of Glass and Carbon Fibre Reinforced Epoxy Cross Ply Laminates and the Effect of Poisson and Thermally Generated Strain," *Proc. R. Soc. Lond. A.*, Vol. 366, p. 599 (1979).
4. Wang, S. D. and Crossman, F. W., "Initiation and Growth of Transverse Cracks and Edge Delamination in Composite Laminates. Part 1. An Energy Method," *J. of Composite Materials*, Vol. 14, p. 71 (1980).
5. Dvorak, G. J. and Johnson, W. S., "Fatigue of Metal Matrix Composites," *International Journal of Fracture*, Vol. 16, 6, p. 585 (1980).
6. Hwang, D. G., "The Proof Testing and Fatigue Behavior of Gr/Ep Laminates," D.Sc. Dissertation, Washington University, St. Louis, Mo (August 1982).
7. Crossman, F. W., Warren, W. J., Wang, A. S. D. and Law, G. E. Jr., "Initiation and Growth of Transverse Cracks and Edge Delamination in Composite Laminates, Part 2. Experimental Correlation," *J. Composite Materials*, Vol. 14, p. 88 (1980).

8. Laws, N., Dvorak, G. J. and Hejazi, M., "Stiffness Changes in Unidirectional Composites Caused by Crack Systems," *Mechanics of Materials*, Vol. 2, p. 123 (1983).
9. Cook, T. S. and Erdogan, F., "Stresses in Bonded Materials with a Crack Perpendicular to the Interface," *Int. J. Engineering Science*, Vol. 10, p. 677 (1972).
10. Gottesman, T., Hashin, Z. and Brull, M. A., "Effective Elastic Moduli of Cracked Fiber Composites." In *Advances in Composite Materials*, ed. A. R. Bunsell, et al., Pergamon Press, Oxford, pp. 749–758.
11. Laws, N., "A Note on Interaction Energies Associated with Cracks in Anisotropic Solids," *Phil. Mag.*, Vol. 36, p. 367 (1977).
12. Laws, N., "On the Thermostatics of Composite Materials," *J. Mech. Phys. Solids*, Vol. 21, p. 9 (1973).
13. Horii, H. and Nemat-Nasser, S., "Overall Moduli of Solids with Microcracks: Load Induced Anisotropy," *J. Mech. Phys. Solids*, Vol. 31, p. 155 (1983).
14. Hill, R., "Theory of Mechanical Properties of Fibre-Strengthened Materials III. Self-Consistent Model," *J. Mech. Phys. Solids*, Vol. 13, p. 189 (1965).

APPENDIX

Selected Properties of Orthotropic Materials

The constitutive equation for orthotropic materials have the following form:

$$\underline{\sigma} = L\,\underline{\varepsilon}\,, \qquad \underline{\varepsilon} = M\,\underline{\sigma} \tag{1}$$

Stresses and strains are:

$$\begin{aligned}\underline{\sigma} &= [\sigma_{11}\ \sigma_{22}\ \sigma_{33}\ \sigma_{23}\ \sigma_{13}\ \sigma_{12}]^T \\ &= [\sigma_1\ \ \sigma_2\ \ \sigma_3\ \ \sigma_4\ \ \sigma_5\ \ \sigma_6\ ]^T\end{aligned} \tag{A-1}$$

$$\begin{aligned}\underline{\varepsilon} &= [\varepsilon_{11}\ \varepsilon_{22}\ \varepsilon_{33}\ 2\varepsilon_{23}\ 2\varepsilon_{13}\ 2\varepsilon_{12}]^T \\ &= [\varepsilon_1\ \ \varepsilon_2\ \ \varepsilon_3\ \ \ \varepsilon_4\ \ \ \varepsilon_5\ \ \ \varepsilon_6]^T\,.\end{aligned} \tag{A-2}$$

Stiffness and compliance matrices are given in the form

$$L = \begin{bmatrix} L_{11} & L_{12} & L_{13} & 0 & 0 & 0 \\ & L_{22} & L_{23} & 0 & 0 & 0 \\ & & L_{33} & 0 & 0 & 0 \\ & & & L_{44} & 0 & 0 \\ & & & & L_{55} & 0 \\ \textit{Sym.} & & & & & L_{66} \end{bmatrix} \tag{A-3}$$

$$M = \begin{bmatrix} M_{11} & M_{12} & M_{13} & 0 & 0 & 0 \\ & M_{22} & M_{23} & 0 & 0 & 0 \\ & & M_{33} & 0 & 0 & 0 \\ & & & M_{44} & 0 & 0 \\ & & & & M_{55} & 0 \\ \text{Sym.} & & & & & M_{66} \end{bmatrix} \tag{A-4}$$

It is sometimes convenient to express the compliance coefficients in terms of elastic Young's and shear moduli, and Poisson's ratios. In an orthotropic material we write

$$\begin{bmatrix} \varepsilon_{11} \\ \varepsilon_{22} \\ \varepsilon_{33} \\ 2\varepsilon_{23} \\ 2\varepsilon_{13} \\ 2\varepsilon_{12} \end{bmatrix} = \begin{bmatrix} \frac{1}{E_{11}} & -\frac{\nu_{12}}{E_{11}} & -\frac{\nu_{13}}{E_{11}} & 0 & 0 & 0 \\ -\frac{\nu_{21}}{E_{22}} & \frac{1}{E_{22}} & -\frac{\nu_{23}}{E_{22}} & 0 & 0 & 0 \\ -\frac{\nu_{31}}{E_{33}} & -\frac{\nu_{32}}{E_{33}} & \frac{1}{E_{33}} & 0 & 0 & 0 \\ 0 & 0 & 0 & \frac{1}{L_{44}} & 0 & 0 \\ 0 & 0 & 0 & 0 & \frac{1}{L_{55}} & 0 \\ 0 & 0 & 0 & 0 & 0 & \frac{1}{L_{66}} \end{bmatrix} \begin{bmatrix} \sigma_{11} \\ \sigma_{22} \\ \sigma_{33} \\ \sigma_{23} \\ \sigma_{13} \\ \sigma_{12} \end{bmatrix} \tag{A-5}$$

Note that M is symmetric, hence $\nu_{12}/E_{11} = \nu_{21}/E_{22}$, etc.

Stiffness L can be written as the inverse of M, or as an expansion of (2) in terms of Λ_{ij}; the result is

$$L_{11} = \frac{1}{\Delta_M}[M_{22}M_{33} - M_{23}^2] = L_{11}^0 - \bar{\beta}(L_{12}^0)^2(1 + \bar{\beta}\, L_{22}^0\Lambda_{22})^{-1}\Lambda_{22}$$

$$L_{12} = \frac{1}{\Delta_M}[M_{13}M_{23} - M_{12}M_{33}] = L_{12}^0(1 + \bar{\beta}\, L_{22}^0\Lambda_{22})^{-1}$$

$$L_{13} = \frac{1}{\Delta_M}[M_{12}M_{32} - M_{13}M_{22}] = L_{13}^0 - \bar{\beta}\, L_{23}^0 L_{12}^0(1 + \bar{\beta}\, L_{22}^0\Lambda_{22})^{-1}\Lambda_{22}$$

$$L_{22} = \frac{1}{\Delta_M}[M_{11}M_{33} - M_{13}^2] = L_{22}^0(1 + \bar{\beta}\, L_{22}^0\Lambda_{22})^{-1} \tag{A-6}$$

$$L_{23} = \frac{1}{\Delta_M}[M_{21}M_{31} - M_{23}M_{11}] = L_{23}^0(1 + \bar{\beta}\, L_{22}^0\Lambda_{22})^{-1}$$

$$L_{33} = \frac{1}{\Delta_M}[M_{11}M_{22} - M_{12}^2] = L_{33}^0 - \bar{\beta}(L_{23}^0)^2(1 + \bar{\beta}\, L_{22}^0\Lambda_{22})^{-1}\,\Lambda_{22}$$

$$L_{44} = 1/M_{44} = L_{44}^0(1 + \bar{\beta}\, L_{44}^0\,\Lambda_{44})^{-1}$$

$$L_{55} = 1/M_{55} = L_{55}^0$$

$$L_{66} = 1/M_{66} = L_{66}^0\,(1 + \bar{\beta}\, L_{66}^0\,\Lambda_{66})^{-1}$$

Also

$$\Delta_M = \{(M_{11}M_{33} - M_{13}^2)\,(M_{22}M_{33} - M_{23}^2) - (M_{13}M_{23} - M_{12}M_{33})^2\}/M_{33} \tag{A-7}$$

which follows from inversion of (A-4).

Analysis of Progressive Matrix Cracking In Composite Laminates II. First Ply Failure

GEORGE J. DVORAK
Civil Engineering Department
Rensselaer Polytechnic Institute
Troy, NY 12180

NORMAN LAWS
Mechanical Engineering Department
University of Pittsburgh
Pittsburgh, PA 15260

(Received July 10, 1985)
(Revised October 30, 1985)

ABSTRACT

The mechanics of transverse cracking in an elastic fibrous composite ply is explored for the case of low crack density. Cracks are assumed to initiate from a nucleus created by localized fiber debonding and matrix cracking. Conditions for onset of unstable cracking from such nuclei are evaluated with regard to interaction of cracks with adjacent plies of different elastic properties. It is found that cracks may propagate in two directions on planes which are parallel to the fiber axis and perpendicular to the midplane of the ply. In general, crack propagation in the direction of the fiber axis controls the strength of thin plies, while cracking in the direction perpendicular to the fiber axis determines the strength of thick plies. The theory relates ply thickness, crack geometry, and ply toughness to ply strength. It predicts a significant increase in strength with decreasing ply thickness in constrained thin plies. The strength of thick plies is found to be constant, but it may be reduced by preexisting damage. Strength of plies of intermediate thickness, and of unconstrained thick plies is evaluated as well. Results are illustrated by comparison with experimental data.

1. INTRODUCTION

IN THE FIRST PAPER OF THIS SERIES [1] WE DESCRIBED THE EVALUATION OF thermoelastic properties of a unidirectional composite containing a certain density of aligned slit cracks which grow in the direction of the fiber and across the thickness of the ply. These cracks are usually referred to as ply cracks or transverse cracks. Now we focus our attention on a single ply in a typical part

Reprinted from *Journal of* COMPOSITE MATERIALS, *Vol. 21–April 1987*

of a laminated structure, removed from free edges and other stress concentrations, and examine the mechanics of transverse cracking in the ply. In particular, we consider the initial stage of the cracking process which consists of first ply failure, and perhaps subsequent failures of the ply at locations which are far apart from each other, so that the cracks do not interact. Our goal is to identify the failure modes which cause transverse cracking, to evaluate the corresponding energy release rates, and to present failure criteria for the cracking process.

Of course, if the composite laminate is loaded beyond the first ply failure, then many transverse cracks may develop in each ply. While this progressive cracking process is essentially a sequence of repetitive ply failures of the type discussed herein, the formation of each individual crack is influenced by interaction with adjacent cracks. This subject will be discussed in a separate paper.

2. CRACK GEOMETRY

Consider a unidirectionally reinforced ply of thickness 2a, which is embedded in a laminated plate, shell, or a similar composite structure. The structure is subjected to a certain incremental loading program which, at each loading step, causes a known instantaneous strain state $\underset{\sim}{\epsilon}$ in the ply. A uniform thermal change θ can also be prescribed. When the ply is free of cracks, the local strains $\underset{\sim}{\epsilon}$ are assumed to be uniform, or nearly uniform in the sense that their wavelength is much larger than the ply thickness. The local strains are then equal to their volume averages, or overall strains, $\bar{\underset{\sim}{\epsilon}}$. The given strain state $\bar{\underset{\sim}{\epsilon}}$ and uniform thermal change θ are related to the resulting overall stress $\bar{\underset{\sim}{\sigma}}$ in the ply, in analogy with (1-17)*, as:

$$\bar{\underset{\sim}{\sigma}} = L_o\bar{\underset{\sim}{\epsilon}} - \theta\,\underset{\sim}{\ell}_o \qquad \bar{\underset{\sim}{\epsilon}} = M_o\bar{\underset{\sim}{\sigma}} + \theta\,\underset{\sim}{m}_o, \tag{1}$$

where L_o, M_o are stiffness and compliance matrices of the uncracked ply, and $\underset{\sim}{\ell}_o$, $\underset{\sim}{m}_o$ are the thermal stress and strain vectors. We emphasize that $\bar{\underset{\sim}{\sigma}}$, $\bar{\underset{\sim}{\epsilon}}$ are ply averages, not laminate averages.

Suppose that at a certain magnitude of $\bar{\underset{\sim}{\epsilon}}$, which is much smaller than the failure strain of the fiber, a single crack appears in the ply. The crack geometry depends on the strength anisotropy of the fibrous ply, and on the state of stress $\bar{\underset{\sim}{\sigma}}$. Clearly, cracks may propagate most easily on planes parallel to fiber direction. In a typical part of a laminated plate or shell, each ply usually supports a plane stress state. In the coordinates of Figure 1 this suggests that overall stress components $\bar{\sigma}_{22}$, $\bar{\sigma}_{23}$, and $\bar{\sigma}_{33}$ are large in comparison to $\bar{\sigma}_{11}$, $\bar{\sigma}_{12}$, and $\bar{\sigma}_{13}$. It is easy to see that stresses $\bar{\sigma}_{22}$ and $\bar{\sigma}_{23}$ favor cracking on x_1x_3-planes. The stress $\bar{\sigma}_{33}$ does not affect these cracks; it may cause cracking on planes perpendicular to the fibers [2], but such cracks are seldom observed in polymer matrix composites. The remaining minor shear components $\bar{\sigma}_{12}$ and $\bar{\sigma}_{13}$ may exist in bent plates, a small $\bar{\sigma}_{12}$ contributes to crack growth on x_1x_3-planes, $\bar{\sigma}_{13}$ does not have an effect. Of

*Equations which appear in Reference [1] will be referred to by their numbers preceded by 1, e.g., (1-17) denotes Equation (17) in [1].

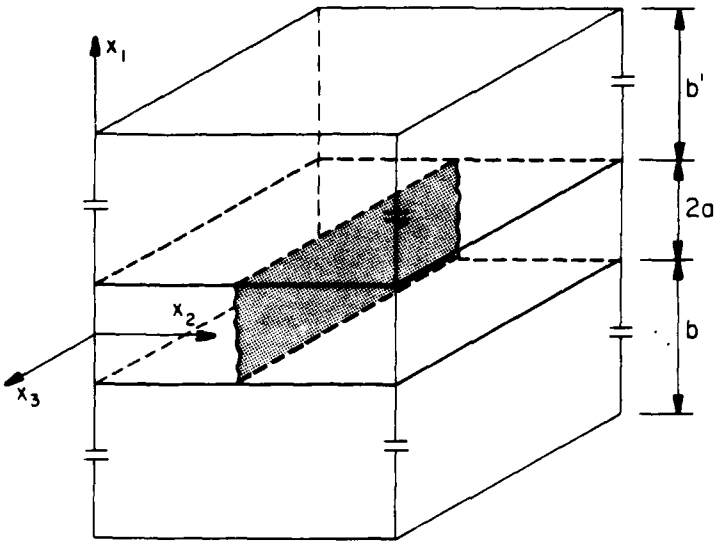

Figure 1. *Slit crack in a uniformly strained composite ply. Fibers and crack are aligned with x_3 axis.*

course, it is essential that $\bar{\sigma}_{11}$ be low or zero so that splitting or delamination of the lamina or laminate, respectively, do not take place.

Under such circumstances the ply will crack as indicated in Figure 1. A typical ply crack is a slit crack which extends in the fiber direction x_3 across the entire loaded area of the ply. Therefore, its length can be very large, whereas its width is essentially equal to the ply thickness 2a. The laminate layers on either side of the ply have certain thicknesses b and b', let $b \geq b'$. If the ply is an exterior layer, then $b' = 0$, and the crack becomes a surface crack.

3. STAGES OF CRACK FORMATION

Analysis of ply cracking requires a reasonably accurate model of the process. As in other fracture events, one may anticipate that there will be an initiation stage leading to formation of a localized crack nucleus, and a propagation stage in which the crack extends in the fiber direction across the entire loaded area of the ply.

In polymer matrix systems, cracks are often initiated at locations where several fibers debond from the matrix under load [3]. Such debonded regions may also be present as, or start from, initial flaws in the ply, but these should be infrequent in well-made materials [4]. There is no need to assume the presence of initial flaws. Instead, fiber debonding can be regarded as a consequence of a statistical distribution of bond strength, within a certain stress interval, along the length of

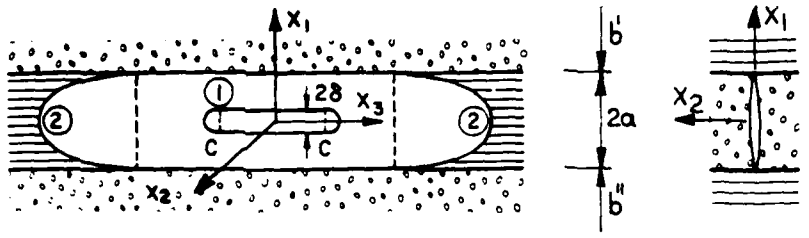

① CRACK NUCLEUS

② RUNNING LONGITUDINAL (TYPE L) SLIT CRACK

Figure 2. *Schematic of crack nucleus and type L slit crack.*

the fiber. Debonding is also influenced by stress distribution on the microscale which depends on fiber spacing. Garrett and Bailey [5] point to numerous studies which suggest that debonding is more likely to occur in regions of high fiber density, or if the fibers are in contact.

The net effect of these factors on the total number of debonded regions is difficult to quantify. However, since the number of cracks increases slowly, especially in the initial stages of cracking, one can conclude that debonded regions of significant size, which can actually initiate cracks at a given level of applied strain, are not particularly numerous. Clearly, while the crack density is low, the distances between initiation sites are many times larger than ply thickness. Therefore, each crack propagates from a single initiation site at which a sufficiently large crack nucleus has formed from a debonded region.

In the absence of experimental information about the actual geometry of a debonded region, we assume that when one or more adjacent fibers debond from the matrix, and these debonds join up, a larger, stable microcrack appears in the ply. This microcrack lies in the x_1x_3-plane, where the ply crack eventually forms, Figure 1. The in-plane contour of each fiber debond should resemble an elongated ellipse, or an oval, and it seems reasonable to adopt the same contour for the initial microcrack. The resulting shape appears in Figure 2. Let the width of the microcrack be denoted by 2δ; the length dimension in x_3, which may be much larger than 2δ, need not be specified. The thickness of the ply is $2a$, and the microcrack is located at mid-thickness.

Now, if the ply is strained in an incremental way, the microcrack will grow slowly until it becomes a crack nucleus of certain critical width $2\delta_c$, and starts to propagate as a Griffith crack. The slow growth process is probably time-dependent in most polymer matrix systems, and one should relate the growth rate to loading history. The rapid crack propagation can be regarded as inviscid, at least in brittle resin matrices.

4. ENERGY RELEASE RATES

To evaluate the critical size 2δ of the crack nucleus under a given stress, and to determine the direction of crack propagation, it is necessary to derive expressions for energy release rates of the crack nucleus in a ply at constant overall strain. Clearly, the crack may extend either in the x_1 direction, in the x_3 direction, or simultaneously in both directions. To distinguish between the direction related quantities, we indicate the relevant direction by the letter L, or T, written in parentheses next to the appropriate symbol. For example, the energy release rate $G(T)$ refers to crack extension in the transverse direction x_1, and $G(L)$ to crack extension in the longitudinal direction x_3. The corresponding toughnesses are $G_c(T)$, $G_c(L)$, critical crack widths $\delta_c(T)$, $\delta_c(L)$, etc.

In general, we shall refer to a crack that propagates in the x_1 direction as type T crack, and to that which propagates in the x_3 direction as type L crack.

It is probably obvious that due to $\bar{\sigma}_{22}$, both crack types open in the x_2 direction, or in Mode I. In addition, there are two shear modes, one along the fiber direction, and one transverse to the fiber direction. These will be designated for both crack types as follows: Mode II represents longitudinal shear displacement in x_3, caused by $\bar{\sigma}_{23}$, and Mode III is the transverse shear mode in x_2 caused by $\bar{\sigma}_{12}$. This notation is derived from the type L cracking and adopted for type T cracks. Subscripts I, II, and III will denote the modes. While the crack front may change direction, the mode designation remains related to stress components in a fixed coordinate system.

Consider first *the case of a thick ply* with a small crack nucleus $\delta << a$, Figure 2. The nucleus is not affected by the presence of adjacent plies, and can be regarded as a slit crack in an infinite orthotropic medium. In this case, the energy release rates for both type T and type L can be obtained from the interaction energy W_δ, which is equal to the total energy released by a slit crack of unit length x_3 and width δ under constant $\bar{\epsilon}$. Expressions for W_δ in anisotropic solids were derived by Stroh [6] and in the orthotropic case by Laws [7]. In the notation used in [1]; for $\delta << a$,

$$W_\delta = \frac{1}{2}\,\pi\,\delta^2[\Lambda^\circ_{22}\,\bar{\sigma}^2_{22} + \Lambda^\circ_{44}\,\bar{\sigma}^2_{23} + \Lambda^\circ_{66}\,\bar{\sigma}^2_{12}] \tag{2}$$

Here, Λ°_{ij} are nonvanishing components of the crack tensor derived in [1], taken for a dilute concentration of cracks, i.e. for crack density parameter $\beta \to 0$. With the help of (1-4) to (1-6) and (1-A5) one can write

$$\Lambda^\circ_{22} = \Lambda^\circ_{66} = 2\left(\frac{1}{E_T} - \frac{\nu_L^2}{E_L}\right) \qquad \Lambda^\circ_{44} = 1/G_L \tag{3}$$

where $E_L = E_{33}$, $E_T = E_{11} = E_{22}$ are the longitudinal and transverse Young's moduli, $G_L = L_{44} = L_{55}$ in [1] is the longitudinal shear modulus, and $\nu_L = \nu_{13} = \nu_{23}$ is the corresponding Poisson's ratio.

The energy release rate of a crack of length 2δ, for an elementary extension in the x_1 direction in an unbounded orthotropic solid is equal to $\frac{1}{2}\,\partial W_\delta/\partial\delta$, or

$$G(T) = \frac{1}{2}\,\pi\,\delta[\Lambda^\circ_{22}\,\bar{\sigma}^2_{22} + \Lambda^\circ_{44}\,\bar{\sigma}^2_{23} + \Lambda^\circ_{66}\,\bar{\sigma}^2_{12}], \qquad \text{for } \delta << a. \tag{4}$$

One can easily verify that (2) and (4) reduce to their familiar plane-strain forms if the solid becomes isotropic.

We now turn our attention to extension of an oval crack of width 2δ in the fiber direction x_3, Figure 2. The energy release rate $G(L)$ of this (type L) crack is equal to the interaction energy W_δ released by a crack of width 2δ as it extends by a unit distance x_3, and thus creates a new surface area $2\delta_*1$. This is the amount of energy change caused by unit extension of the prismatic part $C\bar{C}$ of the stage 2 crack in Figure 2. Hence,

$$G(L) = W_\delta/2\delta \tag{5}$$

or,

$$G(L) = \frac{1}{\delta}\int_o^\delta G(T)\,d\delta \tag{6}$$

From (2) and (4) one obtains

$$G(L) = \frac{1}{4}\,\pi\,\delta[\Lambda^\circ_{22}\,\bar{\sigma}^2_{22} + \Lambda^\circ_{44}\,\bar{\sigma}^2_{23} + \Lambda^\circ_{66}\,\bar{\sigma}^2_{12}] \qquad \text{for } \delta << a \tag{7}$$

Note that $G(L)$ does not depend on the actual length of the crack nucleus in x_3 direction, i.e., of the segment CC in Figure 2. The crack width δ is the only parameter reflecting crack geometry, and if its value is fixed, then $G(L)$ is constant.

Consider now the case of a crack nucleus in a *ply of intermediate thickness* $0 < \delta/a < 1$. As the crack approaches the interface between its own ply and an adjacent ply of different elastic properties, W_δ is influenced by the proximity of the adjacent ply. In the direction x_2, perpendicular to the crack plane, the adjacent plies are usually much stiffer than the ply under consideration, and this causes a reduction in W_δ as $\delta/a \to 1$. To reflect this, (4) can be written in the form valid for type T crack of any length

$$G(T) = \frac{1}{2}\,\pi\,\delta[\eta_I^2\Lambda^\circ_{22}\bar{\sigma}^2_{22} + \eta^2_{II}\,\Lambda^\circ_{44}\,\bar{\sigma}^2_{23} + \eta^2_{III}\,\Lambda^\circ_{66}\,\bar{\sigma}^2_{12}] \quad \text{for} \quad (0 < \delta/a < 1) \tag{8}$$

where

$$\eta_i = \eta_i\left(\frac{\delta}{a}\right) = K_i/(\bar{\sigma}\sqrt{\delta}) \qquad i = I,\ II,\ III \tag{9}$$

are stress intensity reduction coefficients which depend on crack geometry and elastic properties of layers. The stress $\bar{\sigma} = \bar{\sigma}_{22}$ for $i = I$, etc.

For a unit extension in the x_3 direction of a crack nucleus of width 2δ, Figure 2, when $0 < \delta/a < 1$, the energy release rate is given again by (5) and (6). However, since the interaction energy W_δ is now influenced by the proximity of the next ply, (7) now becomes, for $0 < \delta/a < 1$:

$$G(L) = \frac{1}{4}\pi\,\delta[\xi_I\,\Lambda^o_{22}\,\bar{\sigma}^2_{22} + \xi_{II}\,\Lambda^o_{44}\,\bar{\sigma}^2_{23} + \xi_{III}\,\Lambda^o_{66}\,\bar{\sigma}^2_{12}] \tag{10}$$

where, from (6) and (8):

$$\xi_i = 2\,\frac{a^2}{\delta^2}\int_o^{\delta/a} \eta^2\left(\frac{\delta'}{a}\right)\frac{\delta'}{a}\,d\left(\frac{\delta'}{a}\right) \qquad i = I,\ II,\ III \tag{11}$$

Again, the effect of crack geometry is reflected only through δ, and if that is fixed, say at $\delta = a$, then $G(L)$ is constant.

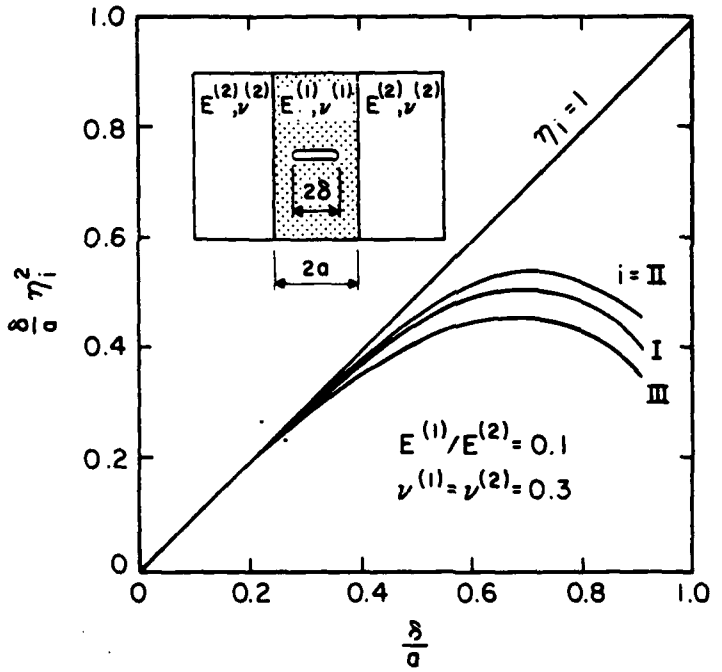

Figure 3. *Stress intensity reduction coefficients $\eta_i = K_i/(\bar{\sigma}\sqrt{\delta})$ for the three fracture modes. The longitudinal shear mode is denoted by $i = II$.*

Coefficients η_i can be found for many crack configurations in nonhomogeneous media. For transverse cracks in layered media one can refer to the results of Hilton and Sih [8], and Cook and Erdogan [9] in the case of isotropic layers. Similar results for laminates made of orthotropic layers can be found in [10], and a finite element evaluation of η_i for a graphite-epoxy laminate appeared in [11].

These and related results indicate that η_i are influenced by the differences in elastic constants between the layers, and particularly so by the ratio $E_{22}^{(1)}/E_{22}^{(2)}$ of the Young's moduli of the cracked layer (1) to that of adjacent layer (2), in direction x_2, perpendicular to crack plane x_1x_3. Additional effects of elastic constants exist and are discussed in [10]. A significant feature of these results is that η_i are not very sensitive to values of the moduli ratio for $E_{22}^{(1)}/E_{22}^{(2)} < 0.1$ or so, the outer layer is perceived by the crack as very stiff or rigid. The relative thicknesses of the layers can have an important effect, particularly in thin laminates where η_i increase if the crack interacts with a surface ply [8,9,12]. Thermal stress effects in cracked laminates have apparently not received much attention, except for [11], and at this time can be examined only in terms of their contribution to overall applied stress $\bar{\sigma}_{ij}$, via Equation (1).

For illustration, Figure 3 shows the coefficients η_i for a crack in a laminate consisting of isotropic layers, for $E_{22}^{(1)}/E_{22}^{(2)} = 0.1$, $\nu = 0.3$ [8,9]. These coefficients can be used as an approximation for laminates consisting of transversely isotropic

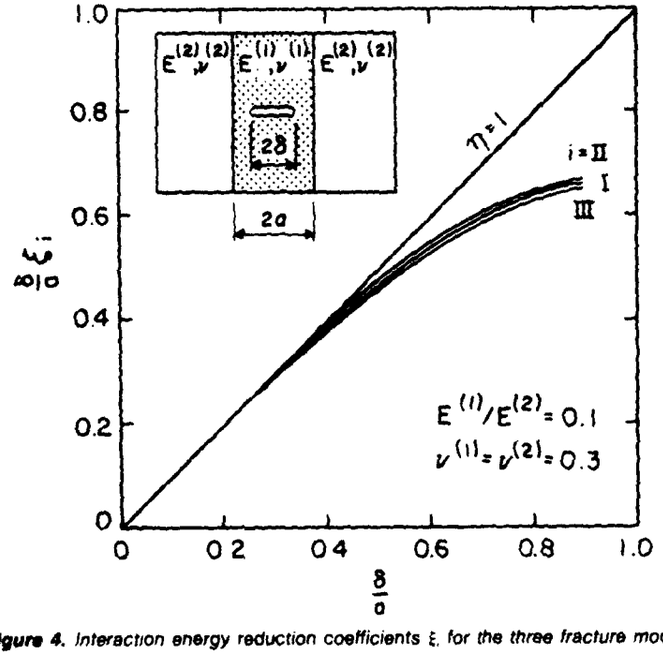

Figure 4. Interaction energy reduction coefficients ξ_i for the three fracture modes.

layers, providing that one takes $E_{22}^{(1)} = E_T^{(1)}$ and $E_{22}^{(2)} = E_L^{(2)}$. The selected ratio of moduli corresponds to that of (0/90) graphite-epoxy.

Figure 4 shows values of $(\delta/a)\xi$, calculated from the η_i in Figure 3 and (11). These refer to a crack which has a certain width δ, and are plotted as functions of δ/a.

We note that η_i are generally available only up to $\delta/a = 0.90$. Also, the order of stress singularity changes when the crack reaches the interface.

As in the case of η_i, the estimates of ξ_i in Figure 4 are rather conservative, taken for adjacent plies of very different properties such as one encounters in (0/90) graphite-epoxy. Somewhat higher values can be expected in glass-epoxy laminates, and also in thin laminates where the crack interacts with one or two surface plies. For example, Chou et al., [11] give values for $(\pm 25/90_3)_s$ and $(0_2/90_2)_s$ in AS-3501-06 graphite-epoxy system which are about 25% higher than those shown in Figure 4.

Finally, consider *the case of a thin ply* in which the crack nucleus extends across the entire ply width, i.e., $\delta/a = 1$. Only $G(L)$ is of interest in this case, and it can be found from (10) provided that ξ_i are known. Unstable type T cracking cannot occur, however; one should keep in mind that the crack tips at $x_1 = \pm a$ reside in a soft matrix which may not be able to support the high crack tip stresses. Therefore, local crack extension, across or along the ply interface, may take place to relieve the stress singularity. Such localized crack extensions have been observed experimentally [5]. More recent studies suggest that delaminations as well as numerous fiber breaks can be found in the axial plies next to transverse cracks [13]. These observations are not surprising in view of analytical studies of cracks terminating at interfaces, which suggest that the stress intensity factor in the next ply and the magnitude of tension stresses perpendicular to the interface both increase at higher ratios of $E_{22}^{(1)}/E_{22}^{(2)}$ [9,12]. Therefore, one should expect that in the presence of additional cracking at ply interface the coefficients ξ_i are actually larger than those predicted theoretically for cracks terminating at the interface. Until the effect of interface damage is clarified, one can use a simple estimate, e.g., $\xi_i = 1$, as in [1].

For a selected ξ_i, one can find $G(L)$ of a thin ply from (10). Note that (8) and (9) are not affected by interface damage but (6) and (11) no longer apply.

5. FAILURE CRITERIA

If a composite ply is loaded only by a simple stress state, such as $\bar{\sigma}_{22}$ or $\bar{\sigma}_{23}$ acting alone, then unstable propagation of type T or type L cracks takes place when the appropriate value of G_I or G_{II} equals or exceeds the corresponding ply toughness G_{Ic} or G_{IIc}, respectively.

It is useful to point out that fracture surface topography depends on fracture mode. Modes I and II in a composite ply always create asperities on the fracture surface, as the crack seeks its way between densely packed fibers. These asperities can be interlocked and thus impede mode III cracking. Also in a typical part of laminated plate or shell, the corresponding stress $\bar{\sigma}_{12}$ is usually

small or equal to zero. Therefore, mode III need not be considered in many applications. For simplicity, we neglect mode III in the sequel.

Apart from the creation of asperities, fracture surface topography is quite different in modes I and II. Mode II favors formation of hackles, and higher energy absorption. For example, a recent review of experimental results [14] quotes toughness values for graphite-epoxy and glass-epoxy for which $K_{IIc}/K_{Ic} \approx 5$.

In mixed mode fracture, the toughness values are interrelated. Specific criteria which describe this effect need to be derived from experimental data. Hahn [14] offers a form based on fracture mechanics considerations that fits data obtained for certain glass-epoxy and graphite-epoxy systems:

$$(1 - g)\left(\frac{G_I}{G_{Ic}}\right)^{1/2} + g\left(\frac{G_I}{G_{Ic}}\right) + \left(\frac{G_{II}}{G_{IIc}}\right) \geq 1 \tag{12}$$

where $g = G_{Ic}/G_{IIc}$.

If G_c are independent of loading mode, then $g = 1$, and (12) assumes a familiar form. In actual composite plies with epoxy matrices $g \doteq 0.1$ [14].

More complex criteria can be derived as needed. In what follows we shall use (12) as a representative mixed mode criterion, both for type T and type L cracks. However, we allow for possible differences between toughness values in the two modes by writing:

$$\begin{aligned} G_{Ic}(L) &= \gamma_I\, G_{Ic}(T) \\ G_{IIc}(L) &= \gamma_{II}\, G_{IIc}(T) \end{aligned} \tag{13}$$

Results reported in [4] and [15] indicate that γ_I ranges from 0.6 to 0.8 for certain graphite-epoxy plies. Data of this kind are apparently very rare, therefore no general conclusions about γ_I and γ_{II} magnitudes can be drawn at this time.

6. FAILURE OF THICK PLIES

Consider a ply in a composite laminate which is subjected to a certain prescribed strain, such that within the ply the stress state is $\bar{\sigma}_{23} = q\,\bar{\sigma}_{22}$ and is applied incrementally until first ply failure. The ply fails by unstable propagation of a crack nucleus, Figure 2, when the width δ grows to a certain critical magnitude δ_c. We recall that δ may increase slowly under load, possibly as a function of time, especially during cyclic loading

$$\delta = \delta[\underline{\bar{\varepsilon}}(t)] \qquad \text{for } \delta \leq \delta_c \tag{14}$$

but once δ_c has been reached, the propagation process is rapid and regarded as time-independent.

The thickness $2a$ of the ply is large, so that $\delta_c/a << 1$.

Our objective is to determine the relationship between δ_c and the measured ply strength, and the directional sequence of the cracking process.

We recall that according to (4)

$$G_I(T) = \frac{1}{2}\pi\,\delta\,\Lambda^0_{22}\,\bar{\sigma}^2_{22}$$
$$G_{II}(T) = \frac{1}{2}\pi\,\delta\,\Lambda^0_{44}\,\bar{\sigma}^2_{23} \tag{15}$$

are the energy release rates for type T cracking in x_1 direction. Also, from (7),

$$G_I(L) = \frac{1}{4}\pi\,\delta\,\Lambda^0_{22}\,\bar{\sigma}^2_{22}$$
$$G_{II}(L) = \frac{1}{4}\pi\,\delta\,\Lambda^0_{44}\,\bar{\sigma}^2_{23} \tag{16}$$

are the rates for type L cracking in x_3 direction.

At any given stress state,

$$G_I(L) = \frac{1}{2}G_I(T)$$
$$\text{for } \delta << a \tag{17}$$
$$G_{II}(L) = \frac{1}{2}G_{II}(T)$$

Suppose that for the special case of loading $\bar{\sigma}_{22} \neq 0$, $\bar{\sigma}_{23} = 0$, the ply fails at $\bar{\sigma}_{22} = (\bar{\sigma}_{22})_{cr}$. At failure load, at least one of the following conditions must be satisfied:

$$G_I(T) \geq G_{Ic}(T),\ \delta \geq \delta_{Ic}(T)$$
and/or, $$G_I(L) \geq G_{Ic}(L),\ \delta \geq \delta_{Ic}(L) \tag{18}$$

where $\delta_{Ic}(T)$, $\delta_{Ic}(L)$ are critical widths of the crack nucleus in Figure 2, at onset of crack propagation in directions x_1, or x_3, respectively.

When (18) are taken as equalities, it follows from (13) and (15) to (17) that

$$\delta_{Ic}(T) = 2G_{Ic}(T)/\pi\Lambda^0_{22}(\bar{\sigma}_{22})^2_{cr} \tag{19}$$

$$\delta_{Ic}(L) = 4G_{Ic}(L)/\pi\Lambda^0_{22}(\bar{\sigma}_{22})^2_{cr} \tag{20}$$

and

$$\delta_{Ic}(L) = 2\gamma_I\,\delta_{Ic}(T) \tag{21}$$

We remark that a slightly different form of (19) has been obtained by Hahn and Johnnesson in [14]. Since the available data indicate that $2\gamma_I > 1$, then $\delta_{Ic}(1) < \delta_{Ic}(3)$. *Therefore, first ply failure in thick plies occurs as a result of type T cracking followed by type L cracking*. The crack starts to propagate as the type T crack in the x_1 direction. After the crack has propagated under constant stress $\bar{\sigma}_{22} = (\bar{\sigma}_{22})_{cr}$ to width $\delta = \delta_{Ic}(L)$, it also may start to propagate in the x_3 direction, as the type L crack. This bidirectional propagation continues until 2δ has reached a certain maximum value which may not exceed the ply thickness $2a$, but may be smaller than $2a$ if the type T crack becomes arrested because of its interaction with an adjacent ply. In any case, the type L cracking continues in the x_3 direction at any $\delta \geq \delta_{Ic}(L)$ across the entire area of the ply where $\bar{\sigma}_{22} > (\bar{\sigma}_{22})_{cr}$. We recall that $G(L)$ does not depend on crack length, hence the type L crack may be arrested quite easily if the crack enters a region of low stress or locally higher toughness.

Next, suppose that the ply is loaded in pure shear, $\bar{\sigma}_{22} = 0$, $\bar{\sigma}_{23} \neq 0$. Analogous to the tension case, one finds at failure load $\bar{\sigma}_{23} = (\bar{\sigma}_{23})_{cr}$ that

$$G_{II}(T) \geq G_{IIc}(T), \quad \delta \geq \delta_{IIc}(T) \tag{22}$$

and/or

$$G_{II}(L) \geq G_{IIc}(L), \quad \delta \geq \delta_{IIc}(L) \tag{23}$$

where

$$\delta_{IIc}(T) = 2G_{IIc}(T)/\pi \, \Lambda^{\circ}_{44}(\bar{\sigma}_{23})^2_{cr}$$

$$\delta_{IIc}(L) = 4G_{IIc}(L)/\pi \, \Lambda^{\circ}_{44}(\bar{\sigma}_{23})^2_{cr}$$

and

$$\delta_{IIc}(L) = 2\gamma_{II} \, \delta_{IIc}(T) \tag{24}$$

Now, if one defines g in (12) for the two crack types as

$$g(T) = G_{Ic}(T)/G_{IIc}(T) \tag{25}$$

$$g(L) = G_{Ic}(L)/G_{IIc}(L) \tag{26}$$

then it follows that

$$\delta_{Ic}(T) = g(T) \, \delta_{IIc}(T) \tag{27}$$

$$\delta_{Ic}(L) = g(L) \, \delta_{IIc}(L) \tag{28}$$

Recall that $g = 0.1$ according to [14] for certain graphite epoxy systems. This

value is actually $g(L)$, no information seems to be available about $g(T)$. However, it appears that the critical width of the crack nucleus in thick plies is generally smaller for Mode I cracking.

Again, if the ply is loaded by simple shear, the crack nucleus starts to propagate in the x_1 direction if $2\gamma_{II} > 1$ and $\delta_{IIc}(T) < \delta_{IIc}(L)$. Bidirectional propagation may start when $\delta = \delta_{IIc}(L)$. As in the previous case, $G(L)$ is constant at fixed δ. Type L cracking continues across the loaded area of the ply as long as $\bar{\sigma}_{23} \geq (\bar{\sigma}_{23})_{cr}$.

Finally, we consider the general case of loading $\bar{\sigma}_{23} = q\bar{\sigma}_{22}$ in the ply, which is applied until failure at $(\bar{\sigma}_{23})_{cr} = q(\bar{\sigma}_{22})_{cr}$. Critical width of the crack nucleus must be found from (12) for each q. For type T cracking one can write

$$[1 - g(T)][R_I(T)]^{1/2} + g(T)\, R_I(T) + R_{II}(T) \geq 1 \tag{29}$$

where

$$\begin{aligned} R_I(T) &= G_I(T)/G_{Ic}(T) \\ R_{II}(T) &= G_{II}(T)/G_{IIc}(T) \end{aligned} \tag{30}$$

Equation (29) can be solved to yield $\delta_c(T)$.

Similarly, for type L cracking, the equation that can be used to find $\delta_c(L)$ is

$$[1 - g(L)][R_I(L)]^{1/2} + g(L)\, R_I(L) + R_{II}(L) \geq 1 \tag{31}$$

where $R_I(L)$, $R_{II}(L)$ are defined in analogy with (30).

Type T cracking precedes type L if

$$\delta_c(T) < \delta_c(L) \tag{32}$$

and vice versa. In any event, bidirectional crack propagation starts when

$$\delta = \max[\delta_c(T), \delta_c(L)] \tag{33}$$

The results derived so far suggest that if many thick plies of different thickness are tested in such a way that the loading history $\underline{\xi}(t)$ is kept constant in each test, then δ in (14) and (33) is also constant, and the measured strength must be constant, regardless of actual ply thickness.

For the special case of loading by $\bar{\sigma}_{23} = 0$, $\bar{\sigma}_{22} \neq 0$, the strength is given by the smaller of the two expressions

$$\begin{aligned} (\bar{\sigma}_{22})_{cr} &= [2G_{Ic}(T)/\pi\, \Lambda_{22}^{\circ}\, \delta_{Ic}(T)]^{1/2} \\ (\bar{\sigma}_{22})_{cr} &= [4G_{Ic}(L)/\pi\, \Lambda_{22}^{\circ}\, \delta_{Ic}(L)]^{1/2} \end{aligned} \tag{34}$$

For $\bar{\sigma}_{22} = 0$, $\bar{\sigma}_{23} \neq 0$, the strength is given by the smaller of the two expressions

$$(\bar{\sigma}_{23})_{cr} = [2G_{IIc}(T)/\pi\ \Lambda^{\circ}_{44}\ \delta_{IIc}(T)]^{1/2}$$
$$(\bar{\sigma}_{23})_{cr} = [4G_{IIc}(L)/\pi\ \Lambda^{\circ}_{44}\ \delta_{IIc}(L)]^{1/2} \tag{35}$$

Constant strength is seen in experimental results discussed in the sequel. Similar relations can be found from (29) and (31) for combined loading.

The strength of unidirectional laminates, or unconstrained thick plies, can be estimated along similar lines by assuming that the crack nucleus may most probably form at the surface. If the rate of slow growth of δ depends only on applied strain history as in (14), one should anticipate that crack nuclei of whidth $2\delta_c$ may be found at the surface of unconstrained unidirectional laminate, as well as in the interior. This implies that the estimate of transverse strength of unconstrained plies is

$$(\bar{\sigma}_{22})^{u}_{cr} = (\bar{\sigma}_{22})_{cr}/(1.12\sqrt{2}) \tag{36}$$

where $(\bar{\sigma}_{22})_{cr}$ follows from (34) and vice versa. The multiplier 1.12 accounts for the stress intensity magnification of a surface crack.

7. STRENGTH OF PLIES OF INTERMEDIATE THICKNESS

Here we consider plies of any thickness $2a$, subjected to a certain strain history, such that at onset of unstable crack propagation, the critical width of the crack nucleus $2\delta_c$ is comparable to $2a$, i.e.

$$0 < \delta_c/a < 1.$$

To evaluate this condition in an approximate manner, one may utilize δ_c found for a thick ply of the same system.

We recall that according to (8)

$$G_I(T) = \frac{1}{2}\pi\ \delta\ \eta_I^2 \Lambda^{\circ}_{22}\ \bar{\sigma}^2_{22}$$
$$G_{II}(T) = \frac{1}{2}\pi\ \delta\ \eta_{II}^2 \Lambda^{\circ}_{44}\ \bar{\sigma}^2_{23} \tag{37}$$

are the release rates for type T cracking in x_1 direction, and that from (10), for type L cracks,

$$G_I(L) = \frac{1}{4}\pi\ \delta\quad \xi_I\ \Lambda^{\circ}_{22}\ \bar{\sigma}^2_{22}$$
$$G_{II}(L) = \frac{1}{4}\pi\ \delta\quad \xi_{II}\ \Lambda^{\circ}_{44}\ \bar{\sigma}^2_{23} \tag{38}$$

At any given stress state,

$$G_I(L) = \frac{1}{2}(\xi_I/\eta_I^2)\, G_I(T)$$
$$G_{II}(L) = \frac{1}{2}(\xi_{II}/\eta_{II}^2)\, G_{II}(T) \qquad \text{for } 0 < \delta/a < 1 \tag{39}$$

Consider first the special case of loading $\bar{\sigma}_{22} \neq 0$, $\bar{\sigma}_{23} = 0$. At failure load $\bar{\sigma}_{22} = (\bar{\sigma}_{22})_{cr}$, the conditions (18) must again be met. When (18) are taken as equalities, it follows from (13) and (37) to (39) that

$$\delta_{Ic}(T) = 2G_{Ic}(T)/\pi\, \eta_I^2\, \Lambda_{22}^2\, (\bar{\sigma}_{22})_{cr}^2$$
$$\delta_{Ic}(L) = 4G_{Ic}(L)/\pi\, \xi_I\, \Lambda_{22}^2\, (\bar{\sigma}_{22})_{cr}^2 \tag{40}$$

and

$$\delta_{Ic}(L) = 2\gamma_I(\xi_I/\eta_I^2)\, \delta_{Ic}(T) \tag{41}$$

Hence, if $2\gamma_I(\xi_I/\eta_I^2) > 1$, then $\delta_{Ic}(T) < \delta_{Ic}(L)$, and the crack starts to propagate as a type T crack in the x_1 direction, and vice versa. In any case, bidirectional propagation starts when

$$\delta = \max\ \{\delta_{Ic}(T), \delta_{Ic}(L)\} \tag{42}$$

Analogous formulae can be found for the special case $\bar{\sigma}_{22} = 0$, $\bar{\sigma}_{23} \neq 0$:

$$\delta_{IIc}(T) = 2G_{IIc}(T)/\pi\, \eta_{II}^2\, \Lambda_{44}^2\, (\bar{\sigma}_{23})_{cr}^2$$
$$\delta_{IIc}(L) = 4G_{IIc}(L)/\pi\, \xi_{II}\, \Lambda_{44}^2\, (\bar{\sigma}_{23})_{cr}^2 \tag{43}$$

and

$$\delta_{IIc}(L) = 2\gamma_{II}(\xi_{II}/\eta_{II}^2)\, \delta_{IIc}(T) \tag{44}$$

Under general loading, $\bar{\sigma}_{23} = q\,\bar{\sigma}_{22}$, which continues until a critical stress level $(\bar{\sigma}_{23})_{cr} = q(\bar{\sigma}_{22})_{cr}$ has been reached, it is necessary to find $\delta_c(T)$ and $\delta_c(L)$ from (12). The equation for $\delta_c(T)$ is formally identical with (29) and (30) but $G_I(T)$, $G_{II}(T)$ must now be taken from (37). Also, for $\delta_c(L)$ one can use (31) with $G_I(L)$ and $G_{II}(L)$ from (38). Once $\delta_c(T)$ and $\delta_c(L)$ have been found from the measured ply strength and toughness, one can find that type T cracking precedes type L if

$$\delta_c(T) < \delta_c(L) \tag{45}$$

and vice versa. Bidirectional propagation starts when

$$\delta = \max |\delta_c(T), \delta_c(L)| \tag{46}$$

In theory, one can use inversion of (40) and (43) in conjunction with Figures 3 and 4 to calculate ply strength. Current experimental data is insufficient to justify a detailed analysis of (40) and (43), as well as (41) and (44).

The propagation process of both types of cracks is affected by crack interaction with the adjacent ply. For type T cracking this is evident from Figure 3, where $(\eta_1^2\, \delta/a)$ reaches a maximum at a certain value of $(\delta/a)_{max}$ and then decreases. According to (37), $G(T)$ also decreases. Therefore, one may find that $G(T) < G_c(T)$ along the crack path, and the crack will stop. In fact, if $\delta_c(T)/a$ coincides with or is larger than $(\delta/a)_{max}$, then unstable type T cracking may be prevented altogether, and only slow growth may take place in x_1 direction until $\delta = \delta_c(L)$.

On the other hand, type L cracks may propagate across the entire loaded area of the ply as soon as $\delta = \delta_c(L)$. It is not certain that the crack retains its initial width during propagation. The width will probably increase to $2\delta = 2a$ because this will enhance $G_I(L)$ and $G_{II}(L)$. The width adjustment may occur even during slow growth of the crack nucleus in x_3 direction. The crack will probably try to fan out across ply width, especially when γ_I and γ_{II} are small. This is a three-dimensional crack problem that cannot be resolved on the basis of two-dimensional solutions which have been used therein.

8. STRENGTH OF THIN PLIES

Here we consider plies of any thickness $2a$, subjected to a certain strain history, such that at onset of unstable crack propagation

$$2\delta_c(L) = 2a \tag{47}$$

It follows from (40_2), (43_2), and their mixed mode equivalents that the strength of thin plies is

$$\begin{aligned} (\bar{\sigma}_{22})_{cr} &= [4G_{Ic}(L)/\pi\, \xi_I\, \Lambda_{22}^2\, a]^{1/2} \quad , \quad \text{at } \bar{\sigma}_{23} = 0 \\ (\bar{\sigma}_{23})_{cr} &= [4G_{IIc}(L)/\pi\, \xi_{II}\, \Lambda_{44}^2\, a]^{1/2} \quad , \quad \text{at } \bar{\sigma}_{22} = 0 \end{aligned} \tag{48}$$

In the general loading case $\bar{\sigma}_{23} = q\, \bar{\sigma}_{22}$ one can calculate $(\bar{\sigma}_{22})_{cr}$ from (31), providing that $G_I(L)$ and $G_{II}(L)$ are taken from (38) with $\delta = a$.

Accordingly, the strength of thin plies becomes related only to onset of unstable type L cracking, much as the strength of a thick ply was related to type T cracking.

If experimentally measured strength data are available for thin plies of variable thickness, then one can always find $G_{Ic}(L)$ and $G_{IIc}(L)$ of the composite system in question.

At this stage it may well be necessary to consider the possibility of interface

damage discussed at the end of Section 4. As a consequence, ξ_i may increase beyond their theoretical estimate. In the absence of adequate experimental information one can tentatively take

$$\xi_I = \xi_{II} = 1, \text{ and } \delta_c(L) = a \tag{49}$$

With this adjustment, one can calculate ply strength from (48) and (49) providing that $G_{Ic}(L)$ and/or $G_{IIc}(L)$ are known. In the general loading case $\bar{\sigma}_{23} = q\,\bar{\sigma}_{22}$ one can calculate $(\bar{\sigma}_{22})_{cr}$ from (31), if $G_I(L)$ and $G_{II}(L)$ are taken from (38) at $\delta = a$.

As long as the strength of plies of intermediate thickness cannot be completely analyzed with available data, it suffices to consider only thick and thin plies. The transition between these two extremes can be defined as the intersection of strength curves calculated from (34), (35), and (48), respectively. Since at either side of this transition point the ply strength is controlled by either type (T) or type (L) cracking, there will be a discontinuous change in the critical width of crack nucleus from $\delta_c(T)$ to $\delta_c(L)$. Of course, if it were possible to analyze plies of intermediate thickness, this discontinuity would be bridged.

9. COMPARISON WITH EXPERIMENTS

To illustrate the theoretical derivation, we interpret results presented by Bailey, et al. [3], and by Crossman, Wang, et al., [15,16]. Figure 5 shows the first set

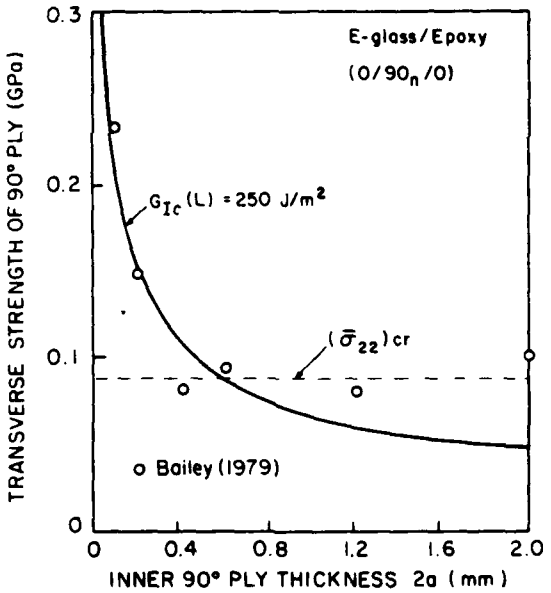

Figure 5. *Comparison of theoretical results with experimental data.*

Table 1. Material properties of selected plies.

	E-Glass/Epoxy	T300/934
E_L (GPa)	42	163.4
E_T (GPa)	14	11.9
ν_L	0.27	0.3
α_L (10^{-6}/°C)	4.3	0.35
α_T (10^{-6}/°C)	14.3	28.8
$\Delta\theta$ (°C)	−125	−125

of results. Several $(0/90_n)_s$ coupons made of a E-glass/epoxy laminated plate were loaded in tension, and the laminate stress or strain was recorded at first failure of the 90° ply (c.f., Figure 13, p. 616 in [3]). To interpret the data, laminated plate theory was used to calculate initial thermal stresses in the 90° ply after cooling from the curing temperature to room temperature, $\Delta\theta = -125°C$. Then, the transverse normal stress $\bar{\sigma}_{22}$ caused in the 90° ply by loading of the laminate was found, and superimposed with thermal stress. In this way, the original data points were converted to ply stress $\bar{\sigma}_{22}$, and then plotted in Figure 5. Thermoelastic properties of the ply were taken from Table 1; these were found in Table 1 in [3], and confirmed by comparison of calculated and measured laminate properties.

Next, ply toughness $G_{Ic}(L) = 250\ J/m^2$ was found by inversion of $(48)_s$ such that the resulting $(\bar{\sigma}_{22})_{cr}$ curve fitted the experimental points at low ply thicknesses.

Then, experimental points for thick plies were used to find the average strength of thick plies as $(\bar{\sigma}_{22})_{cr} = 0.089$ GPa. This strength exceeds the value measured on free 90° plies, which was found as 0.056 GPa, and must be converted to constrained 90° ply strength of $0.056^* (1.12\ \sqrt{2}) = 0.0885$ GPa, with the help of (36). The prediction agrees well with the measured values. The transition between thin and thick plies is found at $2a = 0.5$ mm in this case.

Table 2. Critical widths of type T crack nuclei in thick plies, calculated from (19).

	E-Glass/Epoxy	T300/934
$G_{Ic}(T)$ (J/m²)	$2\delta_{Ic}(T)$ (mm)	$2\delta_{Ic}(T)$ (mm)
200	0.231	0.372
400	0.461	0.745
600	0.692	1.117
800	0.922	1.489
Thick ply strength (GPa)	0.089	0.064

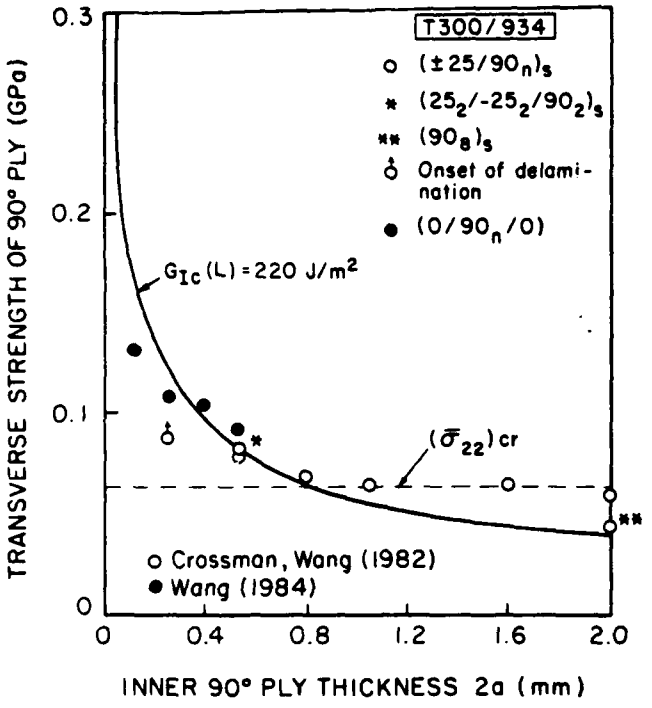

Figure 6. *Comparison of theoretical results with experimental data.*

No definite evaluation of $\delta_{tc}(T)$ can be made, because $G_{tc}(T)$ was not measured. However, expected values at specified G_{tc} are shown in Table 2. For example, if $G_{tc}(T)$ is taken as equal to $G_{tc}(L) = 250$ J/m², then $2\delta_{tc}(T) = 0.288$ mm. In any event, $\delta_{tc}(T) < a$. At the transition point between thin and thick plies $2a = 0.5$ mm, hence $2\delta_{tc}(T) < 0.5$ mm. At the measured strength of thick plies (0.089 GPa), this suggests that $G_{tc}(T) < 433$ J/m². In reality, both $2\delta_{tc}(T)$ and $G_{tc}(T)$ should be much smaller, so that type T cracking may take place even as ply thickness approaches the transition value of 0.5 mm.

Figure 6 shows similar results for a T300/934 graphite/epoxy system, which appeared in [15,16]. Data for three different layups, $(\pm 25/90_n)_s$, $(25_2/-25_2/90_2)_s$, and $(0/90_n/0)$, were superimposed to find $G_{tc}(L)$ in the 90° plies. The results are apparently not affected by the differences in layup of outside layers. Also shown is the strength of a free $(90_8)_s$ ply, which again conforms with (36). The $G_{tc}(L)$ values are somewhat lower than those found by Slepetz and Carlson [17] for glass and graphite-epoxy systems.

Note that the G_{tc} values shown in Figures 5 and 6 are actually values of G_{tc}/ξ_t with ξ_t taken as equal to unity, because of possible interface damage. If ξ_t was taken as equal to calculated values, e.g. $\xi_t = 0.8$ in E-glass/epoxy, then one

would obtain $G_{Ic} = 200$ J/m² in Figure 5, which compares better with the $G_{Ic} = 120 \pm 30$ J/m² indicated for this material in Table 1 of [3].

Finally, we recall that $G(L)$ does not depend on crack length, hence type L cracks mayh be arrested rather easily due to local reduction in applied stress or ply toughness $G_{Ic}(L)$. Figure 2 in [5] shows photographs of crack patterns in plies of various thicknesses. An examination of these results reveals many arrested cracks in a thin ply (0.75 mm) where failure depends on type L cracking. Only very few arrested cracks can be seen in thicker plies which start to fail by type T cracks, and where $G(L)$, although still constant, should be much larger than $G_c(L)$ when the type L crack propagates along a wide front $\delta = a > \delta_c(L)$.

10. DISCUSSION

The theoretical results can predict strength of plies in a laminate as a function of ply thickness and applied stress state, provided experimental values of ply toughnesses in (13) are known. Also, the correct form of (12), and the ratios $g(T)$ and $g(L)$ in (25) and (26) are needed in case of combined loading. While some of these parameters may not be readily available in certain applications, the results are of value in estimating the benefit that enhanced ply toughness may have on strength.

Furthermore, the results suggest that strength of thick plies may be significantly reduced by damage which introduces crack nuclei of sufficient size into the ply. Free edge damage caused in the process of delamination or machining, as well as impact damage or penetrations can be sources of such initial cracks. For plies which have been damaged in this manner, one should assume that crack nuclei of width $2\delta = 2a$ are present from the outset, and that all ply cracking takes place in the fiber direction x_3. The strength of such damaged plies, regardless of their thickness, is given by thin ply formulae (46) and their equivalents, and can be substantially lower than that of undamaged thick plies.

Another application of the present results can be made if the growth rate of the crack nucleus δ in (14) is known for specific loading histories. As long as the material properties in (13) are given constants, one can calculate $\delta_c(t)$, and from that the effect of the loading history on ply strength.

ACKNOWLEDGEMENT

This work was supported by a grant from the Air Force Office of Scientific Research. Dr. M. Hejazi and Dr. C. J. Wung provided assistance in interpretation of experimental data.

REFERENCES

1. Dvorak, G. J., N. Laws and M. Hejazi. "Analysis of Progressive Matrix Cracking in Composite Laminates. I. Thermoelastic Properties of a Unidirectional Composite with Cracks," *J. Composite Materials*, 18 (1985).
2. Dvorak, G. J. and W. S. Johnson. "Fatigue of Metal Matrix Composites," *International Journal of Fracture*, 16:585 (1980).

3. Bailey, J. E., P. T. Curtis and A. Parvizi. "On the Transverse Cracking and Longitudinal Splitting Behaviour of Glass and Carbon Fibre Reinforced Epoxy Cross Ply Laminates and the Effect of Poisson and Thermally Generated Strain," *Proc. R. Soc. Lond. A.*, 366:599 (1979).
4. Bascom, W. D. Private Communication (1984).
5. Garrett, K. W. and J. E. Bailey. "Multiple Transverse Fracture in 90° Cross-ply Laminates of a Glass Fibre-Reinforced Polyester," *J. Materials Science*, 12:157 (1977).
6. Stroh, A. N. "Dislocations and Cracks in Anisotropic Elasticity," *Phil. Mag.*, 3:625 (1958).
7. Laws, N. "A Note on Interaction Energies Associated with Cracks in Anisotropic Media," *Phil. Mag.*, 36:367 (1977).
8. Hilton, P. D. and G. C. Sih. "A Laminate Composite with a Crack Normal to the Interface," *Int. J. Solids Structures*, 7:913 (1971).
9. Cook, T. S. and F. Erdogan. "Stresses in Bonded Materials with a Crack Perpendicular to the Interface," *Int. J. Engng. Sci.*, 10:677 (1972).
10. Delale, F. and F. Erdogan, "Bonded Orthotropic Strips with Cracks," *Int. J. Fracture*, 15:343 (1979).
11. Chou, P. C., A. S. D. Wang and H. Miller. "Cumulative Damage Model for Advanced Composite Materials," Report AFWAL-TR-82-4083 (1982).
12. Lu, M. C. and F. Erdogan. "Stress Intensity Factors in Two Bonded Elastic Layers Containing Cracks Perpendicular to and on the Interface—I. Analysis—II. Solution and Results," *Engineering Fracture Mechanics*, 18:491-528 (1983).
13. Reifsnider, K. L., W. S. Stinchcomb, E. G. Henneke and J. C. Duke. "Fatigue Damage-Strength Relationships in Composite Laminates," AFWAL-TR-83-3084, Vol. 1 (September 1983).
14. Hahn, H. T. and T. Johnnesson. "Fracture of Unidirectional Composites, Theory and Applications," in *Mechanics of Composite Materials—1983*, G. J. Dvorak, ed. AMD-Vol. 58:135, New York (1983).
15. Wang, A. S. D. "Fracture Mechanics of Sublaminate Cracks in Composite Materials," *Composites Technology Review*, 6:45 (1984).
16. Crossman, F. W. and A. S. D. Wang. "The Dependence of Transverse Cracking and Delamination on Ply Thickness in Graphite/Epoxy Laminates," ASTM-STP 775:118 (1982).
17. Slepetz, J. M. and L. Carlson. "Fracture of Composite Compact Tension Specimens," ASTM-STP 593:143 (1975).

ANALYSIS OF MATRIX CRACKING IN COMPOSITE LAMINATES: THEORY AND EXPERIMENT

G. J. Dvorak
Department of Civil Engineering
Rensselaer Polytechnic Institute
Troy, New York

N. Laws
Department of Mechanical Engineering
University of Pittsburgh
Pittsburgh, Pennsylvania

ABSTRACT

A summary of recent results is presented on the subject of progressive ply cracking in fibrous laminates. First, evaluation of stiffness changes caused by systems of aligned slit cracks which are parallel to the fiber direction in a unidirectional composite lamina is discussed. Results obtained by the self-consistent method are presented. Next, a procedure for estimating instantaneous crack densities and stiffness changes in a lamina subjected to prescribed strain history is outlined. Specific examples and comparisons of analytical and experimental results are presented for two graphite-epoxy systems.

INTRODUCTION

In many fibrous composite systems the failure strain of the fiber far exceeds that of the matrix. Under load, the difference is usually accommodated by matrix cracking. This is frequently observed in monotonically or cyclically loaded laminated plates, where each layer may contain a system of aligned slit cracks which grow in the direction of the fibers and across the thickness of the ply. Such cracks are often called ply cracks or transverse cracks, although it is more appropriate to reserve the latter for cracks which are perpendicular to the fiber axis, and refer to cracks which grow parallel to the fiber direction as axial cracks.

In polymer matrix composites axial matrix cracking typically starts at low strain levels in the weakest off-axis ply. As loading continues, cracks appear in other off-axis plies; also, their density increases until it reaches a certain saturation level. For example, in statically loaded $(0/90)_s$ graphite-epoxy laminates the minimum crack spacing was observed to be equal to 3.5-4.0 thicknesses [1]. In metal matrix composites, matrix cracking appears to be caused only by cyclic loads which exceed the shakedown limit of the laminate [2]. Under such circumstances the matrix experiences cyclic plastic straining and, consequently, low-cycle fatigue failure. Both axial and transverse cracking is present, the former in off-axis plies, the latter in zero degree plies. The crack patterns and densities are generally similar to those found in polymer matrix systems. However, saturation density increases with load amplitude, and it is not unusual to find cracks as close as one ply thickness.

In polymer matrix systems each crack apparently propagates very rapidly, as a Griffith crack. In metal matrix systems, under cyclic loading the cracks grow slowly. However, each single crack creates only a small increment in average crack density of the ply. Therefore, transverse cracking is <u>progressive</u> in the sense that crack density increases gradually with applied load, regardless of the rate of local crack progagation.

In a typical part of a laminated composite structure, removed from concentrated loads and free edges, matrix cracking is the initial, low-stress damage mode under applied load. It is eventually followed by other types of damage, such as delamination between layers and fiber breaks; but these appear at relatively high loads which may exceed allowable design magnitudes. In contrast, matrix cracks grow at low loads, and they can significantly impair stiffness and strength of composite structures, especially those containing many off-axis plies. For example, fatigue tests on both polymer and metal matrix laminated plates indicate that stiffness and residual static strength reductions caused by cracking in plies may be as high as 10-50% after 2×10^6 cycles of loading [2,3]. It is therefore desirable to consider the effect of matrix cracking on composite properties in design. Furthermore, matrix cracking is unavoidable, whereas certain other damage modes, such as free edge delamination can be prevented if appropriate precautions are taken in design.

Sufficiently general theoretical models of progressive cracking in composite laminates are apparently not to be found in the literature. Such results as are available for angle-ply laminates have been obtained from finite element calculations [1], while other studies have focused on $(0/90_n)_s$ laminates [4].

The purpose of this research is to develop a procedure for prediction of crack densities in individual plies of a laminated composite structure as a function of applied load, and to evaluate the effect of cracks on stiffness of the structure.

The analysis has been performed in the following steps:

a) Evaluation of overall thermoelastic properties of a fibrous composite which contains a certain density of aligned slit cracks.

b) Evaluation of crack densities and stiffness changes in a single ply which is strained in a prescribed way.

c) Evaluation of crack densities and stiffness changes in a laminated composite plate which is subjected to prescribed loading. Specific examples were solved for laminated plates under in-plane loads.

STIFFNESS CHANGES CAUSED BY A SYSTEM OF CRACKS IN A PLY

First we are concerned with evaluation of overall compliance, thermal expansion coefficients (or thermal strain and stress vectors), and strain and stress averages in the phases of a fibrous lamina which contains aligned slit cracks, and is subjected to uniform mechanical loads and thermal changes. The approach to the problem was outlined in reference [5], where we suggested that the effect of matrix crack systems on properties of fibrous composites can be analyzed, in principle, by the same techniques which are commonly used in evaluation of elastic constants of composite materials and fibrous laminates, e.g., by the self-consistent method.

TWO-PHASE MODEL OF A CRACKED LAMINA

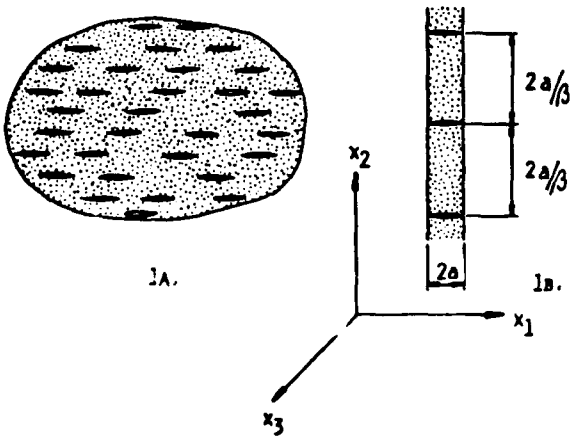

Figure 1.

1A. An infinite fibrous medium with aligned slit cracks,

1B. A fiber lamina with parallel slit cracks.

THREE-PHASE MODEL OF A CRACKED LAMINA

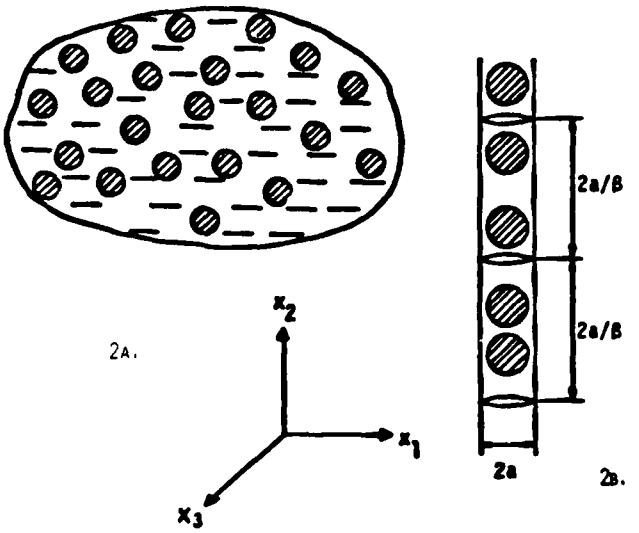

Figure 2.

2A. An infinite medium with aligned fibers and slit cracks,

2B. A fiber monolayer with cracks.

The essential approximation in the evaluation of stiffness and compliance changes of laminates consists in the replacement of a cracked layer, Figure 1b, by an effective medium which contains many cracks, Figure 1a. The crack densities can be exactly matched to provide identical stiffnesses. However, the cracks in the layer are not entirely surrounded by the layer material, instead they interact with neighboring layers which have different elastic properties. This interaction is limited to the vicinity of the crack tip, thus it may be important in analysis of local crack growth at the interface, but it has only a minor effect on lamina stiffness. We note that a similar approximation is commonly accepted in evaluation of elastic moduli of laminated composite structures reinforced by monolayers of large diameter fibers.

When the composite is reinforced by monolayers of fibers, such as boron or silicon carbide, the cracks and fibers may be of similar size. The appropriate model is shown in Figure 2. It is analogous to that of Figure 1, except that it contains three phases (fiber, matrix, and cracks), whereas the model of Figure 1 can be reduced to two phases (composite "matrix", and cracks). Accordingly, the models in Figures 1 and 2 are referred to a two-phase and three-phase models, respectively. From the practical standpoint, the effect of model choice on composite stiffness is small. The simpler two-phase model is thus sufficient for analysis of all fibrous systems.

In the three phase model we designated the fiber as phase 1, matrix as phase 2, and cracks as phase 3. In the two phase model phases 1 and 2 are joined in a homogeneous "matrix" and designated as phase 2; the voids or cracks remain phase 3.

The self-consistent analysis of the cracked composite, as outlined in [5-7], starts with a composite geometry in which the cracks are initially regarded as ellitical cylindrical inclusions. A self-consistent estimate of overall stiffness of this medium is obtained. Next, the inclusions are evacuated, i.e., replaced by voids. Finally, the aspect ratio of the voids is adjusted so that in the limit the voids change to cracks.

To evaluate crack density, the cracks in Figure 1 are first replaced by elliptic cylindrical voids, with *a*, b, *denoting the major and minor semiaxes.* If η is the number of voids per unit area in the x_1x_2-plane, then the volume fraction of voids is equal to $c_3 = \pi ab\eta$, and $c_2 + c_3 = 1$. Next, let the voids be reduced to cracks, i.e., $\delta = b/a \to 0$. Then

$$c_3 = \pi a^2 \eta \delta = \frac{1}{4} \pi \beta \delta \tag{1}$$

where $\beta = 4\eta a^2$ is the crack density parameter. In fact, β is equal to the number of cracks of fixed length, e.g., 2*a*, *in a square of side 2a. For example, if the* cracks are located in a ply, Figure 1b, then β measures the distance between regularly spaced cracks in terms of ply thickness 2a. At $\beta = 1$, the distance between cracks is equal to 2a, as β decreases the distance increases and at $\beta = 0$ the cracks vanish. We recall that the observed *minimum distances between cracks in a saturation* state are equal to 3.5-4.0 ply thicknesses, i.e., 7a-8a [1]. Corresponding values of β are 0.28-0.25, but values as high as $\beta = 1$ were observed in the B-Aℓ system [2]. Therefore $0 \leq \beta \leq 1$ is the appropriate range of β.

On the macroscale, the cracked *unidirectional composite* of Figure 1 can be regarded as an orthotropic homogeneous solid. The elastic properties of the "matrix" are identical with those of the fibrous composite and can be easily evaluated. When cracks are introduced, the macroscopic or overall elastic moduli of the solid change. To make the concept of overall moduli meaningful, it is necessary to consider overall uniform loading. Thus, we introduce uniform overall average stresses $\bar{\underset{\sim}{\sigma}}$ and strains $\bar{\underset{\sim}{\varepsilon}}$, with components arranged in (6x1) column vectors and related by constitutive equations[1]

$$\bar{\underset{\sim}{\sigma}} = L\,\bar{\underset{\sim}{\varepsilon}} \quad , \quad \bar{\underset{\sim}{\varepsilon}} = M\,\bar{\underset{\sim}{\sigma}} \quad , \tag{2}$$

where L, and M are the overall stiffness, and compliance (6x6) matrices of the cracked composite, respectively. $M = L^{-1}$ when the inverse exists. Effective properties of uncracked fibrous material (phase 2) are denoted by L^o, M^o, or by L_2, M_2.

For a dilute concentration of aligned slit cracks, the matrices L and M can be evaluated by the self-consistent method. This was done in Reference [5]; the results are:

$$L = L^o - \bar{\beta}\, L^o \Lambda\, L \tag{3}$$

$$M = M^o + \bar{\beta}\, \Lambda \quad , \tag{4}$$

where

$$\bar{\beta} = \frac{1}{4} \pi \beta \tag{5}$$

The matrix Λ has only three nonzero components, which are expressed in terms of compliances M of the effective medium as:

$$\Lambda_{22} = \frac{M_{22}M_{33} - M_{23}^2}{M_{33}} \left(\alpha_1^{1/2} + \alpha_2^{1/2}\right)$$

$$\Lambda_{44} = \left(M_{44}\, M_{55}\right)^{1/2} \tag{6}$$

$$\Lambda_{66} = \frac{(M_{22}M_{33} - M_{23}^2)^{1/2}(M_{11}M_{33} - M_{13}^2)^{1/2}}{M_{33}} \left(\alpha_2^{1/2} + \alpha_2^{1/2}\right)$$

where α_1 and α_2 are the roots of

$$(M_{22}M_{33} - M_{23}^2)\alpha^2 - \{M_{33}M_{66} + 2(M_{12}M_{33} - M_{13}M_{23})\}\alpha$$

$$+M_{11}M_{33} - M_{13}^2 = 0 \tag{7}$$

These results imply that only three compliance coefficients M_{22}, M_{44}, and M_{66} are affected by the introduction of cracks, the remaining six terms in M are unchanged, i.e., they remain equal to those of the *uncracked fiber composite.* In particular

$$M_{11} = M_{11}^o \;,\; M_{12} = M_{12}^o \;,\; M_{13} = M_{13}^o$$

$$M_{23} = M_{23}^o \;,\; M_{33} = M_{33}^o \;,\; M_{55} = M_{55}^o$$

$$M_{22} = M_{22}^o + \bar{\beta}(M_{22}M_{33} - M_{23}^2)(\alpha_1^{1/2} + \alpha_2^{1/2})/M_{33} \tag{8}$$

$$M_{44} = M_{44}^o + \bar{\beta}(M_{44}M_{55})^{1/2} \tag{9}$$

$$M_{66} = M_{66}^o + \bar{\beta}(M_{22}M_{33} - M_{23}^2)^{1/2}(M_{11}M_{33} - M_{13}^2)^{1/2}$$
$$(\alpha_1^{1/2} + \alpha_2^{1/2})/M_{33} \tag{10}$$

and from (7):

$$\alpha_1\alpha_2 = (M_{11}M_{33} - M_{13}^2)/(M_{22}M_{33} - M_{23}^2)$$

$$\alpha_1 + \alpha_2 = [M_{33}M_{66} + 2(M_{12}M_{33} - M_{13}M_{23})]/$$
$$[M_{22}M_{33} - M_{23}^2] \;.$$

The unknown shear compliance M_{44} can be obtained directly from (9):

$$M_{44} = M_{44}^o + \frac{\bar{\beta}}{2}[\bar{\beta}\, M_{55} + (\bar{\beta}^2 M_{55}^2 + 4M_{44}^o M_{55})^{1/2}] \tag{11}$$

[1] As in [5-7], (6x6) matrices are denoted by capital Latin or Greek letters, e.g., L, M, Λ, A, B, P, Q, and (6x1) matrices by lower case bold face letters, e.g., $\underset{\sim}{\sigma}$, $\underset{\sim}{\varepsilon}$, $\underset{\sim}{m}$, $\underset{\sim}{\ell}$.

The remaining unknowns M_{22} and M_{66} are found from (8) and (10).

These results can be utilized in (4) for a more direct evaluation of the three nonzero components of the matrix Λ in (6):

$$\Lambda_{ij} = (M_{ij} - \overset{o}{M}_{ij})/\bar{\beta} \quad . \quad (ij = 22, 44, 66) \qquad (12)$$

Of course, the same result follows from (6) and (7). In any case, the Λ_{ij} may now be substituted into (3), and the components of the overall stiffness L can be found in a closed form. The resulting expressions are given in reference [7, eqn. (A-6)].

The above procedure leads also to expressions for thermal response of the cracked lamina. Stress and strain averages in the composite matrix (phase 2) and cracks (phase 3) were evaluated as well. All results were found in closed form, as functions of Λ in (6) or (12). Specific forms appear in [7].

It is seen that the results are remarkably simple, and similar to those that are routinely used for evaluation of elastic moduli of an uncracked composite medium. This similarity is particularly useful in applications of the results to laminated structures. Existing theories for reinforced materials can be adapted to incorporate the effect of matrix cracking. Indeed, one may regard cracks as negative reinforcement which reduces stiffness of a composite, essentially in the same way as fiber reinforcement enhances it.

PROGRESSIVE MATRIX CRACKING IN A PLY

This subject is discussed extensively in [8]. Accumulation of transverse cracks in a uniformly strained fibrous lamina which is a part of a laminated plate is analyzed there by two methods. In the first one, thickness averages of strains and stresses in unbroken segments of the cracked lamina are evaluated in an approximate way and combined with fracture criteria for extension of initial flaws, and for propagation of slit cracks in the lamina. It is found that this approach cannot be applied in practice at this time because of insufficient information about the residual strength of the uncracked segments. An alternative method is proposed which regards the cracked lamina as an effective medium. Volume averages of stresses and strains are estimated by a self-consistent procedure, and combined with effective failure criteria. This approach can be applied with minimum of experimental information about ply strength, such as first ply failure data. The effective failure criterion is satisfied by adjustment of volume stress averages through increments of crack density, and the resulting ply stiffness reductions, under increasing strain. Crack densities and stiffness changes may be overestimated in this case, but the results remain on the safe side in structural applications. Specific results were found for two Gr/Ep systems.

The analysis of progressive cracking in an effective medium is made as follows: Suppose that a composite ply is subjected to current uniform strain $\underset{\sim}{\varepsilon}$, and that the corresponding crack density is $\beta_o \geq 0$. A strain increment $d\underset{\sim}{\varepsilon}$, and a thermal change $d\theta$ are applied, and a new magnitude of β is sought. β is regarded as a continuous function of strain, c.f., [7], Section 2. The overall constitutive equation of the ply is given by (2).

The solution can be obtained in the following steps:

Let $$\bar{\underset{\sim}{\varepsilon}}' = \bar{\underset{\sim}{\varepsilon}} + d\bar{\underset{\sim}{\varepsilon}} \quad , \quad \theta' = \theta + d\theta \qquad (13)$$

be the new applied strain and thermal change. The corresponding average stress in the ply is in analogy with (2)

$$\bar{\underset{\sim}{\sigma}}' = L' \bar{\underset{\sim}{\varepsilon}}' + \theta' \underset{\sim}{\ell}' \quad , \qquad (14)$$

where $L' \equiv L'(\beta)$, $\underset{\sim}{\ell}' = \underset{\sim}{\ell}'(\beta)$ are material properties from (4) and (21) in [7] at as yet unknown value of

$$\beta = \beta_o + d\beta \quad ; \quad d\beta \geq 0 \; . \qquad (15)$$

The stress components of interest in the effective failure criteria below are, according to equations (21) and (A-3) to (A-6) in [7]:

$$\bar{\sigma}'_{22} = L'_{12}(\bar{\varepsilon}'_{11} - \alpha_T \theta') + L'_{22}(\bar{\varepsilon}'_{22} - \alpha_T \theta') + L'_{23}(\bar{\varepsilon}'_{33} - \alpha_A \theta')$$

$$\bar{\sigma}'_{23} = 2L'_{44}\bar{\varepsilon}'_{23} \quad , \qquad (16)$$

The effective failure criteria are selected in the form

$$\left(\frac{\bar{\sigma}'_{22}}{\bar{\sigma}_I}\right)^2 + \left(\frac{\bar{\sigma}'_{23}}{\bar{\sigma}_{II}}\right)^2 = 1 \qquad (17)$$

Or, in analogy with the Tsai-Wu form:

$$\bar{F}_2 \bar{\sigma}'_{22} + \bar{F}_{22}(\bar{\sigma}'_{22})^2 + \bar{F}_{66}(\bar{\sigma}'_{23})^2 = 1 \qquad (18)$$

For $\beta > 0$ the magnitudes of overall strength parameters $\bar{\sigma}_I$, $\bar{\sigma}_{II}$, or $\bar{F}_2$, $\bar{F}_{22}$, $\bar{F}_{66}$ are assumed to be known functions of crack density β and ply thickness 2a. Their values must be adjusted after each increment in β. If these parameters are known only in terms of first ply failure, then the L_{ij} reduction alone must balance the stresses in (17) or (18). The crack density and stiffness reduction are overestimated in such a case, but model predictions remain on safe side in structural applications.

To determine if $d\bar{\underset{\sim}{\varepsilon}}$ and $d\theta$ actually cause additional cracking, it is first necessary to evaluate the stresses (16) with $L' = L(\beta_o)$ and $\underset{\sim}{\ell}' = \underset{\sim}{\ell}(\beta_o)$, i.e., with the material properties at the original crack density β_o. If these stresses make the left-hand side of (17) or (18) larger than unity, then an increment $d\beta$ is required to reduce the coefficients L'_{ij}, and thus the stresses to the level allowed by the particular failure criterion.

We recall that both L and $\underset{\sim}{\ell}$ are decreasing functions of β, thus the ply softens under increasing strain but remains elastic during unloading and reloading to the current stress level (17) or (18).

To illustrate typical results provided by (17), consider a graphite-epoxy ply with properties given in

TABLE I.

40% T300/5208

% OF UNCRACKED MODULUS E_L

Lay-up \ β	0.2	0.6	1.0
$(0_4, 90)$	100	99	99
$(0_2, 90)$	99	98	97
$(0, 90)$	98	96	95
$(0, 90_2)$	97	92	90
$(0, 90_4)$	95	86	82
$(0_2, \pm 45)$	99	97	95
$(0, \pm 45)$	98	94	92
$(0, (\pm 45)_2)$	97	91	86
(± 45)	91	74	59
$(0_2, \pm 75)$	99	96	95
$(0_2, \pm 60)$	99	97	95
$(0_2, \pm 30)$	99	97	95
$(0_2, \pm 15)$	100	99	99

40% T300/5208

% OF UNCRACKED MODULUS E_T

Lay-up \ β	0.2	0.6	1.0
$(0_2, \pm 45)$	97	91	87
$(0, \pm 45)$	96	89	84
$(0, (\pm 45)_2)$	95	87	80
(± 45)	91	74	59
$(0_2, \pm 75)$	100	99	99
$(0_2, \pm 60)$	99	97	96
$(0_2, \pm 30)$	92	79	71
$(0_2, \pm 15)$	88	69	59

Table I. Theoretical predictions of relative changes in axial (E_L) and transverse (E_T) Young's moduli of laminated plates at given values of crack density β in all plies.

Table II in [7]. The ply is deformed by prescribed strains $\bar{\varepsilon}_{22}$ and $\bar{\varepsilon}_{23}$ in several radial directions, while stresses are adjusted so that $\sigma_{11} = \sigma_{12} = \sigma_{13} = \sigma_{33} = 0$. For greater clarity of presentation, the ply strengths are taken as constant:

$$\bar{\sigma}_I = \bar{\sigma}_{22}^{cr} = 28.44 \text{ MPa} , \quad \bar{\sigma}_{II} = \bar{\sigma}_{23}^{cr} = 37.95 \text{ MPa}$$

These values were measured for first ply failure of an unconstrained ply, hence they represent relatively low strengths.

The results appear in Figure 3. In each case, the applied strain is plotted on the horizontal axis, the average stresses and crack densities on the vertical. The constant strengths levels are plotted as well. It is easy to see that if strengths were increasing with β, then the stress components would be elevated accordingly.

A remarkable feature of these results is the strong effect of shear strain $\bar{\varepsilon}_{23}$ on crack density increase. When only shear $\bar{\varepsilon}_{23}$, or only transverse normal strain $\bar{\varepsilon}_{22}$ is applied, one finds that β increases about twice as fast in shear when $2\bar{\varepsilon}_{23}$ is compared in magnitude to $\bar{\varepsilon}_{22}$. At the same time, the shear strength exceeds the transverse tension strength by 33%. This behavior can be related to the rate of change of the relevant stiffnessed L_{22} and L_{44} with β. We recall from Figure 2 in [5] that L_{22} decreases with β much more rapidly than L_{44}, from comparable initial levels. Thus $\bar{\sigma}_{23}$ is relatively large, much larger than $\bar{\sigma}_{22}$ for $2\bar{\varepsilon}_{23} > \bar{\varepsilon}_{22}$. Even at low $\bar{\varepsilon}_{23}/\bar{\varepsilon}_{22}$ ratios $\bar{\sigma}_{23}$ keeps increasing with applied strain while $\bar{\sigma}_{22}$ always decreases after onset of cracking.

In addition to stress changes, the ply experiences stiffness change under deformation conditions of Figure 3. These are summarized in Figure 4.

PROGRESSIVE CRACKING IN LAMINATED PLATES

The above procedure for analysis of crack accumulation in a strained ply can be combined with laminated plate theory and thus extended to cracking laminated plates. The theoretical background has been fully developed, and several examples have been solved. A complete description of the results will appear in reference [9]. Figure 5 illustrates stress and stiffness changes in a plate subjected to combined loads.

As in the case of a lamina, cracking in laminated plates must be analyzed in an incremental way. In many applications one cannot predict the exact loading history, or a detailed analysis may be undesirably complex. Under such circumstances, it is sufficient to estimate the maximum stiffness loss caused by the greatest possible damage in individual plies. Ply properties for this case were found in [7], for large values of β. Actual ply stiffness values in this case are well approximated when β is taken as equal to unity.

The effect of a fixed, uniform crack density in all plies of the laminated plate, on longitudinal (E_L) and transverse (E_T) in-plane moduli of plates of different layups is illustrated in Tables I, II, and III [10]. It is seen that the stiffness loss caused by extensive cracking can be very significant in certain composite systems.

A comparison of the theoretical results with experimental observations is presented in Figure 6. Axial stiffness of a $(0,90_3)_s$ E-glass-epoxy plate is plotted against observed crack density for a uniaxial tension test. The experimental points and shear lag analysis were presented in [11]. The theoretical (SCM) curve was calculated with the self-consistent approximation described earlier. A very good agreement of this curve with experiments is indicated. A remarkable feature of this correlation is that the only material constants used in the analysis were the original elastic moduli of the uncracked composite. With this information the stiffness changes were evaluated for given crack density from (3) for the 90° plies, and overall laminate stiffness change was found from laminated plate theory.

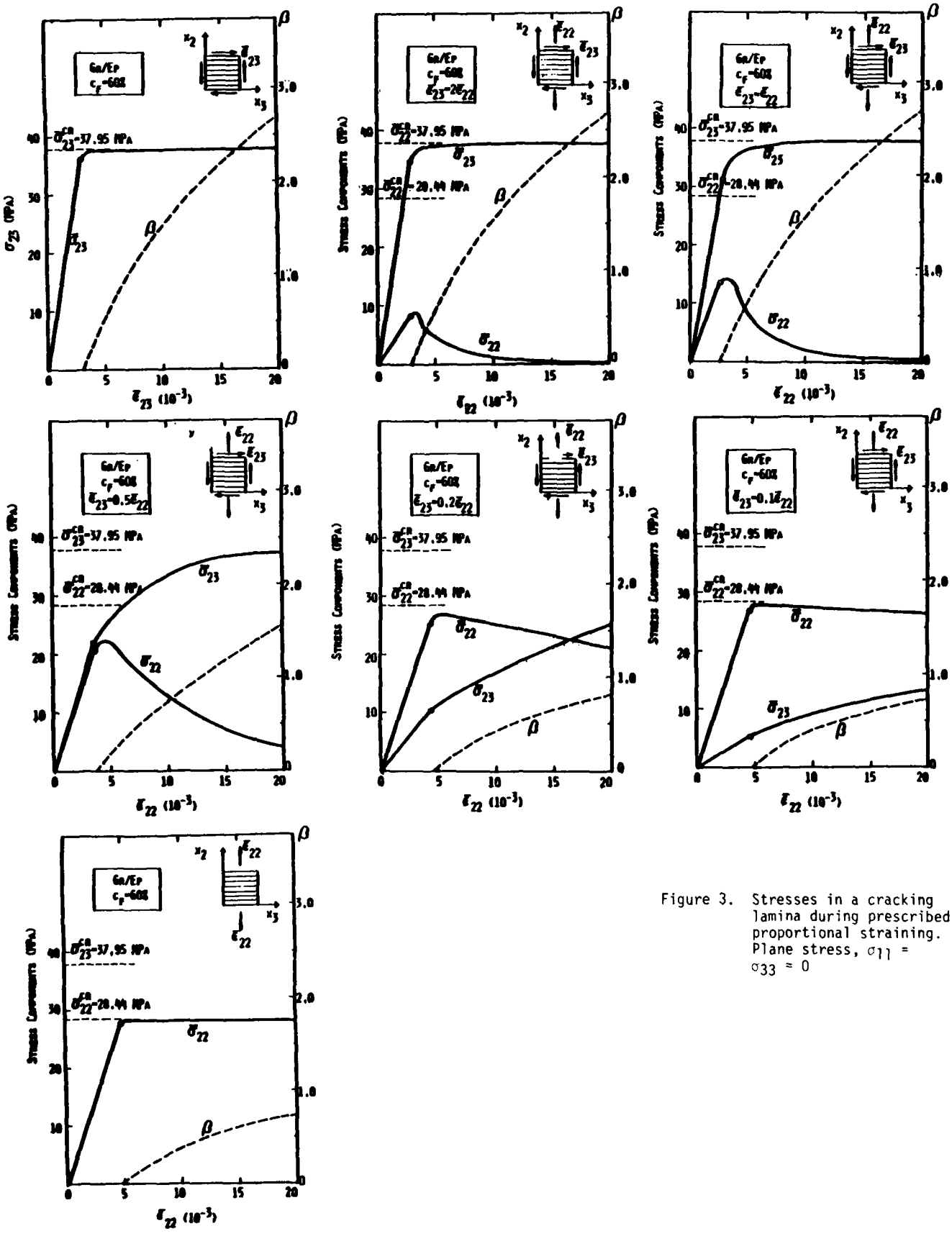

Figure 3. Stresses in a cracking lamina during prescribed proportional straining. Plane stress, $\sigma_{11} = \sigma_{33} \approx 0$

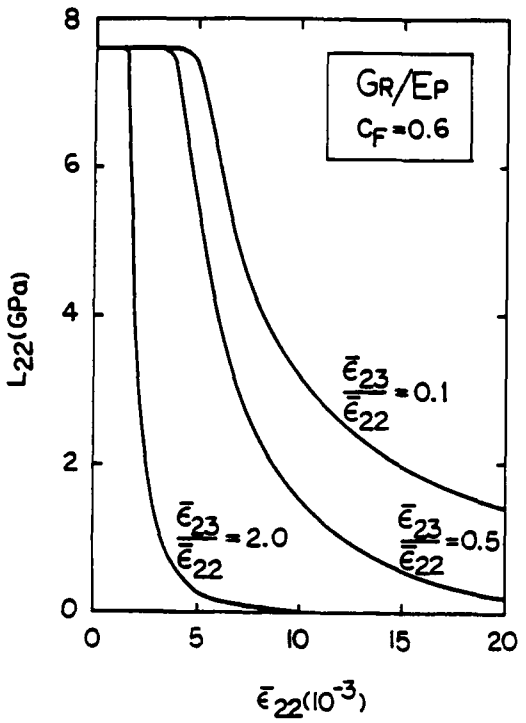

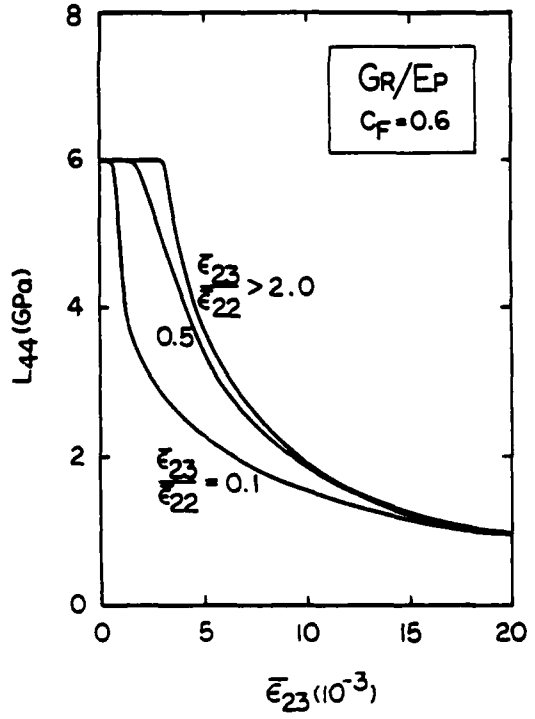

Figure 4. Stiffness changes in the graphite-epoxy ply of Figure 3, as functions of applied strain.

60% E-GLASS/EPOXY

% OF UNCRACKED MODULUS E_L

Lay-up \ β	0.2	0.6	1.0
$(0_2,\pm45)$	92	83	75
$(0,\pm45)$	88	75	63
$(0,(\pm45)_2)$	84	67	50
(±45)	77	51	25

% OF UNCRACKED MODULUS E_T

Lay-up \ β	0.2	0.6	1.0
$(0_2,\pm45)$	86	73	64
$(0,\pm45)$	82	66	53
$(0,(\pm45)_2)$	80	60	44
(±45)	77	51	25

Table II. Theoretical predictions of relative changes in axial (E_L) and transverse (E_T) Young's moduli of laminated plates at given values of crack density β in all plies

40% BORON/ALUMINIUM

% OF UNCRACKED MODULUS E_L

Lay-up \ β	0.2	0.4	0.6
$(0_4,90)$	96	93	91
$(0_2,90)$	93	87	83
$(0,90)$	89	80	73
$(0,90_2)$	85	71	62
$(0,90_4)$	80	64	51
$(0_4,\pm45)$	96	93	90
$(0_2,\pm45)$	94	89	85
$(0,\pm45)$	91	84	78
$(0,(\pm45)_2)$	89	80	73

% OF UNCRACKED MODULUS E_T

Lay-up \ β	0.2	0.4	0.6
$(0_4,\pm45)$	95	90	87
$(0_2,\pm45)$	93	86	81
$(0,\pm45)$	90	82	75
$(0,(\pm45)_2)$	88	78	70

Table III.

Theoretical predictions of relative changes in axial (E_L) and transverse (E_T) Young's moduli of laminated plates at given values of crack density β in all plies.

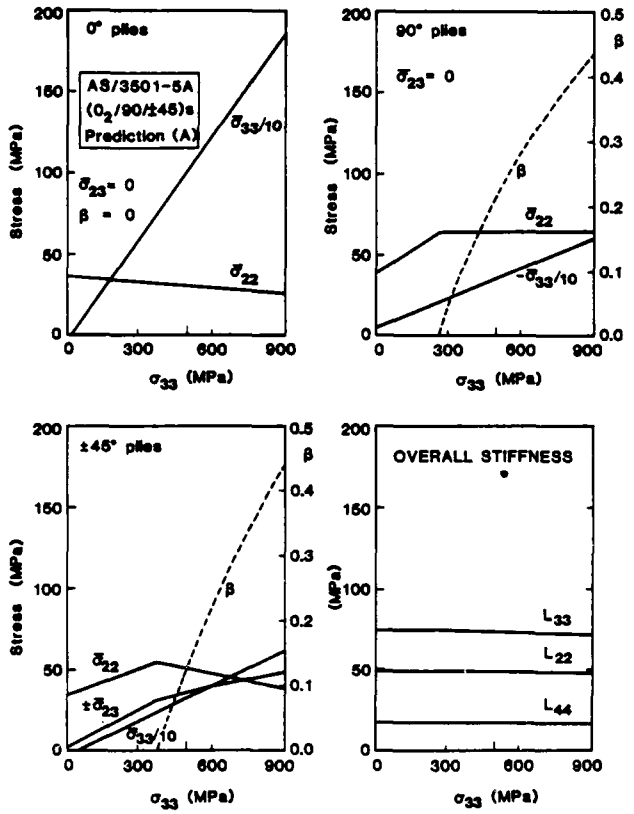

Figure 5. Calculated changes in ply stresses $\bar{\sigma}_{ij}$ and plate stiffnesses L_{ij} in a graphite-epoxy plate loaded in simple tension σ_{33} in the 0° direction. All stresses are in local ply coordinates, the fiber direction coincides with local $\bar{x}_3$ axis of a ply.

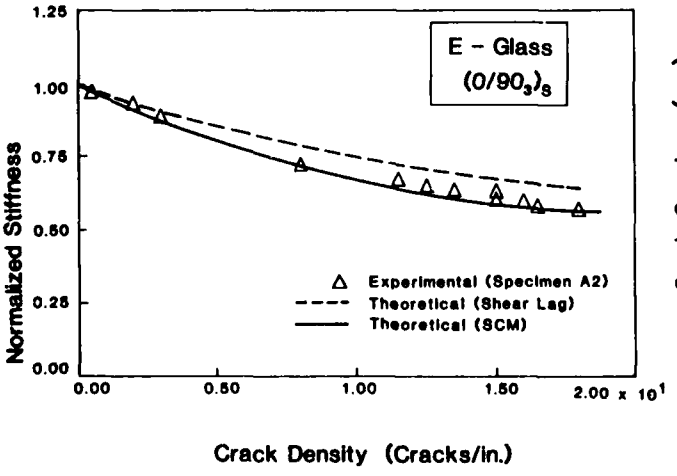

Figure 6. Comparison of experimentally observed stiffness changes and crack densities [11] with theoretical predictions. The (SCM) curve was calculated from the self-consistent estimate of stiffness in 90° plies, Equation (3).

Additional comparisons were made with experimental results obtained by Hwang and Hahn [12] who measured crack density as a function of applied stress or strain in AS/3501-5A laminated plate coupons in tension, and, with similar experiments reported by Ryder and Crossman [13] for laminated T300/5208 plate coupons.

Analytical predictions of crack densities in these laminated plate coupons were made as follows: First, laminated plate theory was used to calculate residual thermal stresses in each ply caused by cooldown from the curing temperature. The temperature difference was ΔT=147°C for both systems. Then ply stresses caused by a uniaxial applied load were evaluated and superimposed on the thermal residual stresses in each ply. Next, (18) was rewritten for each ply in the form given by Hahn [14]:

$$(1-g)\left(\frac{\bar{\sigma}_{22}}{\bar{\sigma}_I}\right) + g\left(\frac{\bar{\sigma}_{22}}{\bar{\sigma}_I}\right)^2 + \left(\frac{\bar{\sigma}_{23}}{\bar{\sigma}_{II}}\right)^2 - 1 = 0 \qquad (19)$$

where the stresses $\bar{\sigma}_{22}$, $\bar{\sigma}_{23}$ are taken in local ply coordinates, x_3 is parallel to local fiber direction. The $\bar{\sigma}_I$, $\bar{\sigma}_{II}$ denote critical stresses at first ply failure. The parameter, which accounts for failure mode interaction in an approximate way was taken as g=0.1.

Now, to determine $\bar{\sigma}_I$ and $\bar{\sigma}_{II}$ for the laminate test data shown in Figures 7 and 8, one calculates the local stress $\bar{\sigma}_{22}$ at first ply failure in the 90° ply. Since σ_{23} = 0 in this ply, one obtains $\bar{\sigma}_I$ from (19). Then, additional stress is applied to the laminate, and crack density β in the 90° ply is calculated incrementally, according to the sequence (13) to (19). The stiffness of the 90° ply gradually decreases in the process. When the applied stress reaches the magnitude required for first ply failure in the +45° ply, $\bar{\sigma}_{II}$ in this ply is again found from (19).

These results are listed in Table IV as predictions (A) and (B) for the two coupons.

In a similar way, the results in Figures 9 and 10 were interpreted and provided values of $\bar{\sigma}_I$ and $\bar{\sigma}_{II}$ in predictions (C), (D) and (E), Table IV.

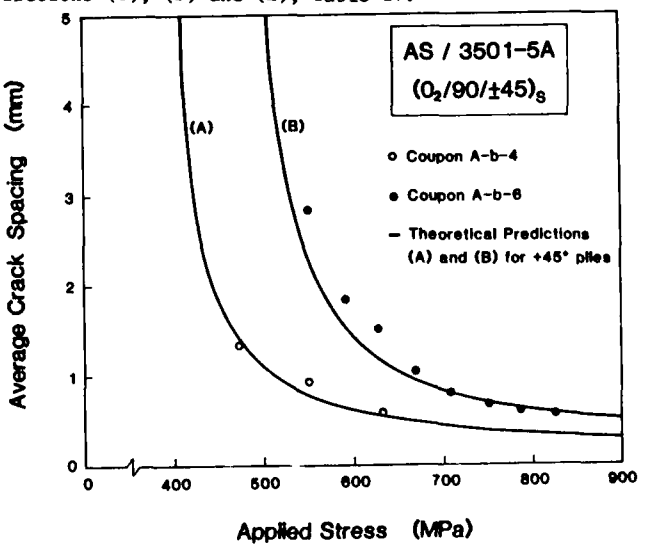

Figure 7. Comparison of predicted and observed average crack spacing in a laminated plate subjected to uniaxial tension. Experimental data from Hwang and Hahn (1982).

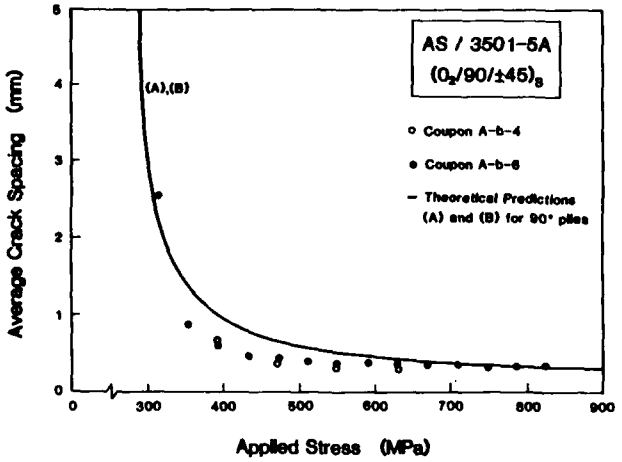

Figure 8. Comparison of predicted and observed average crack spacing in a laminated plate subjected to uniaxial tension. Experimental data from Hwang and Hahn (1982).

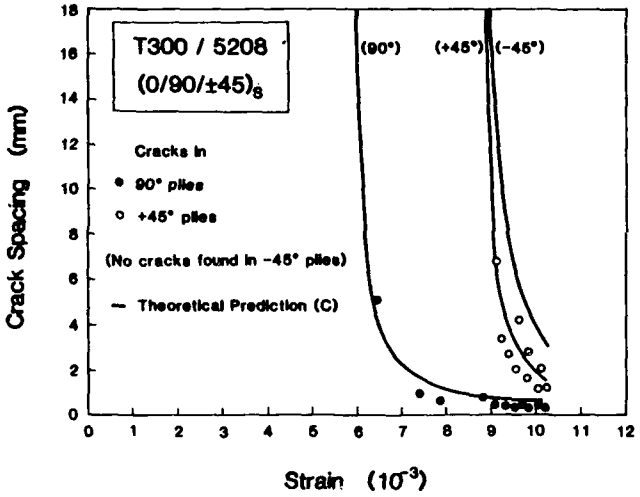

Figure 9. Comparison of predicted and observed average crack spacing in a laminated plate subjected to uniaxial extension. Experimental data from Ryder and Crossman (1984).

Table IV. Effective Ply Strength At First Ply Failure

Prediction	$\bar{\sigma}_I$ MPa	$\bar{\sigma}_{II}$ MPa	Material	Layup	Coupon
A	64.5	73.5	AS/3501-5A	$(0_2/90/\pm45)_s$	A-s-4
B	64.5	125		$(0_2/90/\pm45)_s$	A-s-6
C	83	105	T300/5208	$(0/90/\pm45)_s$	
D	45			$(0_2/90_4)_s$	A2
E	70			$(0_2/90_4)_s$	A1

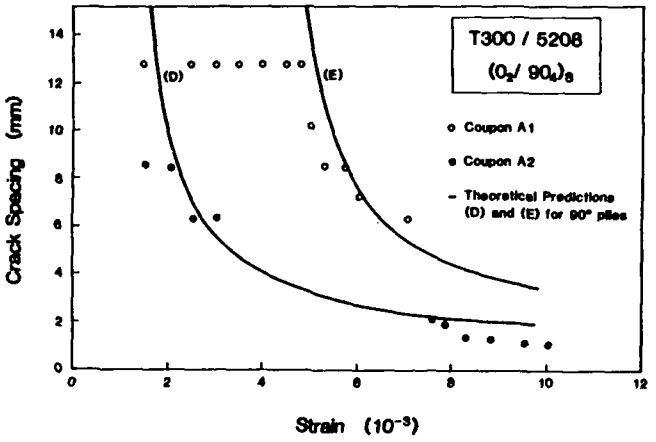

Figure 10. Comparison of predicted and observed average crack spacing in a laminated plate subjected to uniaxial extension. Experimental data from Ryder and Crossman (1984).

The experimentally found values of the critical stress $\bar{\sigma}_I$ and $\bar{\sigma}_{II}$ at first ply failure in (19) are actually the sole material parameters needed to fit the data. The only additional information entering the analysis are original elastic moduli of the undamaged laminate, and the empirical factor g=0.1 in (19).

The magitudes of $\bar{\sigma}_I$ and $\bar{\sigma}_{II}$ are fairly consistent. Note that predictions (A) and (B) apply to both 0° and 45° plies in Figure 7 and 8. Differences between (A) and (B) are caused by differences in experimental data. Prediction (C) is sufficient for all plies in Figure 9, except for the -45° ply as explained below. Predictions (D) and (E) in Figure (10) are different because the data points for the two coupons are so far apart.

It would be desirable to find that one set of critical stresses fits all data for a particular system, or for the two grafite-epoxy systems of Figures 7 to 10. This is not exactly possible but we note that $\bar{\sigma}_I$ in (A) (B) and (D) are similar; ideally they should coincide since they refer to a single system. Still they are closer together than those in (D) and (E) found for not only one system, but also one layup. In fact the two coupons A1 and A2 were taken from the same laminated plate.

Therefore, one can conclude that the differences in effective ply strength at first ply failure in Table IV are caused by variations in material properties that affect the experimental data.

A surprising feature of the experimental results shown in Figures 7 and 9 is that no cracks were observed in the interior -45° plies. One would certainly expect to find cracks in these layers which experience the same average strain state as the +45° plies where numerous cracks were found. In fact, the -45° plies form a single ply of double thickness, and this should make it more susceptible to matrix cracking than the +45° plies of single thickness. This phenomenon requires further study.

CONCLUSIONS

1. An analytical technique has been developed for modeling of progressive transverse matrix cracking in laminated composite plates. The analysis consists of three steps. First, self-consistent estimates of laminate stiffness changes are found for a given crack density from (3) and (4). Next, the rate of crack density increase under applied load is evaluated from (13) to (19) on the basis of a selected ply failure criterion. Finally, the ply analysis is made in terms of ply stress state for a ply embedded in a laminate with several cracking plies. The instantaneous ply stresses follow from a simple adaptation of laminate plate theory.

2. A good agreement of the theory with several sets of experimental data was found. The theoretical predictions require a minimum amount of experimentally derived information, such as first ply failure stresses in the cracking ply, and elastic moduli of the undamaged laminate. No empirical parameters are required outside the ply failure criteria.

3. The theory makes it possible to calculate the instantaneous crack density in each ply, the instantaneous stresses in each ply of the laminate, as well as the average fiber and matrix stresses in each ply, after application of each load or strain increment to the laminate. The laminate can be subjected to combined three dimentional loading, and also to varying uniform thermal changes in the course of mechanical loading.

4. The analysis can be implemented through a simple numerical routine, even on a personal computer. In fact, the entire procedure for each loading step is rather similar to that used in elasticity analysis of laminated plates.

ACKNOWLEDGEMENT

This work was supported by the Air Force Office of Scientific Research and monitored by Major David Glasgow, Ph.D., who provided numerous useful suggestions. Dr. M. Hejazi and Mr. C. J. Wung participated in various stages of this work, performed the numerical calculations and helped to make comparisons of theory with experiments.

REFERENCES

1. Wang, S. D., Crossman, F. W., "Initiation and Growth of Transverse Cracks and Edge Delamination in Composite Laminates, Part 1. An Energy Method," Journal of Composite Materials, Vol. 14, 1980, p. 71.

2. Dvorak, G. J., Johnson, W. S., "Fatigue of Metal Matrix Composites," International Journal of Fracture, Vol. 16, 6, 1980, p. 585.

3. Hwang, D. G., "The Proof Testing and Fatigue Behavior of Gr/Ep Laminates," D.Sc. Dissertation, Washington University, St. Louis, MO, August 1982.

4. Bailey, J., Curtis, P.T., Parvizi, "On the Transverse Cracking and Longitudinal Splitting Behavior of Glass and Carbon Fiber Reinforced Epoxy Cross Ply Laminates and the Effect of Poisson and Thermally Generated Strain," Proc. R. Soc. Lond. A., Vol. 366, 1979, p. 599.

5. Laws, N., Dvorak, G. J., Hejazi, M., "Stiffness Changes in Composites Caused by Crack Systems," Mechanics of Materials, Vol. 2, 1983, p. 123.

6. Dvorak, G. J., Laws, N., Hejazi, M., "Matrix Cracking in Unidirectional Composites," 1983 Advances in Aerospace Structures, Materials, and Dynamics, ASME. Vol. AD-06, November 1983.

7. Dvorak, G. J., Laws, N., Hejazi, M., "Analysis of Progressive Matrix Composite Laminates. I. Thermoelastic Properties of a Unidirectional Composite Ply with Cracks," to be submitted to Journal Composites Materials, 1984.

8. Dvorak, G. J., Laws, N., "Analysis of Progressive Matrix Cracking in Composite Laminates. II. Formation and Accumulation of Cracks in a Ply," to be sumbitted to J. Composite Materials, 1984.

9. Dvorak, G. J., Laws, N. "Analysis of Progressive Matrix Cracking in Composite Laminates. III. Cracking in a Laminated Plate," to be submitted to J. Composite Materials, 1984.

10. Laws, N., Dvorak, G. J., "The Loss of Stiffness of Cracked Laminates," to appear in Fundamentals of Deformation and Fracture, presented at the J. D. Eshelby Memorial Symposium, University of Sheffield, April 1984.

11. Highsmith, A. L., Reifsnider, K. L., "Stiffness-Reduction Mechanisms in Composite Laminates," ASTM-STP 775, p. 103-117, 1982.

12. Hwang, D. G., "The Proof Testing and Fatigue Behavior of Gr/Ep Laminates," D.Sc. Dissertation, Washington University, St. Louis, MO., 1982.

13. Ryder, J. T., Grossman, F. W., "A Study of Stiffness, Residual Strength and Fatigue Life Relationships for Composite Laminates," NASA Contract Report CR-172211,, October 1983.

14. Hahn, H. T., Johannesson, J., "Fracture of Unidirectional Composites, Theory and Applications," in Mechanics of Composite Materials, 1983, G. J. Dvorak, editor, AMD-Vol. 58:13 5, ASME, New York, 1983.

reprinted from

1984 Advances in Aerospace Sciences and Engineering
Structures, Materials, Dynamics, and Space Station Propulsion – AD-08
Editors: U. Yuceoglu and R. Hesser
(Book No. G00276)

published by

THE AMERICAN SOCIETY OF MECHANICAL ENGINEERS
345 East 47th Street, New York, N. Y. 10017
Printed in U.S.A.

Engineering Fracture Mechanics Vol. 25, Nos 5/6, pp. 763–770, 1986
Printed in Great Britain.

0013-7944/86 $3.00 + .00
Pergamon Press Ltd.

ANALYSIS OF FIRST PLY FAILURE IN COMPOSITE LAMINATES

GEORGE J. DVORAK
Department of Civil Engineering, Rensselaer Polytechnic Institute, Troy, NY 12180, U.S.A.

and

NORMAN LAWS
Department of Mechanical Engineering, University of Pittsburgh, Pittsburgh, PA 15260, U.S.A.

Abstract—The mechanics of transverse cracking in an elastic fibrous composite ply is explored for the case of low crack density. Cracks are assumed to initiate from a nucleus created by localized fiber debonding and matrix cracking. It is found that cracks may propagate in two directions on planes which are parallel to the fiber axis and perpendicular to the midplane of the ply. In general, crack propagation in the direction of the fiber axis controls the strength of thin plies, while cracking in the direction perpendicular to the fiber axis determines the strength of thick plies. The theory relates ply thickness, crack geometry and ply toughness to ply strength. It predicts a significant increase in strength with decreasing ply thickness in constrained thin plies. The strength of thick plies is found to be constant, but it may be reduced by preexisting damage. Results are illustrated by comparison with experimental data.

1. INTRODUCTION

IN THIS paper we discuss some fracture mechanics problems associated with transverse cracking in composite laminates. We focus our attention at a single ply in a typical part of a laminated structure, removed from free edges and other stress concentrations. The ply is subjected to a certain deformation history in the course of incremental loading applied to the laminate. In particular, we explore the initial stage of the cracking process which consists of first ply failure, and of few subsequent failures at locations which are far apart from each other, so that the cracks do not interact. Our goal is to identify the failure modes which cause transverse cracking, relate them to appropriate fracture problems, and analyse the different stages of the cracking process.

2. CRACK GEOMETRY

A unidirectionally reinforced ply of thickness $2a$ is embedded in a laminated plate or a similar composite structure. The structure is subjected to a certain incremental loading program which, at each loading step, causes a known instantaneous strain state in the ply. We assume that in a crack-free ply the local strains are uniform, or nearly uniform, and equal to their volume averages, or overall strains $\bar{\boldsymbol{\varepsilon}}$. The strain state $\bar{\boldsymbol{\varepsilon}}$, the thermal change θ, and the resulting overall stress $\bar{\boldsymbol{\sigma}}$ in the ply are related by:

$$\bar{\boldsymbol{\sigma}} = \mathbf{L}_0\bar{\boldsymbol{\varepsilon}} - \theta\mathbf{l}_0, \qquad \bar{\boldsymbol{\varepsilon}} = \mathbf{M}_0\bar{\boldsymbol{\sigma}} + \theta\mathbf{m}_0 \tag{1}$$

where $\mathbf{L}_0$, $\mathbf{M}_0$ are stiffness and compliance matrices of the uncracked ply, and $\mathbf{l}_0$, $\mathbf{m}_0$ are the thermal stress and strain vectors. We emphasize that $\bar{\boldsymbol{\sigma}}$, $\bar{\boldsymbol{\varepsilon}}$ are ply averages, not laminate averages.

In many plate composite structures, each ply usually supports a plane state of stress. In the coordinates of Fig. 1 this suggests that overall stress components $\bar{\sigma}_{22}$, $\bar{\sigma}_{23}$ and $\bar{\sigma}_{33}$ are large in comparison with $\bar{\sigma}_{11}$, $\bar{\sigma}_{12}$ and $\bar{\sigma}_{13}$. It is easy to see that stresses $\bar{\sigma}_{22}$ and $\bar{\sigma}_{23}$ favor cracking on x_1x_3-planes. The stress $\bar{\sigma}_{33}$ does not affect these cracks. The remaining minor shear components $\bar{\sigma}_{12}$ and $\bar{\sigma}_{13}$ may exist in bent plates, but only $\bar{\sigma}_{12}$ may contribute to cracking. The normal stress $\bar{\sigma}_{11}$ is usually small. Under such loading conditions the ply will crack as indicated in Fig. 1. The laminate layers on either side of the ply have a certain thickness b and b'. If $b \geqslant b'$, then we require that $b \gg 2a$, the ply thickness.

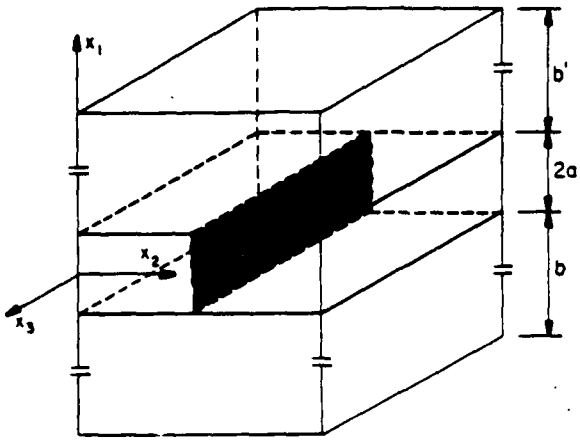

Fig. 1. Slit crack in a uniformly strained composite ply. Fibers and crack are aligned with x_3 axis.

3. CRACK NUCLEATION

It is commonly held that transverse cracks in polymer matrix composites are associated with initial fiber debonding. Several debonds may coalesce into a stable crack nucleus which grows slowly until it reaches a critical size, and then propagates as a Griffith crack. Since the in-plane contour of each fiber debond resembles an ellipse or an elongated oval, it seems reasonable to assume the same contour for the initial microcrack. The resulting shape appears in Fig. 2. Let 2δ denote the width of the microcrack. The length in x_3, which may be much larger than 2δ, need not be specified. The thickness of the ply is $2a$, the microcrack is located at mid-thickness but this does not affect the results that follow.

Now, if the ply is strained in an incremental way, the microcrack will grow slowly until it becomes a crack nucleus of certain critical width $2\delta_c$, and starts to propagate as a Griffith crack. The slow growth process is probably time-dependent in most polymer matrix systems, and one should relate the growth rate to loading history. Therefore, we write

$$\delta = \delta(\bar{\varepsilon}(t)), \qquad \text{for } \delta \leqslant \delta_c. \tag{2}$$

The rapid crack propagation can be regarded as inviscid, at least in brittle resin matrices.

4. STRENGTH OF THIN PLIES

We define thin plies by the relation

$$2\delta = 2a, \qquad \text{for } \delta \leqslant \delta_c. \tag{3}$$

In other words, the ply thickness is such that the debonded region remains stable while it grows in the ply, and it may become unstable only after it has extended across the entire ply thickness. The definition clearly depends on ply properties, such as toughness and crack growth rate (2). It also suggests that plies which contain through the thickness initial flaws or cracks induced by other types of damage must be regarded as "thin" plies regardless of their actual thickness.

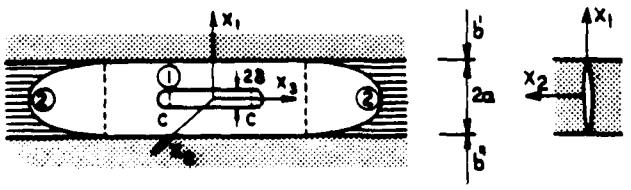

Fig. 2. Schematic of crack nucleus and type L slit crack. ① Crack nucleus, ② running longitudinal (type L) slit crack.

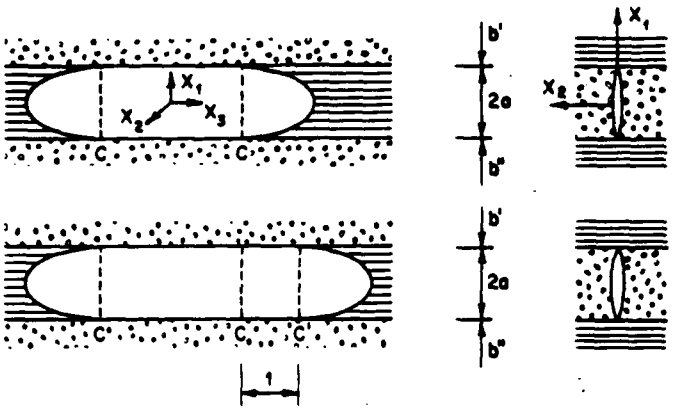

Fig. 3. Extension by unit length of a type L slit crack in a fibrous composite ply.

The energy release rate of the crack nucleus can be derived according to Fig. 3. Initially, the nucleus consists of a prismatic part CC, and precursor regions which are approximated as semielliptical cracks. The crack nucleus can extend only in the fiber direction x_3, and, as it does so, a unit extension CC' will increase the crack area by $2a*1$. The prismatic part extends by unit length and one of the precursor regions translates.

Let W_a denote the energy released by formation of the prismatic section of unit length of a ply crack of width $2a$. This is the interaction energy of the crack section. Then, the energy release rate of the crack can be written as:

$$G(\mathrm{L}) = W_a/2a \tag{4}$$

where (L) indicates that the crack extends in the longitudinal direction in the ply. As in [1], we refer to such cracks as longitudinal or type L cracks.

It is probably obvious that W_a is equal to the energy released by a microcrack of unit width x_3 which has extended in the transverse direction x_1 to length $2a$. One can write:

$$G(\mathrm{L}) = \frac{1}{a}\int_0^a G(\mathrm{T})\,\mathrm{d}\delta, \tag{5}$$

where $G(\mathrm{T})$ is the energy release rate for extension of the microcrack in the transverse direction x_1. Again, cracks growing in the x_1 direction will be referred to as T-type cracks.

If the crack nucleus was located in a very thick ply, $\delta \ll a$, then W_a could be determined from known solutions for cracks in orthotropic solids[2, 3]. In a thin ply, the crack interacts with adjacent plies of different elastic moduli, and this has an influence on W_a. As in [1], this can be reflected by writing (4) in the form

$$G(\mathrm{L}) = \tfrac{1}{4}\pi a[\xi_{\mathrm{I}}\Lambda^0_{22}\bar{\sigma}^2_{22} + \xi_{\mathrm{II}}\Lambda^0_{44}\bar{\sigma}^2_{23} + \xi_{\mathrm{III}}\Lambda^0_{66}\bar{\sigma}^2_{12}]. \tag{6}$$

Here $\bar{\sigma}_{ij}$ are the overall stresses caused in the ply by the applied strains $\bar{\varepsilon}_{ij}$, and by a uniform thermal change θ_i, ξ_i, $i = \mathrm{I}, \mathrm{II}, \mathrm{III}$ are reduction coefficients which reflect interaction of the crack in Fig. 3 with the adjacent plies, for each of the crack opening modes I, II or III. Note that mode I is the opening mode caused by $\bar{\sigma}_{22}$, mode II is the longitudinal shear mode, and mode III is the transverse shear mode. The Λ_{ij} are nonvanishing components of the crack tensor Λ^0_{ij}, derived in [4] and [5], and taken for dilute concentration of cracks:

$$\Lambda^0_{22} = \Lambda^0_{66} = 2\left(\frac{1}{E_{\mathrm{T}}} - \frac{\nu_{\mathrm{L}}^2}{E_{\mathrm{L}}}\right), \qquad \Lambda^0_{44} = 1/G_{\mathrm{L}}, \tag{7}$$

where $E_{\mathrm{L}} = E_{33}$, $E_{\mathrm{T}} = E_{11} = E_{22}$ are the longitudinal and transverse Young's moduli, $G_{\mathrm{L}} = L_{44} = L_{55}$ in [4] is the longitudinal shear modulus, and $\nu_{\mathrm{L}} = \nu_{13} = \nu_{23}$ is the corresponding Poisson's ratio.

Coefficients ξ_i can be found for many crack configurations in layered media; this is discussed in [1]. For example, $\xi_i \doteq 0.65$ in (0/90) graphite–epoxy, and $\xi_i \doteq 0.8$ in (0/90) glass–epoxy. However, one should keep in mind that the crack tips at $x_1 = \pm a$ reside in a soft matrix which may not be able to support the high crack-tip stresses. Therefore, as the crack propagates in the longitudinal direction, local crack extension along ply interface, and across this interface into the adjacent ply may take place to relieve the stress singularity. Such localized crack extension has been observed experimentally; it may be present as delamination as well as extensive fiber cracks in the next ply[6, 7]. This additional cracking will elevate W_a, and the reduction coefficients ξ_i in (6). Exact values of ξ_i are not available for running cracks.

Fracture strength of a thin ply can be found on the grounds that the $G(L)$ reaches a certain critical value. If $\bar{\sigma}_{22}$ or $\bar{\sigma}_{23}$ were acting alone, then one could compare $G_I(L)$ or $G_{II}(L)$ to the corresponding ply toughness $G_{Ic}(L)$ or $G_{IIc}(L)$. However, under combined loading, the modes are interrelated. Specific criteria which describe this effect need to be derived from experimental data. Hahn[8] offers a form based on fracture mechanics considerations that fits data obtained for certain glass–epoxy and graphite–epoxy systems:

$$(1-g)\left(\frac{G_I}{G_{Ic}}\right)^{1/2} + g\left(\frac{G_I}{G_{Ic}}\right) + \left(\frac{G_{II}}{G_{IIc}}\right) \geqslant 1, \tag{8}$$

where $g = G_{Ic}/G_{IIc}$.

If G_c are independent of loading mode, then $g \to 1$ and (8) assumes a familiar form. In actual composite plies with epoxy matrices $g \doteq 0.1$. Note that no allowance is made for mode III cracking. Modes I and II in a composite ply always create asperities on the fracture surface, as the crack seeks its way between densely packed fibers. These asperities can be interlocked and thus impede mode III cracking. Also, in a typical part of laminated plate or shell, the corresponding stress $\bar{\sigma}_{12}$ is usually small or equal to zero. Therefore, mode III need not be considered in most applications.

From (6) and (8) one can find strength of thin plies as

$$(\bar{\sigma}_{22})_{cr} = [4G_{Ic}(L)/(\pi\xi_I\Lambda^0_{22}a)]^{1/2}, \qquad \text{at } \bar{\sigma}_{23} = 0, \tag{9a}$$

$$(\bar{\sigma}_{23})_{cr} = [4G_{IIc}(L)/(\pi\xi_{II}\Lambda^0_{44}a)]^{1/2}, \qquad \text{at } \bar{\sigma}_{22} = 0. \tag{9b}$$

In the general loading case $\bar{\sigma}_{23} = q\bar{\sigma}_{22}$, one can calculate $(\bar{\sigma}_{22})_{cr}$ from (8).

Accordingly, the strength of thin plies becomes related only to onset of unstable longitudinal (type L) cracking.

If experimentally measured strength data are available for thin plies of variable thickness, then one can find $G_{Ic}(L)$ and $G_{IIc}(L)$ of the composite system in question.

5. STRENGTH OF THICK PLIES

In analogy with (3), we define thick plies by the relationship

$$2\delta \ll 2a, \qquad \text{for } \delta \leqslant \delta_c, \tag{10}$$

and adopt the configuration of the crack nucleus in Fig. 2. There is no interaction between the microcrack and the adjacent plies; hence $\xi_i \equiv 1$ in (6), and the crack width is now equal to δ rather than a. For a nucleus of width δ one obtains:

$$G(L) = \tfrac{1}{4}\pi\delta[\Lambda^0_{22}\bar{\sigma}^2_{22} + \Lambda^0_{44}\bar{\sigma}^2_{23} + \Lambda^0_{66}\bar{\sigma}^2_{12}], \qquad \text{for } \delta \ll a. \tag{11}$$

This release rate is appropriate if the nucleus propagates in x_3 direction, as a type L crack. Of course, propagation in the x_1 direction is also possible. Such cracking is referred to as type T cracking. The corresponding energy release rate is

$$G(T) = \partial W_\delta/\partial\delta, \tag{12}$$

and from (4) and (11) it follows that

$$G(\mathrm{T}) = \tfrac{1}{2}\pi\delta[\Lambda^0_{22}\bar{\sigma}^2_{22} + \Lambda^0_{44}\bar{\sigma}^2_{23} + \Lambda^0_{66}\bar{\sigma}^2_{12}], \qquad \text{for } \delta \ll a. \tag{13}$$

or

$$G(\mathrm{T}) = 2G(\mathrm{L}). \tag{14}$$

At this point we again appeal to the mixed mode failure criterion (8). However, we allow for possible differences between toughness values in the two modes by writing:

$$\begin{aligned} G_{\mathrm{Ic}}(\mathrm{L}) &= \gamma_{\mathrm{I}} G_{\mathrm{Ic}}(\mathrm{T}) \\ G_{\mathrm{IIc}}(\mathrm{L}) &= \gamma_{\mathrm{II}} G_{\mathrm{IIc}}(\mathrm{T}). \end{aligned} \tag{15}$$

Results reported in [9] and [10] indicate that γ_{I} ranges from 0.6 to 0.8 for certain graphite–epoxy plies. Data of this kind are apparently very rare, therefore no general conclusions about γ_{I} and γ_{II} magnitudes can be drawn at this time.

To determine if a given crack nucleus of width δ_c will propagate as a type T or type L crack, one can evaluate the critical values $\delta_c(\mathrm{T})$ and $\delta_c(\mathrm{L})$. For example, for modes I and II taken separately, one can find from (14) and (5) that

$$\begin{aligned} \delta_{\mathrm{Ic}}(\mathrm{L}) &= 2\gamma_{\mathrm{I}}\, \delta_{\mathrm{Ic}}(\mathrm{T}) \\ \delta_{\mathrm{IIc}}(\mathrm{L}) &= 2\gamma_{\mathrm{II}}\, \delta_{\mathrm{IIc}}(\mathrm{T}). \end{aligned} \tag{16}$$

In a mixed mode case one needs to invoke (8). Since available data indicate that $2\gamma_{\mathrm{I}} > 1$, one finds that $\delta_{\mathrm{Ic}}(\mathrm{T}) < \delta_{\mathrm{Ic}}(\mathrm{L})$. If one assumes that $\delta_c(\mathrm{T}) < \delta_c(\mathrm{L})$ under mixed loading as well, then it follows that *first ply failure of thick plies occurs as a result of transverse (type T) cracking, followed by longitudinal (type L) cracking.*

The crack starts to propagate as the type T crack in the x_1 direction. After the crack has propagated under constant stress to width $\delta = \delta_c(\mathrm{L})$, it also may start to propagate in the x_3 direction, as the type L crack. This bidirectional propagation continues until 2δ has reached the ply thickness $2a$. In any case, the type L cracking continues in the x_3 direction at any $\delta \geqslant \delta_{\mathrm{Ic}}(\mathrm{L})$ across the entire loaded area of the ply where (8) is satisfied.

The results derived so far suggest that if many thick plies of different thickness are tested in such a way that the loading history $\sigma(t)$ is kept constant in each test, then δ_c in (2) and (16) are also constant, and the measured strength must be constant, regardless of actual ply thickness.

For $\bar{\sigma}_{23} = 0$, $\bar{\sigma}_{22} \neq 0$, the strength is given by

$$(\bar{\sigma}_{22})_{\mathrm{cr}} = [2G_{\mathrm{Ic}}(\mathrm{T})/(\pi\Lambda^0_{22}\, \delta_{\mathrm{Ic}}(\mathrm{T}))]^{1/2}. \tag{17}$$

For $\bar{\sigma}_{22} = 0$, $\bar{\sigma}_{23} \neq 0$, the strength is given by

$$(\bar{\sigma}_{23})_{\mathrm{cr}} = [2G_{\mathrm{IIc}}(\mathrm{T})/(\pi\Lambda^0_{44}\, \delta_{\mathrm{IIc}}(\mathrm{T}))]^{1/2}. \tag{18}$$

Constant strength is seen in experimental results discussed in the sequel. Similar relations can be found from (8) for combined loading.

Equations (17) and (18) can be used to predict strength only if the $\delta_c(\mathrm{T})$ and $G_c(\mathrm{T})$ are known. This is usually not the case since $\delta_c(\mathrm{T})$ cannot be observed. Therefore, actual values of thick ply strength need to be measured directly in experiments.

One possible application of (17) and (18) is in experimental work aimed at evaluation of growth rates of debonded regions under different loading conditions. Such results would provide an experimental foundation for (2).

In conclusion of the theoretical part we note that one can also examine failure of plies of intermediate thickness, where the crack nucleus interacts with adjacent plies. This problem is discussed in [1]. As in the case of thick plies, implementation of the analysis requires knowledge of material properties which is not available at this time.

It is clear that a transition exists between the constant strength of thick plies (17), (18), and the

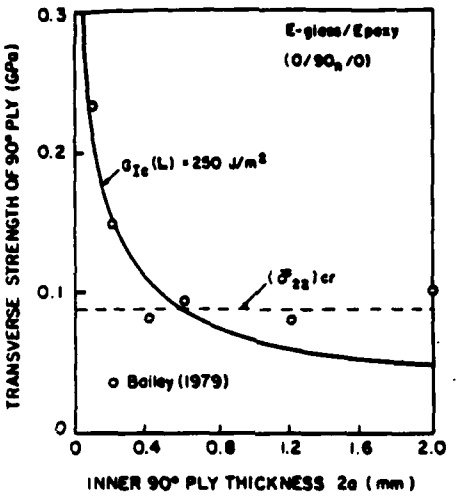

Fig. 4. Comparison of theoretical results with experimental data.

variable strength of thin plies (9). This transition takes place at a certain value of ply thickness $2a$ that can be determined from strength measurements on plies of different thickness; as shown in the sequel.

6. COMPARISON WITH EXPERIMENTS

To illustrate the theoretical derivation, we interpret results presented by Wang[10], Bailey *et al.*[11], and by Crossman and Wang[12]. Figure 4 shows the first set of results. Several $(0/90_n)_s$ coupons made of an E-glass epoxy laminated plate were loaded in tension, and the laminate stress or strain was recorded at first failure of the 90° ply. To interpret the data, laminated plate theory was used to calculate initial thermal stresses in the 90° ply after cooling from the curing temperature to room temperature, $\Delta\theta = -125°C$. Then, the transverse normal stress σ_{22} caused in the 90° ply by loading of the laminate was found, and superimposed with thermal stress. In this way, the original data points were converted to ply stress $\bar{\sigma}_{22}$, and then plotted in Fig. 4. Thermoelastic properties of the ply were taken from Table 1.

Next, ply toughness $G_{Ic}(L) = 250\,J/m^2$ was found by inversion of (9a) such that the resulting $(\bar{\sigma}_{22})_{cr}$ curve fitted the experimental points at low ply thicknesses.

Then, experimental points for thick plies were used to find the average strength of thick plies as $(\bar{\sigma}_{22})_{cr} = 0.089\,GPa$. The transition between thin and thick plies was found at $2a = 0.5\,mm$ in this case.

No definite evaluation of $\delta_{Ic}(T)$ can be made, because $G_{Ic}(T)$ was not measured. However, expected values at specified G_{Ic} are shown in Table 2. For example, if $G_{Ic}(T)$ is taken as equal to $G_{Ic}(L) = 250\,J/m^2$, then $2\delta_{Ic}(T) = 0.288\,mm$. In any event, $\delta_{Ic}(T) < a$. At the transition point between thin and thick plies $2a = 0.5\,mm$, hence $2\delta_{Ic}(T) < 0.5\,mm$. At the measured strength of thick plies (0.089 GPa), this suggests that $G_{Ic}(T) < 433\,J/m^2$. In reality, both $2\delta_{Ic}(T)$ and $G_{Ic}(T)$ should be much smaller, so that type T cracking may take place even as ply thickness approaches the transition value of 0.5 mm.

Figure 5 shows similar results for a T300/934 graphite/epoxy system, which appeared in [10, 12]. Data for three different layups, $(\pm 25/90_n)_s$, $(25_2/-25_2/90_2)_s$, and $(0/90_n/0)_s$ were superimposed to

Table 1. Material properties of selected plies

	E-Glass–epoxy	T300/934
E_L (GPa)	42	163.4
E_T (GPa)	14	11.9
ν_L	0.27	0.3
α_L (10^{-6} C)	4.3	0.36
α_T (10^{-6} C)	14.3	28.8
$\Delta\theta$ (°C)	−125	−125

Table 2. Critical widths δ_{Ic} of type T crack nuclei in thick plies, calculated from eq. (17)

$G_{Ic}(T)$ (J/m^2)	E-Glass–epoxy $2\delta_{Ic}(T)$ (mm)	T300/934 $2\delta_{Ic}(T)$ (mm
100	0.115	0.185
200	0.231	0.372
400	0.461	0.746
600	0.692	1.117
800	0.922	1.489
Thick ply strength (GPa)	0.089	0.064

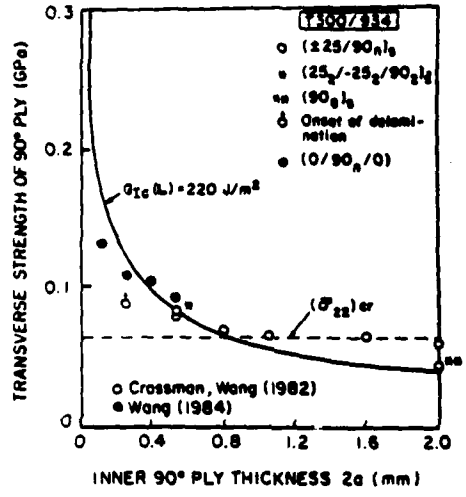

Fig. 5. Comparison of theoretical results with experimental data.

find G_{Ic}(L) in the 90° plies. The results are apparently not significantly affected by the differences in layup of outside layers. Note that the G_{Ic} values shown in Figs 4 and 5 are actually values of G_{Ic}/ξ_1 with ξ_1 taken as equal to unity because of interface damage. If ξ_1 was taken as equal to calculated values, e.g. $\xi_1 = 0.8$ in E-glass–epoxy, then one would obtain $G_{Ic} = 200$ J/m^2 in Fig. 5, which compares better with the $G_{Ic} = 120 \pm 30$ J/m^2 indicated for this material in Table 1 of [11].

7. CONCLUSIONS

(a) First ply failure stress of plies of different thicknesses can be predicted theoretically, providing that ply toughness values and initial flaw sizes are known. In cases of thin plies the ply thickness itself determines the initial flaw size and ply strength can be directly related to toughness via eqs (9). In case of thick or moderately thick plies the analysis cannot be easily implemented for lack of experimental information about relevant material properties.

(b) If a ply of any thickness contains a through-the-thickness flaw—such flaws can be caused by impact, penetrations, or similar types of damage—then it must be regarded as thin ply in strength estimates. Therefore, it is conservative to regard all plies as thin plies, and neglect the additional strength which may be found in undamaged thick plies.

Acknowledgement—This work was supported by a grant from the Air Force Office of Scientific Research. Dr M. Hejazi and Mr C. J. Wung provided assistance in interpretation of experimental data.

REFERENCES

[1] G. J. Dvorak and N. Laws. Analysis of progressive matrix cracking in composite laminates. II. First ply failure. *J. compos. Mater.* in press.

[2] A. N. Stroh, Dislocations and cracks in anisotropic elasticity. *Phil. Mag.* **3**, 625 (1958).
[3] N. Laws, A note on interaction energies associated with cracks in anisotropic media. *Phil. Mag.* **36**, 367 (1977).
[4] G. J. Dvorak, N. Laws and M. Hejazi, Analysis of progressive matrix cracking in composite laminates. I. Thermoelastic properties of a unidirectional composite with cracks. *J. compos. Mater.* **18** (1985).
[5] N. Laws, G. J. Dvorak and M. Hejazi, Stiffness changes in unidirectional composites caused by crack systems. *Mech. Mater.* **2**, 123 (1983).
[6] K. W. Garrett and J. E. Bailey, Multiple transverse fracture in 90° cross-ply laminates of a glass fibre-reinforced polyester. *J. Mater. Sci.* **12**, 157 (1977).
[7] K. L. Reifsnider, W. W. Stinchcomb, E. G. Henneke and J. C. Duke, Fatigue damage–strength relationships in composite laminates. AFWAL-TR-83-3084, Vol. I (September 1983).
[8] H. T. Hahn and T. Johnnesson, Fracture of unidirectional composites, theory and applications, in *Mechanics of Composite Materials—1983* (Edited by G. J. Dvorak), AMD, Vol. 58, p. 135. New York (1983).
[9] W. D. Bascom, Private communication (1984).
[10] A. S. D. Wang, Fracture mechanics of sublaminate cracks in composite materials. *Compos. Technol. Rev.* **6**, 45 (1984).
[11] J. E. Bailey, P. T. Curtis and A. Parvizi, On the transverse cracking and longitudinal splitting behavior of glass and carbon fibre reinforced epoxy cross ply laminates and the effect of Poisson and thermally generated strain. *Proc. R. Soc.* **A366**, 599 (1979).
[12] F. W. Crossman and A. S. D. Wang, The dependence of transverse cracking and delamination on ply thickness in graphite/epoxy laminates. *ASTM STP* **775**, 118 (1982).

Int. J. Solids Structures Vol. 23, No. 9, pp. 1269–1283, 1987
Printed in Great Britain.

0020-7683/87 $3.00+.00

THE EFFECT OF FIBER BREAKS AND ALIGNED PENNY-SHAPED CRACKS ON THE STIFFNESS AND ENERGY RELEASE RATES IN UNIDIRECTIONAL COMPOSITES

N. LAWS
Department of Mechanical Engineering, University of Pittsburgh, Pittsburgh, PA 15261, U.S.A.

and

G. J. DVORAK
Department of Civil Engineering, Rensselaer Polytechnic Institute, Troy, NY 12181, U.S.A.

(*Received* 4 *June* 1986; *in revised form* 11 *November* 1986)

Abstract—The loss of stiffness due to penny-shaped cracks associated with fiber breaks in a unidirectional composite is the main theme of the paper. Explicit results are given for the non-trivial Hashin–Shtrikman bound together with the estimates obtained from the self-consistent and differential schemes. In addition the paper contains some results on energy release rates for two different crack growth mechanisms. It is shown that, in theory, the differential scheme enjoys a distinguished *position*.

1. INTRODUCTION

This paper is mainly concerned with the changes of stiffness and strength of a unidirectional fiber-reinforced solid due to fiber breaks accompanied by penny-shaped cracks at the ends of the broken fibers.

The literature on the effect of crack distributions on the response of solids falls into two categories. First one can consider periodic distributions of cracks, see e.g. Delameter *et al.*[1]. Second, and this is by far the major part of the literature, one can consider random distributions of cracks. Within this second category, the pioneering paper is due to Budiansky and O'Connell[2], although a less general approach was given independently by Salganik[3]. The work of Budiansky and O'Connell[2] was especially directed at predicting the loss of stiffness of an isotropic solid due to a volume distribution of randomly oriented elliptical cracks—leading to isotropy of the cracked solid. Additional work on the effect of slit cracks on the stiffness of anisotropic solids has been given by Gottesman *et al.*[4], and by Laws and Dvorak[5, 6].

It is particularly relevant to the analysis of this paper to call attention to the work of Hoenig[7] who was the first to consider anisotropic distributions of cracks. In addition, it is important to recognize the contributions of Mura and Taya[8] and Taya[9] which were addressed to the problem of determining the effect of fiber breaks on the response of unidirectional fiber-reinforced materials.

In this paper we extend the work of various authors[7–9] in that we obtain self-consistent estimates for the *reduction in* stiffness of unidirectional composites containing penny-shaped cracks. In addition we obtain the only non-trivial Hashin–Shtrikman bound on the moduli of the cracked solid. We also derive the appropriate differential scheme model for the loss of stiffness.

We show how both the self-consistent and differential scheme results are entirely consistent with the Hashin–Shtrikman bound. Further we show explicitly that the results of Mura and Taya[8, 9] *coincide* with the Hashin–Shtrikman bound.

As a further illustration of the results presented herein, we pay brief attention to *isotropic* solids containing distributions of aligned penny-shaped cracks and amongst other things, recover some results first given by Hoenig[7]. The relevance of this analysis in the study of micro-cracking in ceramics is discussed by Laws and Brockenbrough[10].

SAS 23:9-E

Finally we investigate the influence of cracks on energy release rates. Here, we consider two distinct cases. First, we consider situations in which all cracks extend simultaneously. Second, we consider only one crack in the effective cracked solid. It turns out that the differential scheme enjoys a distinguished position as far as the evaluation of energy release rates is concerned. Whether or not this is of physical significance is an open question.

2. PHYSICAL MOTIVATION

Consider a unidirectional graphite–epoxy composite subject to loading parallel to the fibers. It is known that such composite specimens eventually suffer fiber breakage. The density of such fiber breaks can be quite large before final fracture occurs. At the end of each broken fiber, one usually finds penny-shaped cracks (whose normals are in the fiber direction). Under continued loading, these cracks may extend—see the discussion of Mura and Taya[8, 9] and the references contained therein.

In addition there is ample evidence that in cross-ply composite laminates, one often sees fiber breaks in the 0° plies at the end of transverse cracks in the 90° plies. Furthermore, some recent work by Laws and Brockenbrough[10] indicates the relevance of considering aligned penny-shaped micro-cracks in ceramics.

Another application arises in fibrous composites which can develop aligned matrix cracks on planes perpendicular to the fibers. Such cracks are confined to the matrix and do not extend through the fibers. They have been observed in 0° plies of cyclically loaded boron–aluminum laminates by Dvorak and Johnson[11].

It is, therefore, desirable that the effects of aligned penny-shaped cracks on the stiffness and strength of both composites and single phase materials be more fully understood.

3. ANALYSIS

In this section we present the mechanics of the effect of distributions of aligned penny-shaped cracks on the stiffness and strength of solids. For simplicity we shall discuss cracked composites by regarding the uncracked fibrous composite as an effective homogeneous material. This is, of course, commonplace in the theory of composites, but some further explanation is required here since the cracked composite will contain both long and short (broken) fibers.

Now Laws and McLaughlin[12], followed by Chou *et al.*[13], have quantified the effects of fiber aspect ratio on the overall moduli of aligned short fiber-reinforced composites. The general conclusion is that for aspect ratios greater than 100, say, the stiffness of the composite is insensitive to fiber length. Since the applications discussed in Section 2 all indicate broken fibers whose aspect ratios are much larger than 100, there is no loss of generality in considering only long fibers. If we interpret correctly, Taya[9] arrives at the same conclusion, by somewhat different methods.

In addition for transverse cracks in composite laminates the use of a model with cracks in an otherwise homogeneous solid is well established.

The notation and basic ideas presented here are taken directly from the work of Laws and Dvorak[5, 6]. Fourth-order tensors are denoted by upper case letters, e.g. L, Λ and symmetric second-order tensors are denoted by bold-face letters, e.g. $\boldsymbol{\varepsilon}$, $\boldsymbol{\sigma}$. The unit fourth-order tensor is denoted by I and the inverse of a non-singular fourth-order tensor A is denoted by A^{-1}.

Consider a linear elastic solid whose stress tensor, $\boldsymbol{\sigma}$, and strain tensor, $\boldsymbol{\varepsilon}$, are related through

$$\boldsymbol{\sigma} = L\boldsymbol{\varepsilon}, \qquad \boldsymbol{\varepsilon} = M\boldsymbol{\sigma}, \qquad LM = ML = I. \tag{1}$$

We use a standard 6×6 matrix notation for the stiffness tensor L and compliance tensor M. Since we are here concerned with materials which are at worst transversely isotropic with respect to the coordinate axis $0x_3$, it follows that eqns (1) may be written in the form

$$\begin{bmatrix}\sigma_1\\ \sigma_2\\ \sigma_3\\ \sigma_4\\ \sigma_5\\ \sigma_6\end{bmatrix} = \begin{bmatrix} L_{11} & L_{12} & L_{13} & 0 & 0 & 0\\ & L_{11} & L_{13} & 0 & 0 & 0\\ & & L_{33} & 0 & 0 & 0\\ & & & L_{44} & 0 & 0\\ & \text{SYM} & & & L_{44} & 0\\ & & & & & L_{66}\end{bmatrix}\begin{bmatrix}\varepsilon_1\\ \varepsilon_2\\ \varepsilon_3\\ \varepsilon_4\\ \varepsilon_5\\ \varepsilon_6\end{bmatrix}. \tag{2}$$

$$\begin{bmatrix}\varepsilon_1\\ \varepsilon_2\\ \varepsilon_3\\ \varepsilon_4\\ \varepsilon_5\\ \varepsilon_6\end{bmatrix} = \begin{bmatrix} M_{11} & M_{12} & M_{13} & 0 & 0 & 0\\ & M_{11} & M_{13} & 0 & 0 & 0\\ & & M_{33} & 0 & 0 & 0\\ & & & M_{44} & 0 & 0\\ & \text{SYM} & & & M_{44} & 0\\ & & & & & M_{66}\end{bmatrix}\begin{bmatrix}\sigma_1\\ \sigma_2\\ \sigma_3\\ \sigma_4\\ \sigma_5\\ \sigma_6\end{bmatrix}. \tag{3}$$

where

$$L_{66} = \tfrac{1}{2}(L_{11}-L_{12}), \qquad M_{66} = 2(M_{11}-M_{12}). \tag{4}$$

We use the suffix 0 to refer to the initial uncracked solid. Thus, for example L_0 is the stiffness of the uncracked solid, whereas L is the stiffness of the cracked solid. The volume concentration of cavities is denoted by c.

It is convenient, but not essential, to develop the theory by considering a family of aligned spheroidal cavities in a transversely isotropic matrix. A typical spheroid is taken to be

$$\frac{x_1^2}{a^2}+\frac{x_2^2}{a^2}+\frac{x_3^2}{b^2}=1. \tag{5}$$

In addition we suppose all cavities to be of equal size. This assumption is *not* essential as far as theory is concerned, but may well be essential in any application to penny-shaped cracks at the ends of broken fibers in a unidirectional composite. Ultimately we will obtain the required results for aligned penny-shaped cracks by allowing the aspect ratio

$$\varepsilon = b/a \tag{6}$$

to approach zero.

Many methods have been proposed to predict the effect of reinforcement on the effective moduli of composites. It is not our purpose here to give a critical survey of the various methods. Rather, we give the required formula for the Hashin–Shtrikman bounds, the self-consistent method and the differential scheme.

In order to get the Hashin–Shtrikman bounds we refer to the work by Willis[14]. We assume that the cavities are randomly located so that the cracked solid exhibits overall transverse isotropy. Since this envisaged distribution of oblate spheroidal cavities will conform to the statistics assumed by Willis[14], it follows that the overall compliance of the cracked composite must satisfy

$$M \geqslant M_0 + \frac{c}{1-c}Q_0^{-1}. \tag{7}$$

Here Q_0 is a tensor which depends on the uncracked compliance M_0 and the aspect ratio ε. The components of Q_0 can be found explicitly, see Laws and McLaughlin[12] or Laws[15].

The right-hand side of inequality (7) is the Hashin–Shtrikman lower bound for M, denoted here by M^-

$$M^- = M_0 + \frac{c}{1-c} Q_0^{-1}. \tag{8}$$

Since the damaged material contains cavities the Hashin–Shtrikman upper bound for M is here infinite.

Next we recall that the self-consistent estimate is given by Laws *et al.*[5] as

$$M = M_0 + cQ^{-1}. \tag{9}$$

Finally, it is easy to read off the differential scheme estimate from the work of McLaughlin[16]

$$\frac{dM}{dc} = \frac{1}{1-c} Q^{-1} \tag{10}$$

with

$$M = M_0 \quad \text{when} \quad c = 0. \tag{11}$$

In terms of the stiffness tensor L it is easy to show that the upper bound L^+ is given by

$$L^+ = \left[M_0 + \frac{c}{1-c} Q_0^{-1} \right]^{-1}. \tag{12}$$

Also the self-consistent result is

$$L = L_0 [I + cQ^{-1} L_0]^{-1} \tag{13}$$

whereas the differential scheme gives

$$\frac{dL}{dc} = -\frac{1}{1-c} LQ^{-1} L \tag{14}$$

with

$$L = L_0 \quad \text{when} \quad c = 0. \tag{15}$$

We now obtain the required results for penny-shaped cracks by proceeding to the limit as $\varepsilon \to 0$. Let η be the number of cracks per unit volume then

$$c = \frac{4}{3} \pi \eta a^3 \varepsilon$$

$$= \frac{\pi}{6} \alpha \varepsilon$$

where the crack density parameter α is defined by

$$\alpha = 8 \eta a^3. \tag{16}$$

Note that the crack density parameter is *not* the same as the crack density parameter

introduced by Budiansky and O'Connell[2]. The choice of eqn (16) is motivated by the fact that $\alpha = 1$ corresponds to an average of one crack of diameter $2a$ in each cube of side $2a$.

In applications of the theory to composites reinforced by aligned continuous fibers, the crack can, in the first instance, be visualized as a fiber break which has extended into the surrounding matrix and has been arrested by adjacent unbroken fibers. This crack is then regarded as a crack in an effective composite medium. For practical purposes it is desirable to relate the radius of this crack to the fiber radius, r_f, and the fiber volume fraction, v_f. Estimates can be obtained in various ways. For example if the microstructure is such that the fibers are located in a close packed hexagonal array and that failure of one fiber creates a crack which extends through the matrix until it reaches the surfaces of neighboring fibers, then the resulting penny-shaped crack has radius

$$a = r_f\left\{\left(\frac{2\pi}{v_f}\right)^{1/2} 3^{-1/4} - 1\right\}. \tag{17}$$

In the same spirit one obtains the estimate

$$a = r_f\left\{\left(\frac{\pi}{v_f}\right)^{1/2} - 1\right\} \tag{18}$$

for a square array. For typical volume fractions occurring in practice the hexagonal array estimate exceeds the square array estimate by about 13%.

As noted by Eshelby[17] in the isotropic case, and by Hoenig[7] and Laws[15] for orthotropic materials, the limit as ε approaches zero needs to be handled with care. The essential point here is that whereas Q becomes singular, the product εQ^{-1} remains finite. Thus let

$$\lim_{\varepsilon \to 0} \varepsilon Q^{-1} = \Lambda$$

with an analogous definition for Λ_0. The components of Λ are given in the Appendix.

In the limit of aligned penny-shaped cracks it now follows from eqn (8) that

$$M^- = M_0 + \frac{\pi}{6}\alpha\Lambda_0. \tag{19}$$

Further, the self-consistent estimate is obtained from

$$M = M_0 + \frac{\pi}{6}\alpha\Lambda \tag{20}$$

whereas the differential scheme yields

$$\frac{dM}{d\alpha} = \frac{\pi}{6}\Lambda. \tag{21}$$

The dual formulae for the stiffness tensor are

$$L^+ = L_0\left[I + \frac{\pi}{6}\alpha\Lambda_0 L_0\right]^{-1} \tag{22}$$

the self-consistent result being

$$L = L_0\left[I + \frac{\pi}{6}\alpha\Lambda L_0\right]^{-1} \tag{23}$$

and the differential scheme giving

$$\frac{dL}{d\alpha} = -\frac{\pi}{6}L\Lambda L. \tag{24}$$

Since the only non-zero components of Λ (shown in the Appendix) are Λ_{33} and Λ_{44} ($= \Lambda_{55}$) it follows from eqns (20) and (21) that only M_{33} and M_{44} ($= M_{55}$) are predicted to change. This is, of course, only to be expected.

It is instructive to consider the rather special case when the uncracked body is *isotropic*. Thus let E_0, ν_0 be respectively the initial Young's modulus and Poisson's ratio. Then, from the Appendix, we see that

$$\Lambda^0_{33} = \frac{4(1-\nu_0^2)}{\pi E_0}$$

$$\Lambda^0_{44} = \frac{8(1-\nu_0^2)}{\pi E_0(2-\nu_0)}.$$

With the help of a standard notation

$$M_{33} = \frac{1}{E_L}, \qquad M_{44} = \frac{1}{G_L}$$

it now follows from eqn (19) that

$$\frac{E_L^+}{E_0} = \frac{1}{\frac{1}{2} + \frac{2}{3}\alpha(1-\nu_0^2)} \tag{25}$$

$$\frac{G_L^+}{G_0} = \frac{1}{1 + \frac{2}{3}\alpha(1-\nu_0)/(2-\nu_0)}. \tag{26}$$

We emphasize that eqn (25) is *precisely* the formula given by Taya[9]. Hence we see that the Mori–Tanaka[19] back-stress analysis, which is used by Taya[9], yields the non-trivial Hashin–Shtrikman bound. It is noteworthy that it is possible to show that the assumptions of the Mori–Tanaka[19] back-stress analysis lead to formulae which are coincident with the Hashin–Shtrikman bounds in other situations—but we do not include details here.

We remark that there is no difficulty in obtaining eqns (19)–(21) by direct methods instead of using an argument based on cavities. In fact Gottesman *et al.*[4] have given such an argument to obtain the bounds and self-consistent results for a solid with slit cracks. We note that the fully general analysis is given by Laws and Brockenbrough[10].

Numerical results can be found from eqns (19) to (21) or from eqns (22) to (24). In practice, we have found it easier to evaluate the compliances from eqns (19) to (21) and then to determine the stiffness, when required, by matrix inversion.

For the most part we present results for the loss in stiffness of unidirectional fiber-reinforced materials containing a distribution of penny-shaped cracks with common orientation perpendicular to the fiber direction. In other words we attempt to model the loss of stiffness of unidirectional fiber-reinforced materials due to fiber breaks. Data for the uncracked composite is taken directly from Table 2 of the paper by Dvorak *et al.*[6] which is for a T300/5208 graphite–epoxy system with volume fractions $c_f = 0.2, 0.4, 0.6$. As noted earlier the only compliances which change are M_{33}, M_{44} ($= M_{55}$). In Figs 1 and 2 we give

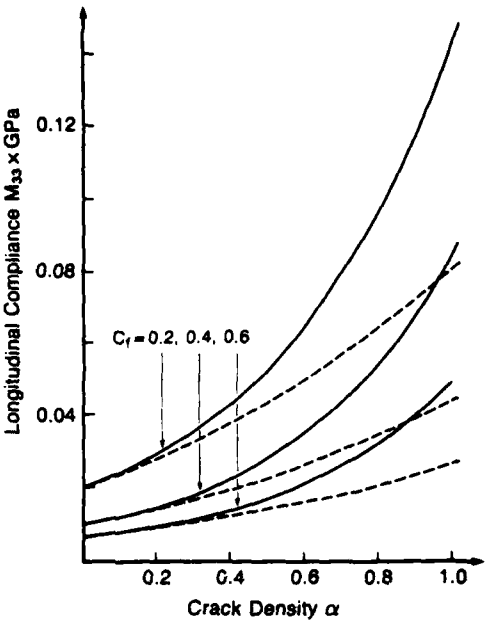

Fig. 1. Longitudinal compliance for various T300/5208 systems: (a) s.c.m. ——; (b) d.s. – – –.

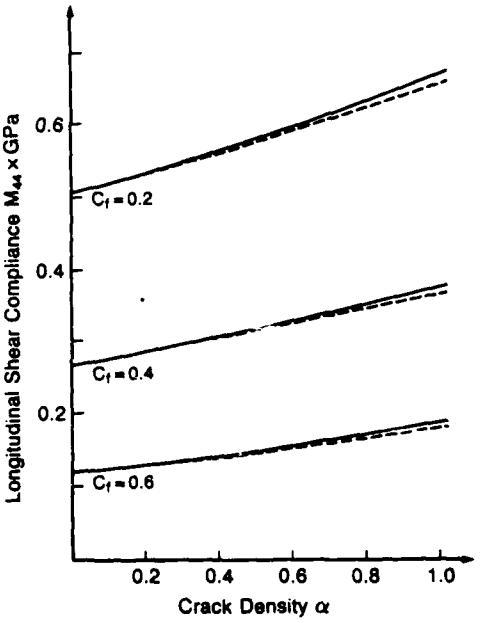

Fig. 2. Longitudinal shear compliance for various T300/5208 systems: (a) s.c.m. ——; (b) d.s. – – –.

the self-consistent and differential scheme predictions for these two compliances. There is no need to display the Hashin–Shtrikman bound since it coincides with the common tangent at $\alpha = 0$. We observe that for each value of c_f the self-consistent result is always greater than the differential scheme result. For small α (<0.1 say) the two results for M_{33} are coincident and equal to the Hashin–Shtrikman bound. On the other hand, we see from Fig. 2 that there is virtually no difference between the self-consistent, the differential scheme and the Hashin–Shtrikman results for M_{44} for $\alpha < 0.5$. Thus for practical purposes it suffices to take

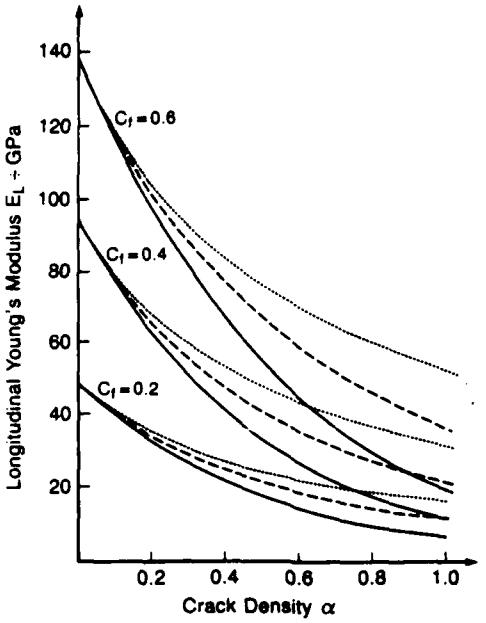

Fig. 3. Longitudinal Young's modulus for various T300/5208 systems: (a) bound ——; (b) s.c.m. – – –; (c) d.s. ·····.

$$M_{44} = M_{\tilde{44}}$$

$$= M^0_{44} + \frac{\pi}{6}\alpha\Lambda^0_{44}$$

where Λ^0_{44} can be found from the formulae given in the Appendix.

The presentation of the results is sometimes clearer when we use the respective Young's moduli, Poisson's ratios and shear moduli. Thus we write

$$M = \begin{bmatrix} \frac{1}{E_T} & -\frac{\nu_{TT}}{E_T} & -\frac{\nu_{TL}}{E_T} & 0 & 0 & 0 \\ -\frac{\nu_{TT}}{E_T} & \frac{1}{E_T} & -\frac{\nu_{TL}}{E_T} & 0 & 0 & 0 \\ -\frac{\nu_{LT}}{E_L} & -\frac{\nu_{LT}}{E_L} & \frac{1}{E_L} & 0 & 0 & 0 \\ 0 & 0 & 0 & \frac{1}{G_L} & 0 & 0 \\ 0 & 0 & 0 & 0 & \frac{1}{G_L} & 0 \\ 0 & 0 & 0 & 0 & 0 & \frac{1}{G_T} \end{bmatrix}.$$

Since the only changed compliances are M_{33}, M_{44} and M_{55}, it follows that E_T and G_T are not changed by the introduction of cracks. Also the only Poisson's ratio which is changed is ν_{LT} (for transverse contraction due to longitudinal extension). Results showing the reduction of E_L and G_L are given in Figs 3 and 4, respectively. In both cases the Hashin–Shtrikman bound is nontrivial; actually

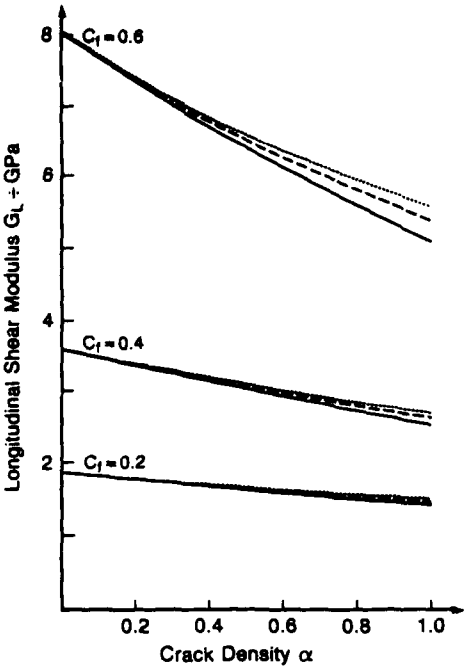

Fig. 4. Longitudinal shear modulus for various T300/5208 systems: (a) bound ——; (b) s.c.m. – – – –; (c) d.s. ·····.

$$\frac{E_L^+}{E_L^0} = \left(1 + \frac{\pi}{6}\alpha E_L^0 \Lambda_{33}^0\right)^{-1}$$

$$\frac{G_L^+}{G_L^0} = \left(1 + \frac{\pi}{6}\alpha G_L^0 \Lambda_{44}^0\right)^{-1}.$$

We note that the self-consistent estimate for both E_L and G_L is always lower than the differential scheme result. Clearly both results are consistent with the Hashin–Shtrikman bound.

As for the reduction in ν_{LT} we note that since $M_{13} = M_{13}^0$ and $M_{13} = M_{31}$, it follows that

$$\frac{\nu_{LT}}{\nu_{LT}^0} = \frac{E_L}{E_L^0}.$$

Hence the fractional reduction of ν_{LT} *is equal to the fractional reduction of* E_L. Also the actual reduction in ν_{LT} can be found from the reduction of E_L merely by a change in scale. For clarity Figs 5 and 6 display only the fractional reduction for E_L and G_L when $c_f = 0.6$. We remark that the appropriate curves for $c_f = 0.2$ and 0.4 are *almost* indistinguishable from the curves indicated in Figs 5 and 6. By way of comparison Figs 7 and 8 show the fractional reduction of E_L and G_L for an *isotropic* material with Poisson's ratio $\nu_0 = 0.3$. Two remarks are in order. First the fractional reduction curves indicated in Figs 6 and 7 are insensitive to the choice of Poisson's ratio: $0.2 \leqslant \nu_0 \leqslant 0.4$. Second the fractional reductions indicated in Figs 5 and 6 compared with those in Figs 7 and 8 show that there is no possibility of constructing "master curves" for anisotropic materials.

4. ENERGY RELEASE RATES

In this section we calculate energy release rates for two different mechanisms of crack growth. First, we consider a solid which contains a family of cracks each of radius a and

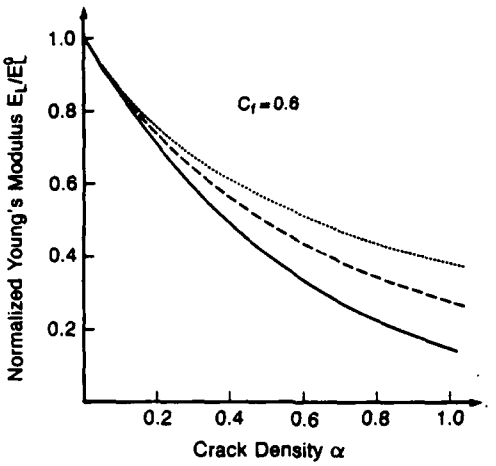

Fig. 5. Normalized longitudinal Young's modulus for the T300/5208 system with $c_f = 0.6$: (a) bound ———; (b) s.c.m. – – – –; (c) d.s. ·····.

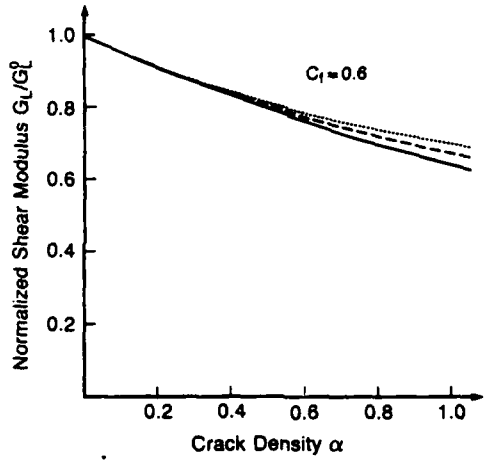

Fig. 6. Normalized longitudinal shear modulus for the T300/5208 system with $c_f = 0.6$: (a) bound ———; (b) s.c.m. – – – –; (c) d.s. ·····.

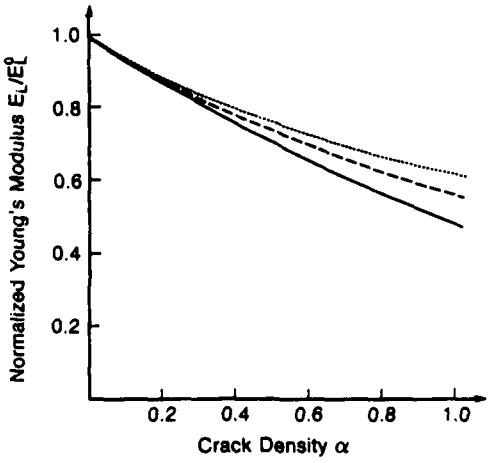

Fig. 7. Normalized longitudinal Young's modulus for isotropic materials with Poisson's ratio = 0.3: (a) bound ———; (b) s.c.m. – – – –; (c) d.s. ·····.

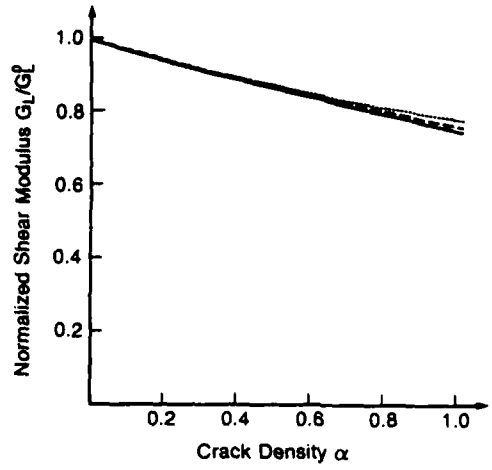

Fig. 8. Normalized longitudinal shear modulus for isotropic materials with Poisson's ratio = 0.3: (a) bound ———; (b) s.c.m. – – –; (c) d.s. · · · · · · ·.

allow each crack to extend by the same amount. Second, we consider a single penny-shaped crack in an otherwise homogeneous (cracked) solid. We show, *inter alia*, that the differential scheme enjoys a peculiar status in that it predicts equality of the two energy release rates.

Thus we first consider a solid containing a family of aligned penny-shaped cracks each of radius a. The corresponding crack density is α. The solid is subject to macroscopically uniform loading with applied stress $\bar{\boldsymbol{\sigma}}$, which is also the average stress. All cracks are assumed to be open. The *total energy* of the cracked solid is

$$E(\alpha) = \frac{1}{2}\int_V \boldsymbol{\sigma}\cdot\boldsymbol{\varepsilon}\,\mathrm{d}V - \int_S \mathbf{T}\cdot\mathbf{u}\,\mathrm{d}S \tag{27}$$

where $\mathbf{T}$, $\mathbf{u}$ are respectively the tractions and displacements on the boundary S. It is easy to show that eqn (27) may be rewritten in the form

$$\begin{aligned} E(\alpha) &= -\tfrac{1}{2}V\bar{\boldsymbol{\sigma}}\cdot M(\alpha)\bar{\boldsymbol{\sigma}} \qquad \text{when } \alpha \neq 0, \\ E_0 &= -\tfrac{1}{2}V\bar{\boldsymbol{\sigma}}\cdot M_0\bar{\boldsymbol{\sigma}} \qquad \text{when } \alpha = 0. \end{aligned} \tag{28}$$

Thus the total energy released by the introduction of cracks is $(E_0 - E(\alpha))$. Accordingly the energy released by *each* crack, $W(\alpha)$, is given by

$$\begin{aligned} W(\alpha) &= \frac{E_0 - E(\alpha)}{\eta V} \\ &= \frac{1}{2\eta}\bar{\boldsymbol{\sigma}}\cdot[M(\alpha) - M_0]\bar{\boldsymbol{\sigma}}. \end{aligned} \tag{29}$$

Suppose now that each crack extends from radius a to radius $(a+\delta a)$ while the *total number of cracks remains constant*. This corresponds to an increase in crack density from α to $(\alpha+\delta\alpha)$. The crack extension force, or energy release rate per unit length, G_A, of each crack is given by

$$G_A = \frac{1}{2\pi a}\frac{\partial W}{\partial \alpha}\frac{\mathrm{d}\alpha}{\mathrm{d}a}. \tag{30}$$

Here the subscript A is used to signify that G_A is the energy release rate of each crack when *all* cracks extend simultaneously. From eqn (16)

$$\frac{d\alpha}{da} = 24\eta a^2$$

so from eqns (29) and (30)

$$G_A = \frac{6a}{\pi}\bar{\sigma}\cdot\frac{\partial M}{\partial \alpha}\bar{\sigma}. \tag{31}$$

The lower bound M^- in eqn (19) gives

$$G_A^- = a\bar{\sigma}\cdot\Lambda_0\bar{\sigma}$$

while the self-consistent estimate of M in eqn (20) yields

$$G_A = a\bar{\sigma}\cdot\left(\Lambda+\alpha\frac{d\Lambda}{d\alpha}\right)\bar{\sigma}$$

and the differential scheme result, eqn (21), gives

$$G_A = a\bar{\sigma}\cdot\Lambda\bar{\sigma}.$$

Next we focus on a single penny-shaped crack in the cracked solid. We now regard the cracked solid as a homogeneous medium with effective compliance $M(\alpha)$. Only one crack is now present in this effective medium and we wish to determine the energy release rate, G_S, for extension of this *single* crack.

In these circumstances we can use the results of Laws[15] to obtain the required energy released by extension of this single crack of radius a

$$\mathscr{E}(a) = \tfrac{2}{3}\pi a^3\bar{\sigma}\cdot\Lambda\bar{\sigma}.$$

Hence

$$G_S = \frac{1}{2\pi a}\frac{\partial \mathscr{E}}{\partial a} = a\bar{\sigma}\cdot\Lambda\bar{\sigma}. \tag{32}$$

We emphasize that different models give rise to different values of M. Since the components of Λ are given in terms of the components of M by the formulae of the Appendix, it follows that each of the three models gives rise to a different value of Λ and hence of G_S.

Whether we consider all cracks simultaneously growing in self-similar fashion or a single growing crack, it is clear that both G_A and G_S are *average* crack extension forces. Of course if we are considering crack extension in a *single phase* brittle solid there is no conceptual problem. However, in the case when the cracks are located in an effective composite matrix some further comments are in order. Thus consider an arbitrary growing penny-shaped crack in a unidirectional fiber-reinforced composite—with the plane of the crack perpendicular to the fiber direction. In the first place this crack will arise from a fiber break followed by extension through the matrix until the circumferential crack tip reaches neighboring fibers. If there is further growth then part of the crack tip must lie in the matrix material whereas the remainder must lie in the fibers. Since here we consider cracks in an effective solid it is clear that the energy release rates G_A and G_S do not apply when the crack radius is smaller than the value given in eqn (17) or eqn (18). However, for subsequent growth an *average* crack extension force is precisely the quantity which is demanded by the physics of the problem.

Taya[9] has reported some work on the second case (G_S) but his work appears to have little in common with the work described here.

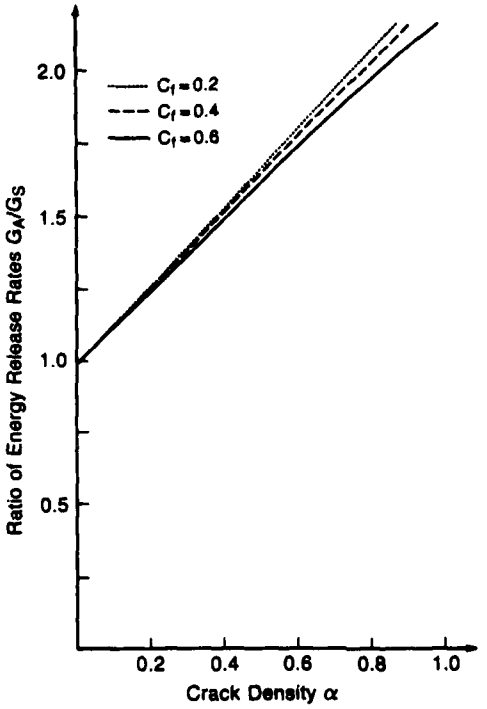

Fig. 9. Ratio of energy release rates for various T300/5208 systems according to s.c.m.

From eqns (21), (29) and (30) we obtain the surprising result that the differential scheme predicts that $G_A = G_S$. Thus the differential scheme can provide a useful border between those models which predict G_A to be greater or smaller than G_S. However, one ought to bear in mind that there is no *a priori* reason why a particular model should not give $G_A > G_S$ for small α and yet $G_A < G_S$ for large α.

Since a general analysis of eqns (29) and (30) is complicated by the fact that both refer to mixed mode loading, we concentrate on mode I loading in which the only non-zero applied stress is $\bar{\sigma}_{33}$. From eqns (31) and (32) we have

$$\frac{G_A}{G_S} = \frac{6}{\pi} \frac{dM_{33}/d\alpha}{\Lambda_{33}}.$$

It is perhaps useful to emphasize here that both G_A and G_S depend upon crack density. This may be contrasted with the usual situation in fracture mechanics wherein a single crack extends in a material of fixed properties. Nevertheless we see from eqns (31) and (32) that if $G_A/G_S \geqslant 1$ extension of all cracks is indicated rather than extension of a single crack. When $G_A/G_S < 1$ the opposite conclusion applies.

Numerical results can be obtained for the T300/5208 graphite–epoxy systems considered earlier. In particular Fig. 9 shows the self-consistent and (trivially) the differential scheme estimates for G_A/G_S. Since $G_A/G_S \geqslant 1$ both models suggest extension of all cracks. By way of comparison Fig. 10 shows the results for initially isotropic solids in which case the value of G_A/G_S is insensitive to the choice of initial Poisson's ratio in the range $0.2 \leqslant \nu_0 \leqslant 0.4$.

A further general conclusion on energy release rates for a *single* crack can be obtained from eqn (30) and the results of Section 3. For simplicity consider the mixed mode loading $\bar{\sigma}_{33} \neq 0$, $\bar{\sigma}_{23} \neq 0$ so that eqn (30) reduces to

$$G_S = a\Lambda_{33}(\bar{\sigma}_{33})^2 + a\Lambda_{44}(\bar{\sigma}_{23})^2.$$

Thus Λ_{33} and Λ_{44} may be interpreted as energy release rate factors. Indeed Figs 11 and 12

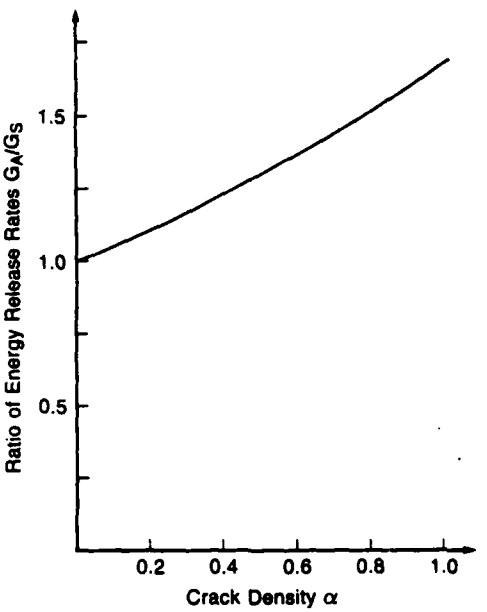

Fig. 10. Ratio of energy release rates for isotropic materials with Poisson's ratio = 0.3 according to s.c.m.

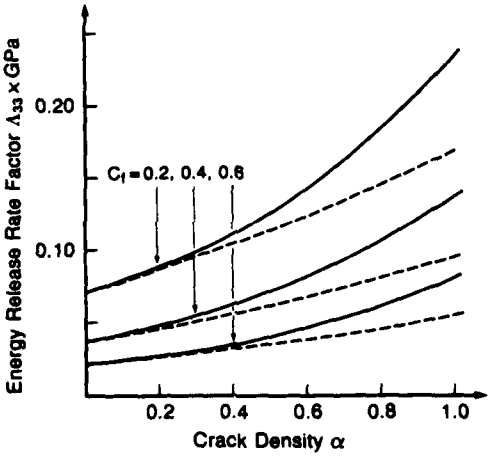

Fig. 11. Energy release rate factor for various T300/5208 systems: (a) s.c.m. ———, (b) d.s. – – – –.

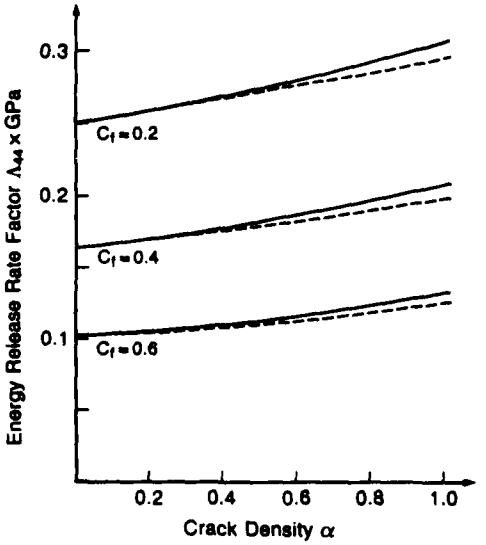

Fig. 12. Energy release rate factor for various T300/5208 systems: (a) s.c.m. ———; (b) d.s. – – – –.

contain the self-consistent and differential scheme results for Λ_{33} and Λ_{44} for the T300/5208 systems considered earlier. It is clear that both models predict that at fixed crack density, Λ_{33} and Λ_{44} decrease as the volume fraction of fiber increases. Hence G_S decreases as the volume fraction of fiber increases in agreement with some results of Taya[9]. Further it is evident that, for fixed c_f, G_S increases with α.

Finally, we note that in the fibrous composite medium the crack density will increase gradually under incremental load, as a result of fiber breaks at randomly distributed locations. Each new crack will require for its formation at least the same amount of crack energy as the first crack, i.e. $W(\alpha) \geq W_0$. Equation (29) indicates that this will be the case for all models considered herein. Therefore, progressive cracking is governed by spatial variation of fiber strength; sufficient crack energy is available for each fiber break to produce a new crack.

Acknowledgement—This work was supported by a grant from the Air Force Office of Scientific Research.

REFERENCES

1. W. R. Delameter, G. Herrmann and D. M. Barnett, *J. Appl. Mech.* **42**, 74 (1975); **44**, 190 (1977).
2. B. Budiansky and R. J. O'Connell, *Int. J. Solids Structures* **12**, 81 (1976).
3. R. L. Salganik, *Mekh. Tverd. Tela* **4**, 149 (1973).
4. T. Gottesman, Z. Hashin and M. A. Brull, *Advances in Composite Materials* (Edited by A. R. Bunsell, A. Martrenchar, D. Menkes, C. Bathias and G. Verchery), p. 749. Pergamon Press, Oxford (1980).
5. N. Laws, G. J. Dvorak and M. Hejazi, *Mech. Mater.* **2**, 123 (1983).
6. G. J. Dvorak, N. Laws and M. Hejazi, *J. Composite Mater.* **19**, 216 (1985).
7. A. Hoenig, *Int. J. Solids Structures* **15**, 137 (1979).
8. T. Mura and M. Taya, *J. Appl. Mech.* **48**, 361 (1981).
9. M. Taya, *J. Composite Mater.* **15**, 198 (1981).
10. N. Laws and J. R. Brockenbrough, *Int. J. Solids Structures* **23**, 1247 (1987).
11. G. J. Dvorak and W. S. Johnson, *Int. J. Fracture* **16**, 585 (1980).
12. N. Laws and R. McLaughlin, *J. Mech. Phys. Solids* **27**, 1 (1979).
13. T. W. Chou, S. Nomura and M. Taya, *J. Composite Mater.* **14**, 178 (1980).
14. J. R. Willis, *J. Mech. Phys. Solids* **25**, 185 (1977).
15. N. Laws, *Mech. Mater.* **4**, 209 (1985).
16. R. McLaughlin, *Int. J. Engng Sci.* **15**, 237 (1977).
17. J. D. Eshelby, *Proc. R. Soc. Lond.* **A241**, 376 (1957).
18. N. Laws, *Phil. Mag.* **36**, 367 (1977).
19. T. Mori and K. Tanaka, *Acta Metall.* **21**, 571 (1973).

APPENDIX

For completeness we give here the formulae for the non-zero components of the Λ tensor, defined in eqn (18), for a penny-shaped crack in a transversely isotropic material. The crack lies in a plane normal to the axis of transverse isotropy. As is shown by Laws[15]

$$\Lambda_{33} = \frac{2\gamma_1\gamma_2(\gamma_1+\gamma_2)}{\pi}\frac{M_{11}^2 - M_{12}^2}{M_{11}}$$

$$\Lambda_{44} = \Lambda_{55} = \frac{4(\gamma_1+\gamma_2)(M_{11}^2 - M_{12}^2)(2M_{44})^{1/2}}{\pi\{M_{11}(2M_{44})^{1/2} + (\gamma_1+\gamma_2)(M_{11}+M_{12})(M_{11}-M_{12})^{1/2}\}}$$

where γ_1^2 and γ_2^2 are the roots of

$$(M_{11}^2 - M_{12}^2)x^2 - [M_{11}M_{44} + 2M_{13}(M_{11} - M_{12})]x + M_{11}M_{33} - M_{13}^2 = 0.$$

When the material is isotropic with Young's modulus E and Poisson's ratio ν, it is easy to see that $\gamma_1 = \gamma_2 = 1$. Hence

$$\Lambda_{33} = \frac{4(1-\nu^2)}{\pi E}$$

$$\Lambda_{44} = \frac{8(1-\nu^2)}{\pi E(2-\nu)}.$$

These results are in complete agreement with those of Eshelby[17].

FATIGUE DAMAGE MECHANICS OF METAL MATRIX COMPOSITE LAMINATES

GEORGE J. DVORAK AND EDWARD C. J. WUNG*

Department of Civil Engineering
Rensselaer Polytechnic Institute
Troy, New York 12180, USA

Technical Report

to

Air Force Office of Scientific Research

Contract No. 84-0366

and

NASA-Air Force Office of Scientific Research

Contract No. NGL-33-018-003

July 1988

To appear in Strain Localization and Size Effect Due to Cracking and Damage, edited by J. Mazars and Z. P. Bazant, Elsevier Applied Science Publishers Limited, London, 1988.

*Now at Materials Sciences Corporation, Spring House, PA, 19477.

FATIGUE DAMAGE MECHANICS OF METAL MATRIX COMPOSITE LAMINATES

GEORGE J. DVORAK AND EDWARD C.J. WUNG
Department of Civil Engineering
Rensselaer Polytechnic Institute
Troy, New York 12180, U.S.A.

ABSTRACT

In their past work, Dvorak and Johnson had shown that fatigue damage in metal composite laminates takes place when the applied loads cause cyclic plastic straining in the matrix. The present work describes an incremental analysis of the plastic deformation and damage accumulation processes in elastic-plastic composite laminates. It is based on a strain space formulation of a plasticity theory of fibrous composites and on a self-consistent analysis of stiffness changes and local fields in cracked fibrous layers which has been extended here to elastic-plastic laminates.

1. INTRODUCTION

In most fiber composite systems, the strength of the fiber far exceeds that of the matrix, hence damage caused by matrix cracking is commonly observed in fibrous composites and laminates. This is certainly an unwelcome disadvantage of composite materials, and of many other heterogeneous media such as concrete and rocks, which is not encountered to a similar extent in metals and indeed in most macroscopically homogeneous materials. The difficulty with composites is that damage may start at relatively low overall loads which do not utilize the superior strength afforded by the reinforcement. Typical consequences of damage are reduction of stiffness, redistribution of internal stresses which may impair strength, and exposure of the microstructure to possible environmental attack.

In some systems and in certain applications, damage does not cause significant problems. For example, the loss of stiffness and strength that may be caused by cracking of a polymer matrix is often quite small, because the matrix itself makes only a limited contribution. On the other hand, mechanical properties of metal and ceramic matrix composites are more sensitive to the effects of matrix damage because the matrix may carry a major part of the applied load in these systems.

In the last fifteen years, damage modeling and analysis have become a major activity in mechanics of composites. Recent surveys by Hashin

(1983) and Wang (1984) describe some of the earlier work that pertains to brittle, mostly polymer systems. Since the geometry and evolution of damage in composites are often rather complex, predictive modeling of the process and of its consequences is very difficult. These problems seem to be magnified in metal matrix systems where damage is seldom caused by monotonic or short variable loads, but frequently appears under sustained cyclic plastic straining which leads to fatigue cracking in the matrix. This particular problem is the subject of the present paper. While certainly not denying the difficulties involved, we outline a relatively simple micromechanical approach to fatigue damage analysis in metal matrix composite laminates. The next section presents some essential results which evaluate the effect of transverse matrix cracks on thermomechanical properties and stress distribution in an elastic fibrous ply. Section 4 reviews some basic concepts of plasticity of fibrous composites. Section 5 is a discussion of certain physical aspects of damage development in metal matrix laminates which identify damage as a shakedown mechanism, and pave the way to quantitative modeling of damage development. The details of the analysis are omitted here, but selected results are used to illustrate the key results.

2. ELASTIC PROPERTIES OF A CRACKED PLY

The first step in the analysis is the evaluation of overall compliance and stiffness tensors of a fibrous ply which is embedded in a laminated plate and contains a certain density of transverse cracks, Fig. 1. For modeling purposes, the cracks are represented by aligned slit cracks which extend in the fiber direction that coincides with the x_3 axis in the local coordinate system of each ply. The remaining parts of the laminate are represented here by layers of thickness b and b'. In reality, the cracks are not uniformly spaced but their average density in a large representative volume V of the ply can be described by a crack density parameter $\beta = 4a^2\eta/V$, where η is the number of cracks in a unit area of the transverse x_1x_2 plane, and 2a is the crack width equal to the ply thickness.

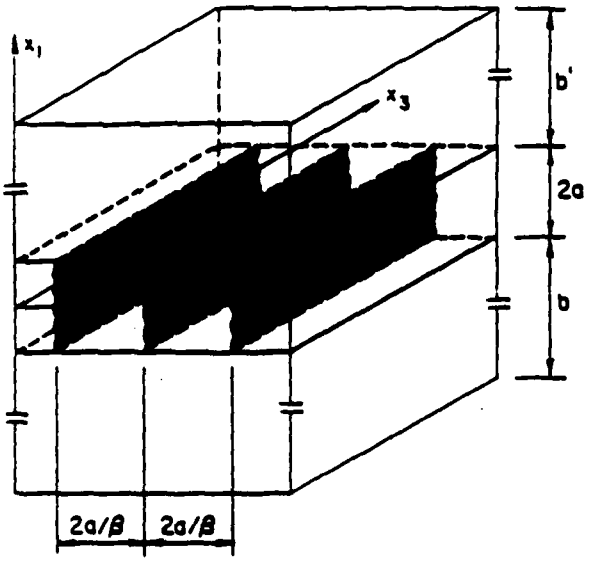

Fig. 1 Schematic representation of transverse cracks in a fibrous composite ply. Fibers are aligned in the x_3 direction.

Suppose that the stiffness and compliance tensors $\underset{\sim}{L}_o$ and $\underset{\sim}{M}_o$ of the ply are known in the undamaged state. These quantities can be estimated in terms of fiber and matrix moduli and fiber volume fractions by approximate averaging techniques, or bracketed by the Hashin-Rosen bounds. Exact evaluation of the corresponding tensors for a damaged ply would have to account not only for the interaction between the cracks, but also for the interaction of each crack with the adjacent plies of arbitrary orientation. To circumvent the considerable difficulty posed by these interactions, and particularly by the latter, we assume that the properties of the cracked ply can be approximated by those of a homogeneous medium which contains a certain density of aligned slit cracks of width 2a. Then, the overall stiffness $\underset{\sim}{L}(\beta)$ and compliance $\underset{\sim}{M}(\beta)$ at certain crack density β can be determined by the following self-consistent approximation, originally suggested by Budiansky and O'Connell (1976).

In the absence of cracks, the potential energy of a homogeneous body of volume V, under uniform overall stress $\underset{\sim}{\sigma}$ can be written in the form

$$E_o = -\frac{1}{2} V \underset{\sim}{\sigma}.\underset{\sim}{M}_o\underset{\sim}{\sigma} . \tag{1}$$

The energy released by formation of a single crack in the homogeneous body can be written in terms of a certain crack tensor $\underset{\sim}{\Lambda}_o$ as:

$$W = \frac{1}{2}\pi\ a^2\ \underset{\sim}{\sigma}.\underset{\sim}{\Lambda}_o\underset{\sim}{\sigma} . \tag{2}$$

Now, if many aligned slit cracks are introduced in such a way that the body remains statistically homogeneous, then the effect of interaction between the cracks on the energy released by a single crack can be expressed in terms of

$$W(\beta) = \frac{1}{2}\pi\ a^2\ \underset{\sim}{\sigma}.\underset{\sim}{\Lambda}(\beta)\underset{\sim}{\sigma}, \tag{3}$$

which is equal to the energy released by a single crack in a homogeneous medium of compliance $\underset{\sim}{M}(\beta)$, or stiffness $\underset{\sim}{L}(\beta)$. Of course, the number of cracks in the volume V is equal to $n = \beta V/4a^2$. Therefore, the potential energy of the medium with open slit cracks of density β can be written as

$$-\frac{1}{2} V \underset{\sim}{\sigma}.\underset{\sim}{M}(\beta)\underset{\sim}{\sigma} = -\frac{1}{2} V \underset{\sim}{\sigma}.\underset{\sim}{M}_o\underset{\sim}{\sigma} - \frac{1}{2} n \pi\ a^2\ \underset{\sim}{\sigma}.\underset{\sim}{\Lambda}(\beta)\underset{\sim}{\sigma} . \tag{4}$$

This must hold for any V and $\underset{\sim}{\sigma}$, hence the effective compliance of the cracked medium is

$$\underset{\sim}{M}(\beta) = \underset{\sim}{M}_o + \frac{1}{4}\pi\ \beta\ \underset{\sim}{\Lambda}(\beta). \tag{5}$$

Next, use the identity $\underset{\sim}{M}\underset{\sim}{L} = \underset{\sim}{M}_o\underset{\sim}{L}_o = \underset{\sim}{I}$, where $\underset{\sim}{I}$ is the identity tensor, to find the effective stiffness

$$\underset{\sim}{L}(\beta) = \underset{\sim}{L}_o - \frac{1}{4}\pi\ \beta\ \underset{\sim}{L}_o\ \underset{\sim}{\Lambda}(\beta)\ \underset{\sim}{L}(\beta) . \tag{6}$$

Evaluation of the crack tensor $\underset{\sim}{A}(\beta)$ in a transversely isotropic medium with aligned slit cracks was described by Laws, Dvorak, and Hejazi (1983), and Dvorak, Laws, and Hejazi (1985).

The overall thermoelastic constitutive equations of the cracked ply can be written in the form

$$\underset{\sim}{\sigma} = \underset{\sim}{L}\,\underset{\sim}{\varepsilon} - \theta\,\underset{\sim}{\ell}\ , \qquad \underset{\sim}{\varepsilon} = \underset{\sim}{M}\,\underset{\sim}{\sigma} + \theta\,\underset{\sim}{m}\ , \tag{7}$$

where $\underset{\sim}{m}$ is thermal strain vector of expansion coefficients and $\underset{\sim}{\ell} = \underset{\sim}{L}(\beta)\underset{\sim}{m}$ is the thermal stress vector. One can establish from the above analysis that $\underset{\sim}{m} = \underset{\sim}{m}_o$ of the undamaged state, and that $\underset{\sim}{\ell} = [\underset{\sim}{I} - \beta\underset{\sim}{L}(\beta)\,\underset{\sim}{A}(\beta)]\underset{\sim}{\ell}_o$. Also, if the overall strain of the cracked medium is written as the sum

$$\underset{\sim}{\varepsilon} = \underset{\sim}{\varepsilon}_o + \underset{\sim}{\varepsilon}_c\ , \tag{8}$$

of the average strain $\underset{\sim}{\varepsilon}_o$ in the uncracked ligaments, and the average strain $\underset{\sim}{\varepsilon}_c$ accommodated by opening of all the cracks, then Dvorak et al. (1985) show that

$$\underset{\sim}{\varepsilon}_o = \underset{\sim}{A}_o\,\underset{\sim}{\varepsilon} - \theta\,\underset{\sim}{a}_o\ , \qquad \underset{\sim}{\varepsilon}_c = \underset{\sim}{A}_c\,\underset{\sim}{\varepsilon} - \theta\,\underset{\sim}{a}_c \tag{9}$$

where

$$\underset{\sim}{A}_o = \underset{\sim}{I} - \frac{1}{4}\pi\,\beta\,\underset{\sim}{\Lambda}\,\underset{\sim}{L} = \underset{\sim}{M}_o\,\underset{\sim}{L}, \qquad \underset{\sim}{A}_c = \frac{1}{4}\pi\,\beta\,\underset{\sim}{\Lambda}\,\underset{\sim}{L} = \underset{\sim}{M}_o\,(\underset{\sim}{L}_o - \underset{\sim}{L}) \tag{10}$$

$$\underset{\sim}{a}_o = -\frac{1}{4}\pi\,\beta\,\underset{\sim}{\Lambda}\,\underset{\sim}{L}\,\underset{\sim}{m} = -\underset{\sim}{A}_c\,\underset{\sim}{m}, \qquad \underset{\sim}{a}_c = \frac{1}{4}\pi\,\beta\,\underset{\sim}{\Lambda}\,\underset{\sim}{L}\,\underset{\sim}{m} = \underset{\sim}{A}_c\,\underset{\sim}{m} \tag{11}$$

and $\underset{\sim}{\Lambda} = \underset{\sim}{\Lambda}(\beta)$, $\underset{\sim}{L} = \underset{\sim}{L}(\beta)$.

Similar results can be developed for cracks in zero-degree plies. Such plies typically contain matrix cracks on planes perpendicular to the fiber. In well-made systems such cracks bypass the fibers, and the corresponding crack geometry must be analyzed, c.f., Wung (1987).

3. RELAXATION SURFACES

Plastic deformation of heterogeneous media is a very complex process. The initial stages are dominated by local yielding at inhomogeneities, but such contained plastic flow does not significantly affect overall stiffness. Indeed the onset of overall yielding is typically associated with extensive plastic straining in the aggregate. One may then assume that the overall yield condition of a fibrous ply can be expressed in terms of the matrix yield condition and the average matrix stress. Recent experimental observations of plastic behavior of fibrous composites (Dvorak et al. 1988) suggest that in certain but not all cases the experimentally detected overall yield surface of the composite medium can be approximated in this way. Several composite plasticity models have been developed along these lines; in the sequel it will be convenient to use the strain space formulation of Wung and Dvorak (1985).

Let the matrix relaxation condition be expressed in the Mises form

$$g_m(\underset{\sim}{\varepsilon}_m - \underset{\sim}{\beta}_m) \equiv 2G_m^2(\underset{\sim}{\varepsilon}_m - \underset{\sim}{\beta}_m)^T \underset{\sim}{C}(\underset{\sim}{\varepsilon}_m - \underset{\sim}{\beta}_m) - k^2 = 0 , \tag{12}$$

where G_m is the matrix shear modulus, $\underset{\sim}{C}$ is a constant matrix, $\underset{\sim}{\varepsilon}_m$ is the matrix strain, $\underset{\sim}{\beta}_m$ is the position of the center of the relaxation surface in $\underset{\sim}{\varepsilon}_m$ space, and k is the matrix yield stress in simple shear. If the matrix strain concentration factors are written in the form used in (9), then the composite relaxation surface in the overall strain space $\underset{\sim}{\varepsilon}$ is:

$$g(\underset{\sim}{\varepsilon} - \underset{\sim}{\beta}) = 2G_m^2(\underset{\sim}{\varepsilon} - \underset{\sim}{\beta})^T \underset{\sim}{A}_{mc}^T \underset{\sim}{C} \underset{\sim}{A}_{mc}(\underset{\sim}{\varepsilon} - \underset{\sim}{\beta}) - k^2 = 0 , \tag{13}$$

where the concentration factors $\underset{\sim}{A}_{mc}$ must be derived from a chosen model of the composite microstructure. This, and the development of hardening and flow laws which can be applied to fibrous plies in a metal matrix laminate, was described in the above reference.

When a system of cracks of density β exists in a ply which has undergone some plastic strain $\underset{\sim}{\varepsilon}_p$ followed by unloading, the total strain in the layer with fully open cracks can be written as

$$\underset{\sim}{\varepsilon} = \underset{\sim}{M}\,\underset{\sim}{\sigma} + \underset{\sim}{\varepsilon}_p , \quad \underset{\sim}{\sigma} = \underset{\sim}{L}\,\underset{\sim}{\varepsilon} + \underset{\sim}{\sigma}_R \tag{14}$$

where $\underset{\sim}{M}$, $\underset{\sim}{L}$ are given by (5) and (6), $\underset{\sim}{\varepsilon}_p$ is the plastic strain, and $\underset{\sim}{\sigma}_R$ is the relaxation stress which is given by $\underset{\sim}{\sigma}_R = \underset{\sim}{L}\,\underset{\sim}{\varepsilon}_p$. Of course, the unbroken ligaments in the ply are now regarded as an effective homogeneous material which has the properties of the composite. At the onset of further plastic loading the ligament material carries, on average, the part of overall ply strain given by $\underset{\sim}{A}_o$ in (10). Again, this strain is not uniformly distributed in the ligament. However, if one extends the argument leading to derivation of the relaxation surface of the undamaged composite to the present case, the relaxation surface of the damaged ply with open cracks is obtained in the form

$$g_\beta(\underset{\sim}{\varepsilon} - \underset{\sim}{\beta}) = 2G_m^2(\underset{\sim}{\varepsilon} - \underset{\sim}{\beta})^T(\underset{\sim}{A}_{mc}\,\underset{\sim}{A}_o)^T \underset{\sim}{C}(\underset{\sim}{A}_{mc}\,\underset{\sim}{A}_o)(\underset{\sim}{\varepsilon} - \underset{\sim}{\beta}) - k^2 = 0. \tag{15}$$

When the cracks are closed, the relaxation surface of the ply is again given by (13), but adjustments must be made if the cracks close with a relative shear displacement which cannot be adjusted by relative sliding. The distinction between open and closed cracks is determined by the inequality that assures crack opening:

$$\varepsilon_{22}^c = \varepsilon_{22} - \varepsilon_{22}^o > 0, \tag{16}$$

in the coordinate system of Fig. 1.

Fig. 2 shows an illustration of relaxation surfaces (15) of a $(0/90)_s$ laminated plate subjected to in-plane uniaxial load from 0 to 500 MPa and to load cycles from 500 MPa to 50 MPa. Note that a steady state response is obtained after the second cycle. In this example, the matrix follows the Ziegler hardening rule, details of the calculation were described by Wung (1987). The surfaces and the loading path are plotted in the in-plane strain coordinates $\bar{\varepsilon}_{22}$, $\bar{\varepsilon}_{33}$. The top bars indicate laminate strains, which are equal in all plies; the x_3 direction coincides with the fiber orientation in the 0° ply, and x_2 is the fiber direction in the 90° ply. In this illustration, the relaxation surface equations (14,15) have been transformed into the laminate strain coordinates. The cracks have been added after completion of the load cycle, and the relaxation surfaces (15) are therefore plotted from the end position at 50 MPa. The dashed

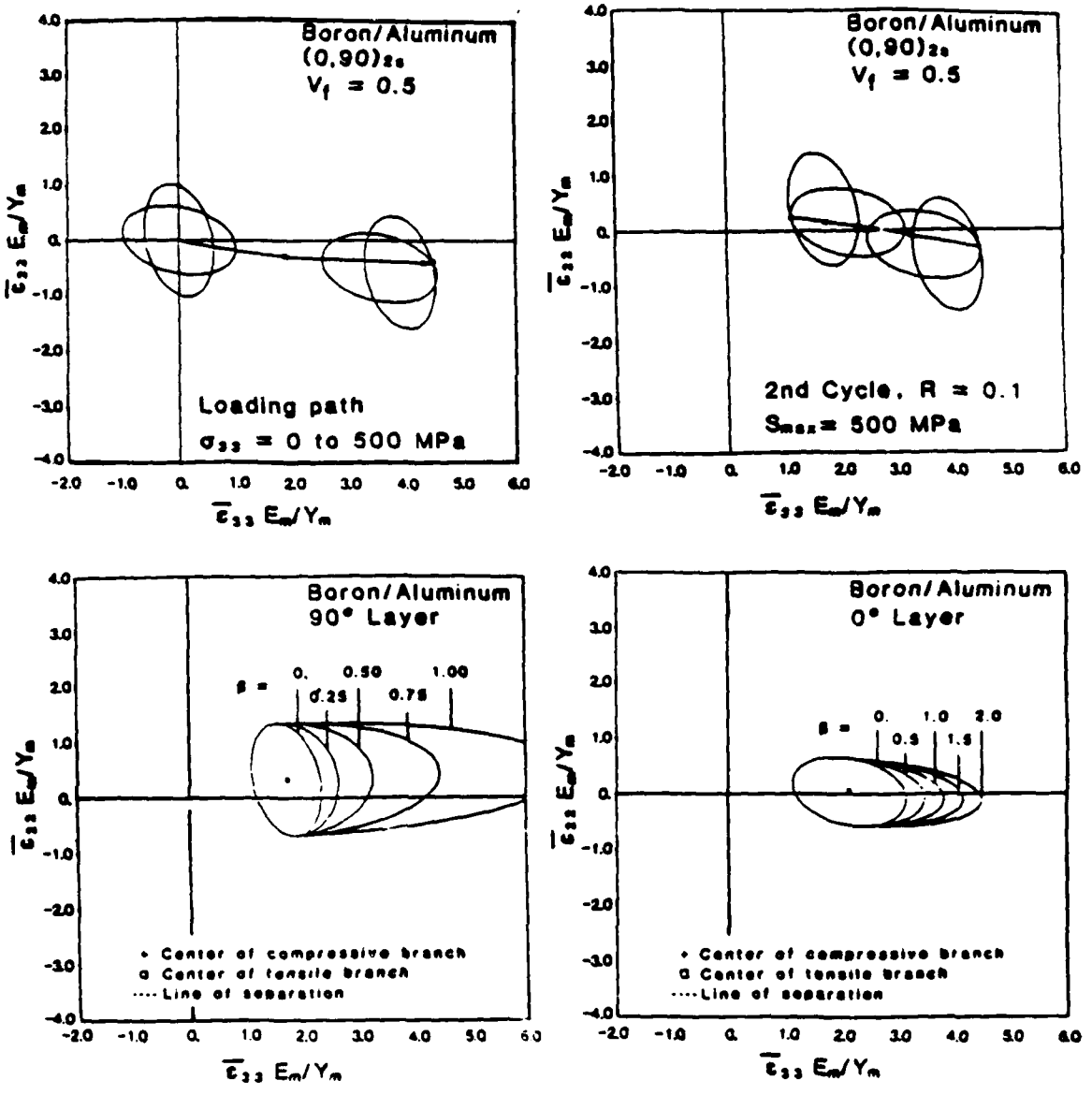

Fig. 2 Motion of ply relaxation surfaces during first and second loading cycle, and expansion of the surfaces at different values of the damage parameter β.

line indicates the crack opening condition (16). As one would expect, a larger overall strain is needed to cause the initial yield strain in the matrix of a cracked ply. Therefore, the open crack branches of the relaxation surfaces expand with increasing crack density. Again, the scalar β denotes the crack density, while the vector $\underset{\sim}{\beta}$ defines the position of the center of the relaxation surface.

4. THE DAMAGE PROCESS

Damage development in metal matrix composites is often observed only under sustained cyclic loading in the platic range. The damage process in these systems has many unusual aspects which deserve attention since they affect the subsequent modeling and analysis.

We focus on a laminated plate which consists of many fibrous layers which at all times remain perfectly bonded. This constrains the plies to identical in-plane strains, and a fairly straightforward procedure based on laminated plate theory can be used to derive overall plate properties from the ply properties. In what follows we assume that all plies are made of the same composite material, the only distinction between the plies being the in-plane orientation of the fiber which also determines the orientation of cracks. Of course, laminates made of dissimilar plies can be considered as well. The plate is subjected only to in-plane mechanical stresses which are assumed to be uniform, and also to a spatially uniform change in temperature.

Each ply consists of an elastic-plastic fibrous composite medium; the macroscopic elastic response of a ply is described by (7), with the overall properties, $\underset{\sim}{L}_o$, $\underset{\sim}{M}_o$ in the undamaged state, and $\underset{\sim}{L}(\beta)$, $\underset{\sim}{M}(\beta)$, given by (5) and (6), in the presence of damage. The elastic state terminates when the stress state in any ply satisfies the yield condition (13) in the undamaged state, and also when (16) is not satisfied in a damaged ply. Similarly, (15) and (16) describe the yield condition of a damaged ply. Normality of the plastic strain increment to the matrix yield surface guarantees normality at the ply and also at the laminate level. This opens the way to formulation of constitutive equations in the plastic range.

Under cyclic loading of a metal matrix laminate in the plastic range, the plastically strained plies eventually develop a certain fatigue damage state which is dominated by transverse cracks of the type shown in Fig. 1 (Dvorak and Johnson 1980). However, other types of damage such as localized delamination at the fiber-matrix interface and between plies, as well as fiber splitting by the transverse cracks are frequently observed. Of course, when two adjacent plies have transverse crack systems, the cracks will intersect at ply boundaries. In fact, if the laminate is made of momolayers reinforced by large diameter fibers, such as boron or silicone carbide, the ply boundaries are not well defined and cracks in one ply will extend up to the layer of inclined fibers in the next ply. Modeling of the various types of damage would be very difficult. However, one may account for the additional damage by increasing the effective density of transverse cracks in each ply. This can be understood as addition of more cracks of width 2a to those which are physically present, or as a magnification of the width of the existing cracks. The second alternative appears to be more plausible as it may well represent the actual reason

for an increase in $W(\beta)$ in (3), which is the extension of the existing cracks by delamination and ply boundary crossing. Then, the scalar β may no longer be regarded as a measure of the actual crack density, but as a damage parameter to be used in the results of Section 2, which are still supposed to predict the effect of damage on stiffness and on averages of local fields.

The experimental results of Dvorak and Johnson (1980) on B/Al laminates, as well as subsequent studies by Johnson on SiC/Ti plates suggest that cyclic plastic straining of the matrix is the principal cause of fatigue damage growth. No damage is typically observed if the laminate is loaded by an elastic load cycle, either in the initial or shakedown state. This argument can be extended to damaged laminates. In particular, one can assume that all damage growth will terminate if the laminate reaches an elastic deformation state. As illustrated by the example in Fig. 2, elastic deformation can be restored under an initially inelastic cycle of loading, if the amount of damage in the plies, and the applied strain cycle cause, respectively, expansion and translation of the ply relaxation surfaces such that the prescribed load cycle or the corresponding strain cycle can be accommodated within the new elastic range. The damage evolution process can then be regarded as a mechanism that the composite laminate employs to reach an elastic state. In this new state, the originally inelastic part of the total strain in each ply is accommodated, in part, by the strain ε_c caused by opening of the cracks.

Viewed from a different perspective, the damage process can be thought of as a part of a shakedown mechanism in the composite laminate. According to the static or Melan shakedown theorem, an elstic-plastic solid or structure will shake down if any admissible residual stress field can be found such that its superposition with the stresses caused by the applied loading will not violate the yield condition anywhere in the solid. In other words, the laminate will shake down if a subsequent yield surface, or its relaxation surface counterpart in the strain space, can be found which contains the applied load or strain cycle. Of course, shakedown can take place only if the structure is loaded within its failure envelope, and if early collapse by incremental plastic straining can be prevented. That is usually the case in laminated plates where the elastic fibers support a major part of the load so that the total strains are small, yet substantially larger than the initial yield strains of a ply.

It is useful to point out that cyclic plastic loading of the laminate creates cyclic plastic strains in individual plies which, as illustrated again by Fig. 2, tend to reach a steady state after relatively few cycles. On the other hand, the plastic deformation cycle also promotes low cycle fatigue damage growth which, in comparison, proceeds very slowly. Typically, several thousand cycles may be needed to cause a significant change. One may then expect the relaxation surfaces to translate much more rapidly than expand. The direction of translation should be such as to minimize the magnitude of plastic work per cycle. Under such circumstances, the relaxation surfaces will tend to translate into such most favorable positions which will assure that, the amount of expansion - which is to say extent of ply damage - will reach only the minimum amount necessary for an elastic accommodation of the loading program.

Another consequence of the large disparity between deformation and damage rates is that in each damage state, or at a particular magnitude of

ß under a prescribed load or strain cycle, the effect of past deformation history will fade very quickly. That is to say that the deformation field in the laminate at a particular state of ply damage will be very similar to that which one would reach if this amount of damage was introduced into an elastic laminate prior to the application of the corresponding load cycle. Of course, that does not suggest that the final shakedown state may be reached by purely elastic deformation of an initially damaged medium. We recall that damage causes only expansion of the relaxation surfaces. But if translation is also needed due to the minimum damage requirement, the shakedown state under the prescribed load or strain cycle may be reached only after several cycles of plastic straining which may be needed to bring the respective ply relaxation surfaces to their final location. However, the implication is that the final deformation state in a damaged laminate subjected to a constant load cycle is independent of previous loading and damage history. Therefore, in arriving at a final damage state, one may follow any convenient path. For example, the damage analysis of the typical case of constant amplitude loading, which causes large excursions into the plastic range during many initial deformation cycles, can be replaced by analysis of damage caused by a load cycle which expands at a rate comparable to that of damage growth. In this particular case each increment in amplitude is followed after few cycles by a saturaion damage increment which restores elastic straining within a new shakedown state.

Of course, the independence of the final damage state on the loading path would be expected to hold only in elastic-plastic systems which have the ability to adjust their internal permanent strain state in response to current cyclic loading conditions. Apart from the above arguments, available results obtained in tension-tension fatigue tests of B/Aℓ metal matrix composite laminates support the path independence concept. For example, Johnson (1982) found that a saturation damage state at a certain maximum load amplitude could be reached by dissimilar loading sequences. Another support for this concept was established by experiments which showed that the amount of damage in a laminate was determined primarily by the load amplitude and not by variations of the mean stress.

5. INCREMENTAL SHAKEDOWN-DAMAGE ANALYSIS

We now present some results which illustrate certain aspects of damage development in B/Aℓ laminates subjected to cyclic tension loading. Our objective is to find, for several different load amplitudes, the amount of damage in each ply that is needed to reach a shakedown state in the laminate. Of course, the stiffness loss and the internal stress distribution, particularly the fiber stress, are also of interest. One specific laminate under consideration, of 0/90 layup, was already discussed in connection with Fig. 2. In addition, a similar analysis was performed for a 0° plate. The final load cycle we wish to reach is from S_{min} = 50 MPa to S_{max} = 500 MPa in both laminates. The actual path we follow starts with cycling of the laminate to a steady state, as in Fig. 2. Then, while S_{min} is kept constant, S_{max} is reduced to bring the laminate into an elastic state. Next, S_{max} is increased in small increments. After each increment, cracks are introduced in the plastically deforming plies to the extent needed to acommodate the deformation path within the expanded relaxation surfaces. This involves both expansion and translation of the surfaces, which cause

a new plastic strain state and a stress redistribution through the laminate. Details of the procedure have been described by Wung (1987). As an example, Fig. 3 shows the current relaxation surfaces at two levels of S_{max}. Note

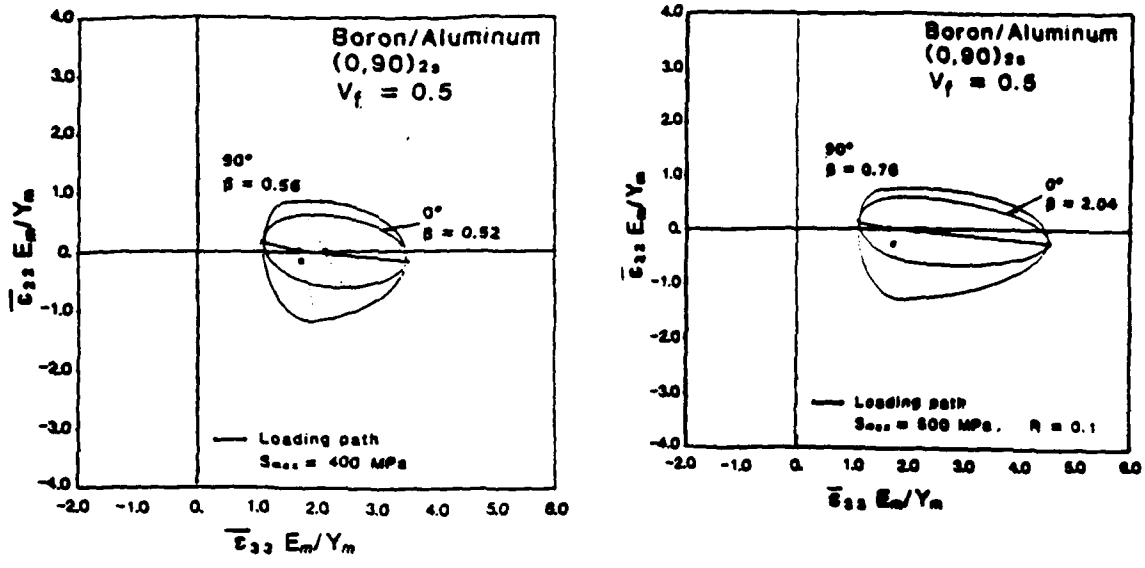

Fig. 3 Translated and expanded relaxation surfaces of a damaged laminate at two different levels of S_{max}.

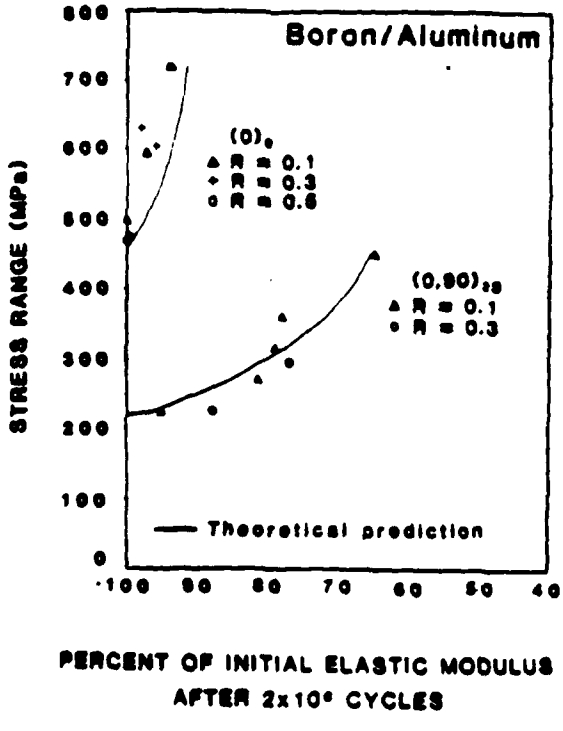

Fig. 4 The effect of sustained cyclic loading on reduction of axial elastic modulus of two B/Aℓ laminates. Comparison of prediction with experimental results obtained under constant load amplitudes.

that high values of 8 are required to accomplish the accommodation, as anticipated in Section 4. The incremental expansion of the loading range continues until one reaches the desired final magnitude of S_{max}.

Fig. 4 shows the change in the axial elastic modulus caused by saturation damage in the two laminates as a function of the applied tension stress range. The computed results are plotted together with experimental data of Dvorak and Johnson (1980). In the experiments, the saturation damage state was defined as the damage state after $2x10^6$ cycles at constant stress amplitude, as noted in Fig. 4, but actual measurements of stiffness loss indicated that damage usually stabilized after $5x10^5$ cycles. Finally, Fig. 5 shows the computed magnitudes of the axial stress in the 0° layer fibers, in the saturation state at different levels of S_{max}. This stress change has been plotted up to S_{max} equal to the experimentally observed endurance limit. Note that while the endurance S_{max} are quite different in the two laminates, the terminal fiber stresses are nearly identical. The implication is that fatigue failure occurs in these composite systems by overloading of the 0° fibers. Of course, the maximum stress is not seen by the fibers until the laminate reaches the saturation damage state at the endurance S_{max}. In the initial stages of damage development, a part of the load is carried by the undamaged off-axis plies, but as damage grows more stress is absorbed by the 0° fibers.

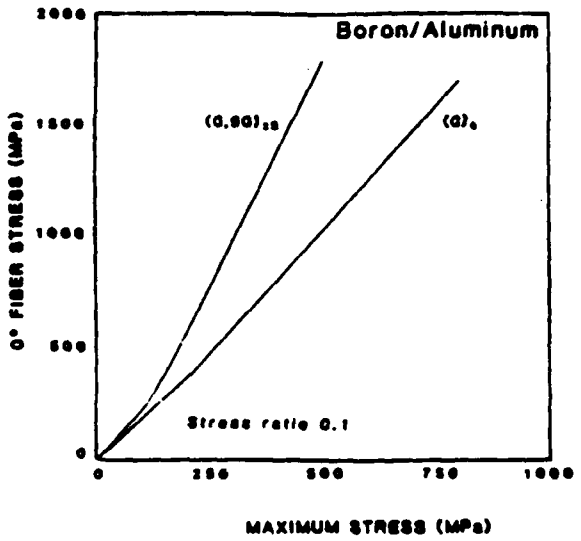

Fig. 5 Fiber stresses in zero-degree plies after damage-induced shakedown.

6. CONCLUSION

The good agreement between experimentally measured stiffness changes and the predictions derived by the present method, Fig. 4, has also been reproduced in an application of the method to fatigue analysis of a $(0/\pm45/90)_s$ laminate. We recall that the predictions were found for an incrementally expanding load cycle, while the experiments were performed under constant load amplitudes. This seems to indicate that the approximations introduced in the model strike a reasonable balance between simplicity and accuracy, and that the damage process is actually path independent. Of course, a more realistic model of the elastic-plastic behavior of the cracked ply would be desirable. However, the significant results are the identification of the saturation damage state as a damage-induced shakedown mechanism, and of the path-independence of the damage process. These aspects of the problem could be exploited in design of a more efficient approach.

Acknowledgement: This work was supported in part by the Air Force Office of Scientific Research, and by the NASA/AFOSR Composite Materials and Structures Grant to Rensselaer.

REFERENCES

Budiansky, B. and O'Connell, R.J. (1976) Elastic moduli of a cracked solid. Intl. Jnl. Solids and Structures, 12, 81-97.

Dvorak, G.J., and Johnson, W.S. (1980) Fatigue of metal matrix composites. Intl. Jnl. Fracture, 16, 585.

Dvorak, G.J., Laws, N., and Hejazi, M. (1985) Analysis of progressive matrix cracking in composite laminates I. Thermoelastic properties of a ply with cracks. Jnl. Composite Materials, 19, 216-234.

Dvorak, G.J., Bahei-El-Din, Y.A., Macheret, Y., and Liu, C.J. (1988) An experimental study of elastic-plastic behavior of a fibrous boron-aluminum composite, Jnl. Mechanics and Physics of Solids, in print.

Hashin, Z. (1983) Analysis of composite materials - a survey. J. Applied Mech., 50, 481-506.

Johnson, W.S. (1982) Mechanisms of fatigue damage in boron/aluminum composites. Damage in Composite Materials, ASTM-STP 775, K.L. Reifsnider, editor, pp. 83-102.

Laws, N., Dvorak, G.J., and Hejazi, M. (1983) Stiffness changes in unidirectional composites caused by crack systems. Mechanics of Materials, 2, 123-137.

Wang, A.S.D. (1984) Fracture mechanics of sublaminate cracks in composite materials. Composites Technology Review, 6, 45-62.

Wung, C.J., and Dvorak, G.J. (1985) Strain-space plasticity analysis of fibrous composites. Intl. Jnl. Plasticity, 1, 125-139.

Wung, C.J. (1987) Strain-space analysis of plasticity, fracture, and fatigue of fibrous composites. Ph.D. Dissertation, University of Utah, 202 pp.